https://doi.org/10.57634/RCR5055

Advances in the chemistry of composites of metal-organic frameworks

Gulzhian I. Dzhardimalieva,[a, b] Vladimir A. Zhinzhilo,[c] Igor E. Uflyand [c]

[a] *Federal Research Center of the Problems of Chemical Physics and Medicinal Chemistry, Russian Academy of Sciences, prosp. Akad. Sakharova 1, 142432 Chernogolovka, Moscow Region, Russian Federation*
[b] *Moscow Aviation Institute (National Research University), Volokolamskoe shosse 4, 125993 Moscow,*
[c] *Southern Federal University, ul. Zorge 7, 344090 Rostov-on-Don, Russian Federation*

The review addresses the current state of research in the synthesis, structure and properties of composites of metal-organic frameworks (MOFs) with functional materials, which are classified into four types depending on their dimensionality: zero-, one-, two- and three-dimensional materials. Due to the wide variety of functional materials, numerous MOF composites with unique properties and characteristics have been obtained. In addition to combining the advantages of MOFs (chemical versatility, structural adaptability and flexibility, high porosity due to hierarchical pore structure) and functional materials of various types (special catalytic, optical, electrical and magnetic properties and mechanical strength), a synergistic effect may appear in the composites. This gives rise to new physicochemical properties or a set of properties. The design of composites based on MOFs represents a new stage in the development of the chemistry of composite materials, in which the surface area, morphology and pore size can be controlled. The interest in these composites is associated with the wide scope of their practical application.
The bibliography includes 480 references.

Contents

1. Introduction 1
2. Composites of metal-organic frameworks with 0D materials 3
3. Composites of metal-organic frameworks with 1D materials 8
4. Composites of metal-organic frameworks with 2D materials 10
5. Composites of metal-organic frameworks with 3D-materials 12
6. Properties of composites of metal-organic frameworks 19
7. Template effects in the composites of metal-organic frameworks 21
8. Conclusion 24
9. List of abbreviations and symbols 25

G.I.Dzhardimalieva. Doctor of Science (Chemistry), Head of Laboratory at FRC PCP and MC, Professor of MAI.
E-mail: dzhardim@icp.ac.ru
Current research interests: metal polymers, composite materials, metal nanoparticles, catalysis
V.A.Zhinzhilo. Candidate of Chemical Sciences, Senior Lecturer at the Faculty of Chemistry of SFU.
E-mail: i06993@yandex.ru
Current research interests: metal-organic frameworks, sorbents.
I.E.Uflyand. Doctor of Science (Chemistry), Professor, Head of a Department of the Faculty of Chemistry of SFU.
E-mail: ieuflyand@sfedu.ru
Current research interests: coordination chemistry, metal-organic frameworks, extraction, metal nanoparticles, tribology.

Translation: Z.P.Svitanko

1. Introduction

Metal-organic frameworks (MOFs), obtained by self-assembly of organic polytopic ligands and metal ions (clusters),[1–18] represent a new class of porous materials. They are characterized by high diversity and structural variability in combination with minor topological restrictions in the formation of porous 3D lattices. Metal-organic frameworks possess unique properties such as high strength and considerable pore volume (> 50% of the total volume). In addition, by choosing appropriate precursors, it is possible to change the size of the formed pores (up to 98 Å),[19] the density (down to 0.124 g cm^{-3})[20] and the specific surface area (up to 10 000 m^2 g^{-1}).[21] Owing to the listed properties, MOFs are promising for the design of catalysts, adsorbents, nanomaterial precursors, tribotechnical materials, *etc.*

In the last two decades, the interest in MOFs has boomed (Fig. 1 *a*); research efforts were mainly concentrated on the fabrication of new structures and study of their various applications.[22–38] Currently, some MOFs are produced on an industrial scale.[39, 40]

Among significant drawbacks that restrict the application of MOFs, mention should be made destruction under the action of high pressure and temperature, low resistance to light and water and poor electrical conductivity. Most of MOFs (> 20 000) have been synthesized in non-aqueous or mixed water–organic media (only 62 MOFs were prepared in water). Many MOFs have smaller pores than analogous materials (zeolites) and moderate pore apertures; in particular, a typical diameter of pore aperture of MOFs (without MOF–MOF interpenetration[21, 41]) is 5–20 Å. Note also

Received July 3 2021

© 2022 Uspekhi Khimii, ZIOC RAS, Russian Academy of Sciences

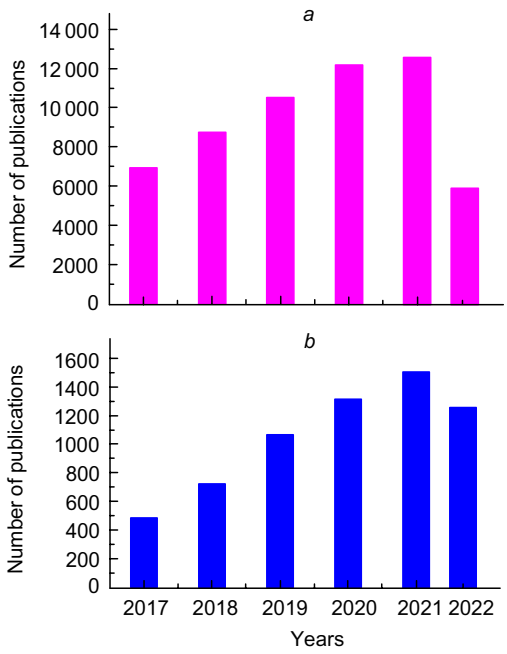


Figure 1. Diagrams illustrating the dynamics of publications addressing MOFs (*a*) and MOF composites (*b*) since 2017 up to the first half of 2022. The Figure was created by the authors using Web of Science data.

the limited thermal stability of MOFs[42,43] and their low chemical stability in aqueous media (Fig. 2).[44]

A promising trend for increasing MOF quality is integration with diverse functional materials (FMs) such as nanoparticles (NPs), quantum dots (QDs), carbon nanotubes (CNTs), polyoxometalates (POMs), silicon dioxide, polymers, enzymes, *etc*. The development of this approach may combine the benefits and mitigate the drawbacks of both components.[45–48] Metal-organic framework composites consist of one MOF and one or several FMs comprising other MOFs. The properties of composites markedly differ from the properties of constituents, that is, MOFs and FMs taken separately. Metal-organic frameworks with large surface areas can form host–guest supramolecular systems in which MOFs may serve as hosts.‡ Owing to large free space in the pores, MOFs can accommodate large amounts of FMs.[49] Apart from combination of the properties of various MOFs (chemical versatility, structural adaptability and flexibility, and high porosity due to hierarchical pore structure) and FMs (mechanical strength and special catalytic, optical, electrical and magnetic properties), synergistic effect may arise, giving rise to new physicochemical properties or sets of properties of the composites.[26,50,51] The use of these composites not only promotes the development of advanced materials, but also expands the scope of applicability of MOFs. An appropriate MOF can be selected from a library of porous materials; alternatively, simulation tools can be used as an efficient screening technique.[52–57] It is necessary to note that ensuring the compatibility of MOFs and FMs is a fairly complex task, the solution of which would promote the targeted synthesis of composites with specified properties.

‡ There is no generally accepted designations of composites in the literature. Here the host and guest components, including for core/shell structures, are separated by a slash.

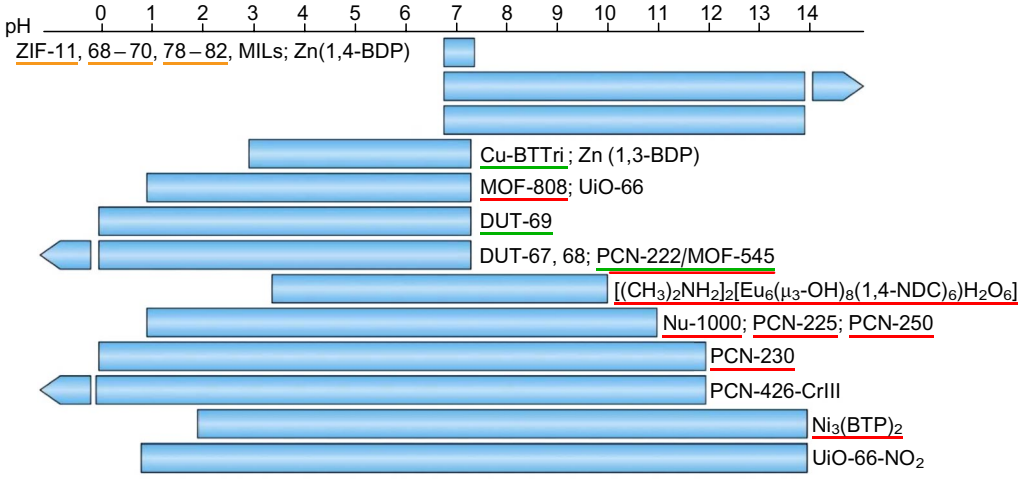


Figure 2. Review of stability of some MOFs to acids and bases in aqueous medium.[44] The length of the band corresponds to the pH range in which MOFs can exist without degradation; the arrow indicates that MOFs are stable at pH <0 or pH >14. The stability was established by powder X-ray diffraction (PXRD). The names of MOFs the stability of which was confirmed by both PXRD and gas sorption experiments are underlined in red; the names of MOFs for which no data on the stability in aqueous acids and bases are available are underlined in green and orange, respectively. Designations (see †): 1,3-BDP is 1,3-benzenedipyrazolate; 1,4-BDP is 1,4-benzenedipyrazolate; 1,4-NDC is 1,4-naphthalenedicarboxylate; BTP is 1,3,5-tris(1*H*-pyrazol-4-yl)benzene; BTTri is 1,3,5-tris(1*H*-1,2,3-triazol-5-yl)benzene; dimb is 1,4-bis(1*H*-imidazol-4-yl)benzene; MOF is metal-organic framework; PCN is porous coordination network; ZIF is zeolite imidazolate framework. Published with permission from Springer Nature.

† For the nomenclature and origin of the MOF names, see, for example, Chapter II in Ref. 3. The letter designations of some MOFs that are frequently mentioned in this review are derived from the names of institutions in which they were first synthesized, *e.g.*, DUT is the Dresden University of Technology, HKUST is the Hong Kong University of Science and Technology, MIL is the Materials Institute Lavoisier, NENU is the Northeast Normal University, NU is the Northwestern University, UiO is Universitetet i Oslo, UTSA is the University of Texas at San Antonio, TMU is the Tarbiat Modares University.

Metal-organic framework composites can be used as the base or precursors for the preparation of nanomaterials, which expands the scope of applications of MOFs in practically important fields such as development of protective and functional coatings,[58] storage and separation of gas mixtures,[59,60] heterogeneous catalysis,[61–63] lithium battery materials,[64] targeted drug delivery systems,[20] artificial photosynthesis and photocatalysis [65] and supercapacitors.[66] In addition, MOF composites with their excellent novel properties and multifunctional performance would be in demand in innovative technologies.

Many research groups have concentrated their efforts on the study of MOF composites; therefore, the publication activity in this area is rapidly increasing (Fig. 1 *b*). A number of reviews appeared, covering various aspects of MOF composites, namely

— general issues of the synthesis and application of MOF composites;[50,67–69]

— porphyrin MOF composites,[5] magnetic MOF composites,[46,70–74] particular types of composites such as MOF/GO (GO is graphene oxide),[75–77] MOF/QD,[78] MOF/polymer,[79–82] MOF/CNT,[83] MOF/biopolymer,[84] MOF/carbon material,[85–91] MOF/2D material,[92] MOF/COF (COFs are covalent organic frameworks),[93] MOF/enzyme,[94] MOF/MOF,[95] MOF/SiO_2,[96–98] MOF/NPs,[49,99–101] MOF/MXene (MXene is a family of 2D transition metal carbides, nitrides and carbonitrides known for their compositional versatility and formation of some structures with a wealthy surface chemistry),[102] MOF/POM,[103] MOF/g-C_3N_4 (g-C_3N_4 is graphite-like carbon nitride);[104]

— application of MOF composites for adsorption,[105–108] biomedicine,[109–113] catalysis,[114–116] energy storage and conversion,[117] electrochemistry [118–122] and as sensor,[85,123–126] antioxidant,[127] antibacterial [128] and luminescent [129] materials;

— films [130,131] and mixed-matrix membranes [131–133] based on MOF composites.

In this review, we analyze the most important studies addressing the preparation of composites of MOFs and discuss components, structures and properties of composites. Particular attention is devoted to synergistic phenomena and their influence on MOF composites. The systems composed of MOFs and FMs are classified into four types depending on their dimensionality: zero- (0D), one- (1D), two- (2D) and three-dimensional (3D) materials.

We hope that the design strategies and functional performance of MOF composites discussed in this review would be useful for developing new composites and their applications.

2. Composites of metal-organic frameworks with 0D materials

Composites of MOFs with 0D materials contain metal and/or metal oxide quantum dots or nanoparticles. The 0D materials with broad absorption bands, narrow and symmetrical emission,[78,134] and high surface energy [135] possess unique characteristics: high degree of dispersion, stability and chemical reactivity. Hence, they are more beneficial than other nanomaterials.[136] Metal nanoparticles with controlled shape, size, crystallinity and functionality are widely used in electronics, optics, energy conversion and storage, solar energy harvesting and catalysis.[137–139] Quantum dots are semiconductor nanocrystals of 2–10 nm size. They are considered to be promising materials owing to high quantum yields of luminescence, size-dependent characteristics, photostability and low cost;[140,141] they are used in biology, chemical analysis, medicine and engineering.[142–145] Due to high surface energy, NPs are thermodynamically unstable and susceptible to aggregation,[146] which leads to the loss of magnetism,[147] catalytic properties [148] and optical activity.[149] This drawback can be eliminated by using MOFs, since numerous coordination sites and highly ordered structure of MOFs make it possible to stabilize NPs in space and prevent them from aggregation.

By utilizing the benefits of 0D materials, one can improve the existing and generate new functional properties of MOFs.[49,150] NP/MOF composites have the following advantages over other nanostructures such as NP/polymer, NP/silica and NP/metal oxide composites: [151–154] unlimited choice of composition, controllable pore size, multifunctional cores and shells and extensive opportunities for tuning the properties.[135] The introduction of metal NPs with a high ratio of the surface area to the volume [155] into the pores enhances the adsorption properties of MOFs and expands the scope of their applicability.[49]

There is a wide range of synthetic methods for integrating NPs into MOFs.[50,70,100] The composites of MOFs and 0D materials are mainly fabricated by three well-developed methods (Fig. 3):[156]

— 'ship-in-the-bottle',

— 'bottle-around-the-ship',

— 'one-pot synthesis'.

These methods have been employed to prepare MOF composites containing metal NPs,[136,156–162] bimetallic (alloy) NPs,[163,164] including core/shell NPs,[165–167] and polyhedral metal nanocrystals [168,169] with a controlled arrangement of NPs in MOF and controlled composition and shape.

The 'ship-in-the-bottle' approach comprises encapsulation of active low-molecular-weight components or NP precursors into the cavities of MOFs followed by *in situ*

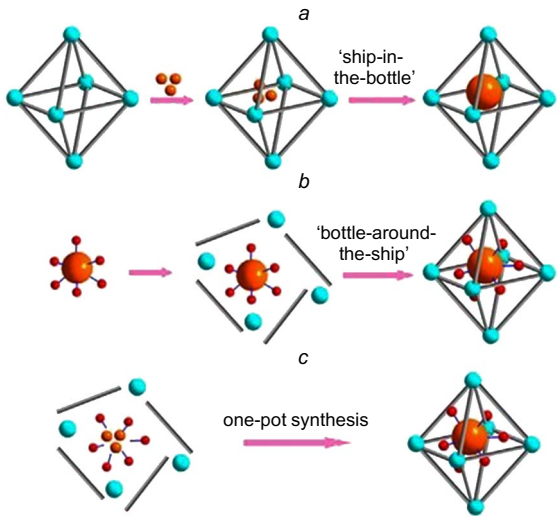


Figure 3. Synthetic routes to metal NP/MOF composites: 'ship-in-the-bottle' (*a*), 'bottle-around-the-ship' (*b*) and one-pot-synthesis (*c*). The inorganic MOF nodes are shown in the turquoise colour, organic linkers are shown in grey, metal or NP precursors are orange and protective groups are red.[156] Published in accordance with the Creative Commons Attribution license (CC BY 4.0).

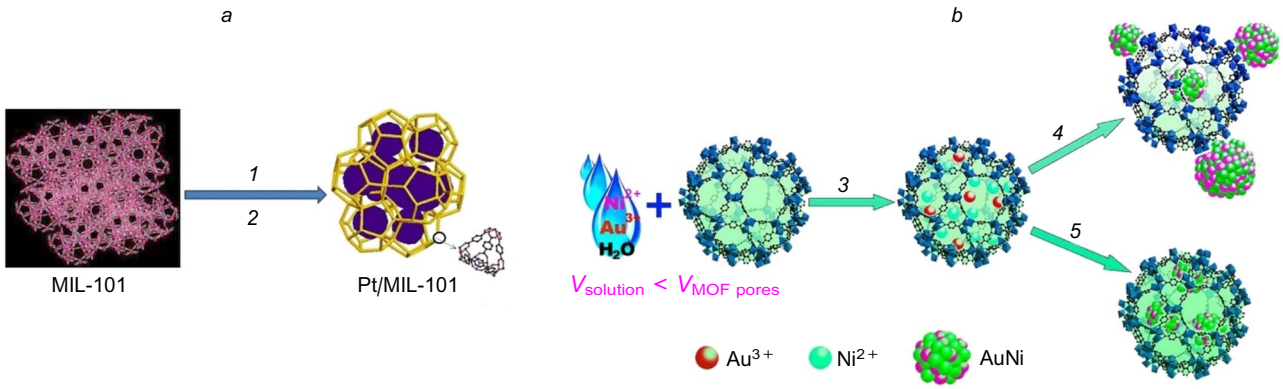


Figure 4. Scheme of the synthesis of Pt (*a*) [177] and AuNi (*b*) [180] nanoparticles in the MIL-101 matrix by double solvent method. (*1*) metal salt in a solvent containing a small amount of water and a large amount of hexane; (*2*) reduction in an H_2 – He flow (1 : 1) at 200 °C for 5 h; (*3*) hexane; (*4*) moderate reduction; (*5*) overwhelming reduction. Published with permission from the American Chemical Society.

synthesis of desired materials in the cavities *via* chemical reduction, photoreaction or thermolysis.[136, 170–173] The NP precursors are introduced into MOFs using a variety of methods: chemical vapour deposition, solution impregnation, solid-phase grinding and microwave irradiation, which are followed by the reduction of the precursors to give metal NPs.[174, 175] These methods differ in the efficiency of control over the size, degree of dispersion and FM location in MOF matrices. For example, in the case of chemical vapour deposition, highly dispersed NPs are located only in pores with a narrow size distribution. However, when the 'ship-in-the-bottle' approach is used, it is difficult to exactly control the location, composition, structure and morphology of the introduced NPs.[176] In particular, it is difficult to entirely introduce metal precursors into MOF pores; the particles are deposited on the external surface of MOFs (being weakly bound to the surface).

The double solvent method provides successful encapsulation of metal nanoparticles into MOF pores without their aggregation on the external surface of the framework.[177–179] This method is based on the use of a hydrophilic solvent (water), the volume of which is equal to or is smaller than the pore volume of the adsorbent (in particular, to obtain MIL-101). The metal-containing precursor (*e.g.*, H_2PtCl_6) is dissolved in the hydrophilic solvent, while a large amount of an adsorbent is suspended in a hydrophobic solvent (hexane), which facilitates the process of impregnation (Fig. 4 *a*).[177] An aqueous solution of H_2PtCl_6 was introduced into the hydrophilic pores of MIL-101 by means of capillary forces; in this case, the deposition of H_2PtCl_6 on the external surface considerably decreased. This gave ultrafine platinum NPs with an average size of 1.8 to 0.2 nm, uniformly distributed in the cavities of the MIL-101 crystals.

It is important that the double solvent method allows *in situ* encapsulation of not only metal NPs, but also bimetallic alloy NPs and core/shell structures into MOF cavities (Fig. 4 *b*).[180–182] In particular, it was found that the size and arrangement of AuNi nanoparticles can be controlled during the reduction of Au^{3+} and Ni^{2+} precursors for NP encapsulation into MOF pores.[166, 180, 181] The reduction with sodium borohydride resulted in ultrafine AuNi nanoparticles (1.8 nm) encapsulated into MIL-101 pores without aggregation on the external surface.[180] Other bimetallic NPs were also introduced into MOF using double solvent approach; in particular, CuNi/MIL-101,[182] Pd – Ni/UiO-67 [183] and PdAg/MIL-101 [184] composites were obtained in this way.

According to the annular dark-field scanning transmission electron microscopy (ADF-STEM) data, after loading platinum NPs into MIL-101 (Fig. 5), the adsorbent remains in the crystalline state and retains its initial morphology.[185] The size of NPs (examples are marked by arrows in Fig. 5 *b*)

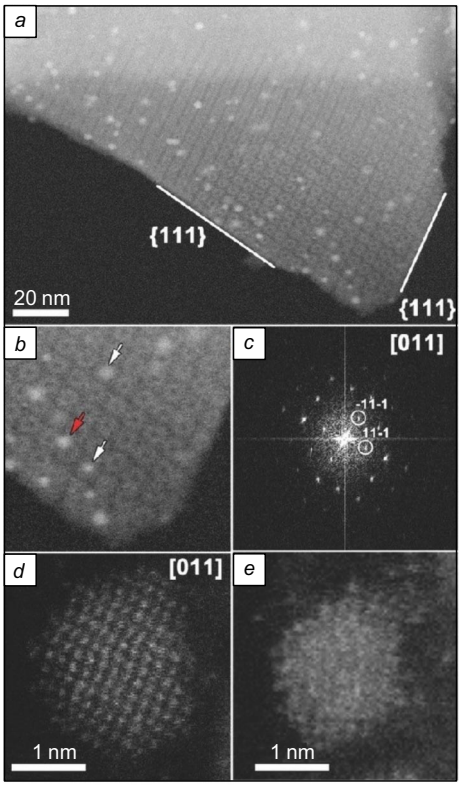


Figure 5. ADF-STEM images of the MIL-101 crystal containing Pt nanoparticles after 40 cycles of chemical vapour deposition (*a*), the same crystal viewed along the [011] direction (*b*) (it can be seen that the size of Pt nanoparticles is adapted to the size of MIL-101 pores; white and red arrows indicate nanoparticles in small and large cages, respectively); Fourier transformation (*c*) of the image shown in Fig. *b*; high-resolution ADF-STEM images of the crystalline (*d*) and partly crystallized Pt nanoparticle (*e*).[185] Published with permission from John Wiley and Sons.

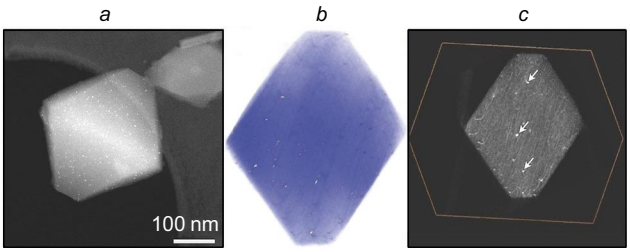


Figure 6. ADF-STEM image of the MIL-101 crystal encapsulating Pt nanoparticles after 40 chemical vapour deposition cycles (*a*), tomographic volume reconstruction of the same crystal (*b*) and orthoslice through the reconstruction indicating that the Pt nanoparticles are located inside the MIL-101 crystal (*c*). The arrows point out several nanoparticles.[185] Published with permission from John Wiley and Sons.

corresponds to the diameter of the MIL-101 cavity, which is indicative of restricted growth of Pt nanoparticles inside MIL-101. The location of NPs confirms that they are embedded into MIL-101 cavities; the NPs marked by white and red arrows are embedded into small and large cavities, respectively. Analysis of ADF-STEM images with atomic resolution showed that NPs can be either crystalline (Fig. 5 *d*) or partly crystallized (Fig. 5 *e*).

An electron tomography experiment was carried out to confirm the incorporation of platinum NPs into MIL-101 cavities. The reconstructed volume of the MIL-101 crystal shaped as a truncated octahedron containing Pt nanoparticles and tomographic slices (Fig. 6) provide direct evidence for the fact that platinum NPs are actually embedded into MIL-101. In combination with high-resolution ADF-STEM image (see Fig. 5), the electron tomography results proved that platinum NPs are embedded into both small and large pores of the MIL-101 framework, without degrading the framework structure during loading.

The 'bottle-around-the-ship' method, which is also known as template synthesis, usually includes two stages.[186–190] First, NPs with similar size, structure and morphology are obtained. Often, they are stabilized by protective coatings or surfactants. Then the pre-synthesized NPs are added into a solution containing MOF precursors. When this method is used, NPs do not occupy the pore space of MOFs, but are surrounded by the MOFs being formed. This prevents the aggregation of NPs on the external surface of MOFs, and the size, morphology and structure of encapsulated NPs can be readily controlled during their preliminary formation (before the MOF assembly).[67, 134] However, introduction of NPs into a solution in some cases hampers the MOF growth due to the high interfacial energy barrier between the two components of the composite. To overcome this barrier, MOFs are linked to encapsulated particles *via* structurally flexibe agents.

For example, controlled encapsulation method was proposed in which the NP surface was coated by a surfactant such as polyvinylpyrrolidone (PVP) or hexadecyltrimethylammonium bromide, and the modified NPs were used in the synthesis of MOFs.[191–193] This method can also be used to introduce several types of functional NPs into MOFs. For example, PVP was added to promote the crystallization of ZIF-8 on the surfaces of some metal NPs (in particular, Au, Pt NPs).[191, 194] Encapsulated NPs were thoroughly dispersed and completely embedded into ZIF-8 crystals (Fig. 7). The spatial distribution of NPs in the ZIF-8 crystals can be controlled by varying the order of addition of the components during the composite synthesis: either in the beginning of the process (τ_0) or after some period of time (τ). The spatial arrangement of NPs in the resulting composites can be represented as the distribution of NPs of one type in the central areas (Fig. 7 *a*) or beyond the central areas (Fig. 7 *b*) of MOF crystals, or as two types of NPs in the central areas (Fig. 7 *c*), or as one type of NPs in the central area and the other type in the transition layers (Fig. 7 *d*) of MOF crystals.

However, it is very difficult to remove surfactants from the surface of metal NPs after the synthesis of NP/MOF composites, and this hampers the application of the composites, for example, in catalysis. Apart from surfactants, some metal oxides or hydroxides are used to modify NPs and to grow a MOF on them.[195–198] A metal oxide shell can be leached, and the metal ions formed in the solution would react with organic ligands to give MOFs around nanoparticles. Using this method, NPs differing in size and morphology can be encapsulated into MOFs. Unfortunately, the activity of encapsulated NPs is somewhat reduced due to the presence of protective coatings or metal oxide layers. In addition, complex interfacial interactions hamper studying the structure–property relationships for such composite materials.

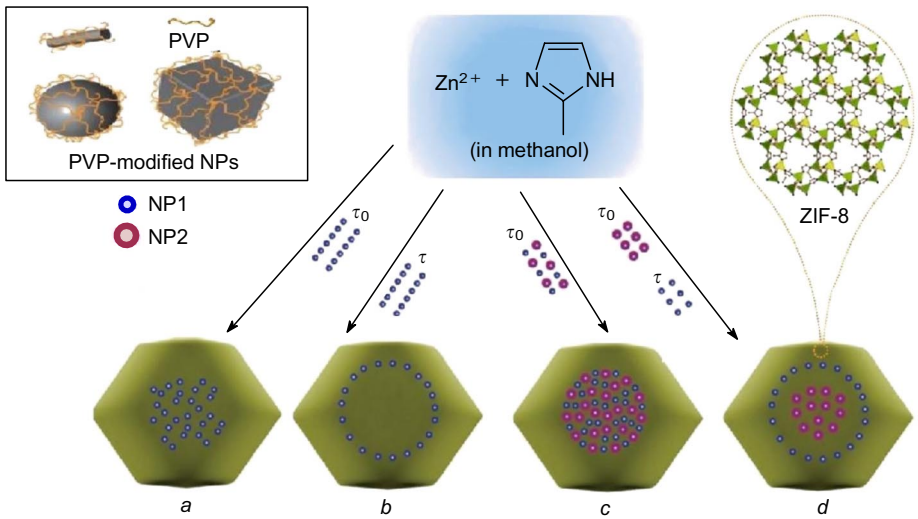


Figure 7. Scheme of the controlled encapsulation of NPs into ZIF-8 crystal.[191] For positions *a*–*d*, see the text. Published with permission from Springer Nature.

Due to the solid-state nature of the reaction and relatively slow kinetics, the 'bottle-around-the-ship' method is effective for the formation of core/shell structures or hollow nanostructures.[199–202] The key issue for the successful use of this method for the preparation of NP/MOF composites is to choose appropriate template materials and reaction conditions to ensure that the rate of release of metal ions from the template corresponds to the rate of their coordination to organic ligands for targeted formation of the MOF shell on the surface of the sacrificial template rather than in solution. This method is simple and versatile and can be implemented using metal oxides and alloys containing transition metals as template materials.[203–205] The PtNi alloy NPs were used as templates to obtain the PtNi/MOF-74 composites by means of oxidative etching.[200]

In comparison with other approaches, the 'bottle-around-the-ship' approach provides the possibility of accurate control of the structure, thickness and morphology of MOF shells. For example, in the synthesis of the RhNi/MOF-74(Ni) nanoflowers, the thickness of the MOF shell was successfully controlled by varying the nickel content in the self-sacrificial template, the RhNi alloy.[203] For the formation of MOF-74(Ni) and ZIF-67(Co) shells on the surface of the RhCoNi ternary alloy, 2-methylimidazole (2MI) or 2,5-dihydroxyterephthalic acid were used as etching agents for the selective dissolution of nickel or cobalt.[204] In view of the pronounced size difference between MOF-74(Ni) and ZIF-67(Co), the cavities of the obtained composites can serve as objects for systematic study of the relationship between characteristics of composites and the structure of MOF shells. The multicomponent MOF shells can also be obtained by adding another metal source for the formation of MOFs.[206]

Inert silica was used as the template for the synthesis of metal NP/MOF composites with uncoated surface or with the yolk/shell structure § (Fig. 8).[207, 208] A typical synthesis of such composites includes several stages: coating of SiO_2 layer on metal NPs; growth of MOFs on the SiO_2 surface to form sandwich nanostructures; and selective removal of the SiO_2 layer in a NaOH solution to obtain the final product.

The one-pot, or direct *in situ* synthesis, which consists in the addition of NP precursors to a mixture of reactants to obtain MOFs and the subsequent self-assembly of the framework, has lately attracted considerable attention of researchers due to the possibility of decreasing the prime cost of the product and the time of the synthesis and easy scaling-up.[188, 190, 209] This method is based on the rational control of the rate of reduction of metal ions and/or the rate of MOF growth. It is important to balance the metal NP nucleation and growth processes with the assembly of MOFs around NPs.[189, 208] In particular, the one-pot method was used to obtain the Pd NPs/MOF composites, which made it possible to attach highly dispersed metal NPs to the MOF surface in one stage without using surfactants.[210]

The encapsulation of platinum clusters into UiO-66 was successfully controlled using one-pot method with hydrogen as an auxiliary reducing agent and/or acetic acid as a MOF-formation modulator (Fig. 9 *a*).[211, 212] An important role in this process is played by the solvent, dimethylformamide (DMF), because DMF and Me_2NCOOH, formed in trace amounts upon DMF oxidation, provide bridges to link MOF precursors to the reduced platinum clusters, thus initiating the anisotropic growth of MOFs. However, unfortunately, the one-pot synthesis is not a universal strategy, although it is simple and efficient.

The restriction of FM formation either inside or outside the MOF matrix is often a complicated task. A random distribution of functional NPs in the matrix not only leads to poor practical reproducibility of composite synthesis, but also considerably affects analysis of the structure – property relationships. To solve this problem, sandwich-like composites were obtained by growing additional MOF layers.[213–215] For example, Zhao *et al.*[213] first synthesized MIL-101 with encapsulated platinum NPs, and after that, one more MIL-101 shell was epitaxially grown on the surface of the MIL-101/Pt composite. As a result, all platinum NPs were encapsulated into a very thin layer of MIL-101, which did not affect the diffusion of substances, for example, during catalysis (Fig. 9 *b*). The sizes of thick MOF shells were ~296 and ~243 nm for MIL-101(Fe) and MIL-101(Cr), respectively, and the diameter of Pt nanoparticles was 2.8 nm. Altogether five composites were obtained, with the shell size being 5.1 nm for MIL-101(Cr) and 2.9, 8.8, 9.2 and 22.0 nm for MIL-101(Fe). Thick shells would have restricted the diffusion of reactants and products, thus considerably decreasing the substrate conversion in catalyzed reactions, although the selectivity should increase to the same extent.[215]

Owing to high porosity of MOFs, it is possible to encapsulate QDs, the luminescent properties of which can serve to monitor various objects. Luminescent semiconductor QDs were encapsulated into MOF-5 crystals to endow the composites with new functional properties.[50] The composites of QDs with MOF-5 retain the optical characteristics of QDs and the porosity of the MOF-5 framework, even if the QD size is larger than the MOF-5 cavity.[216] A similar method was used to obtain the Eu^{3+}/carbon QDs/MIL-53 composite, which combined characteristics of the

§ The yolk/shell (or core/cavity/shell) structure is similar to the core/shell structure, but differs by the presence of empty space between the core and the shell.

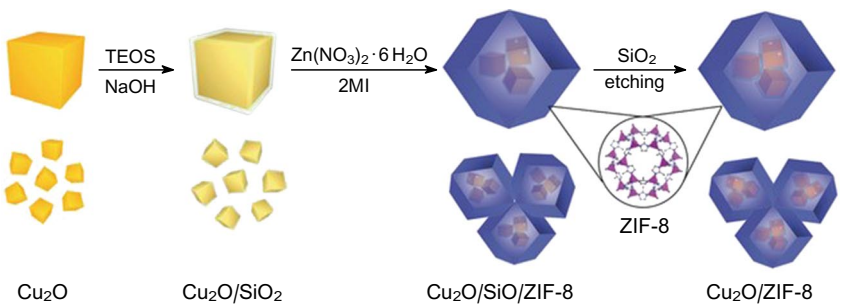


Figure 8. Scheme of the synthesis of the Cu_2O/ZIF-8 composite. TEOS is tetraethoxysilane.[207] Published with permission from John Wiley and Sons.

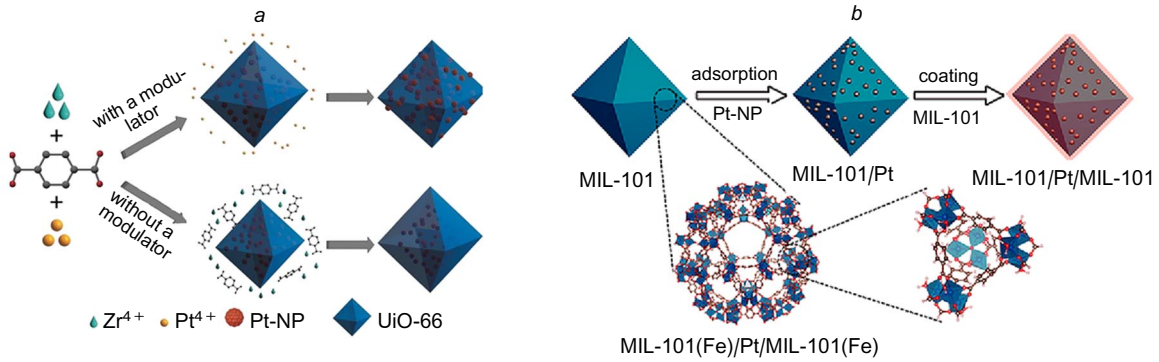


Figure 9. Scheme of incorporation of Pt nanoparticles into UiO-66 by *in situ* one-pot method with and without a modulator (*a*),[217] and synthetic route towards multilayer MIL-101/Pt/MIL-101 composites (*b*).[213] Figure 9 *a* is published with permission from Springer Nature, Fig. 9 *b* is published in accordance with the Creative Commons Attribution license (CC BY 4.0).

MOF matrix, luminescence of the lanthanide ion and luminescence and properties of carbon QDs.[217]

A simple method of *in situ* deposition was used to prepare the SnO_2 QDs/ZIF-8 composites, which were employed as electrodes of supercapacitors with a high specific capacitance and good cycling stability.[218] The HKUST-1/TiO_2 quantum dot composite with a core/shell structure was synthesized by hydrolysis. In this case, MOF was a sorbent for gas molecules, and TiO_2 was a photocatalyst for the CO_2 conversion to CH_4. Charge transfer could take place between the photoexcited inorganic semiconductors and MOF to give long-lived electrons for the reduction of gas molecules adsorbed on MOF.[219]

Among the nitride QD/MOF composites, mention should be made of the synthesis of semiconductor QDs based on gallium nitride inside MOF crystals by encapsulation of trimethylamine gallane into ZIF-8 micropores followed by treatment with ammonia to form GaN (13 mass %).[220]

In most cases, the pre-synthesized QDs are coated by a protective agent, which prevents them from aggregation during the growth of MOFs from precursors.[221] Huang *et al.*[222] obtained the QD/MOF composite by a procedure consisting of two stages: synthesis of nitrogen-doped TiO_2 nanoparticles (N-TiO_2) and their encapsulation into MIL-100(Fe). As compared with the initial MIL-100(Fe), the N-TiO_2/MIL-100(Fe) composite showed a higher capacity for photodegradation of methylene blue or Rhodamine B dye upon visible light irradiation. The material operated for up to four cycles without leaching or loss of activity of QDs.

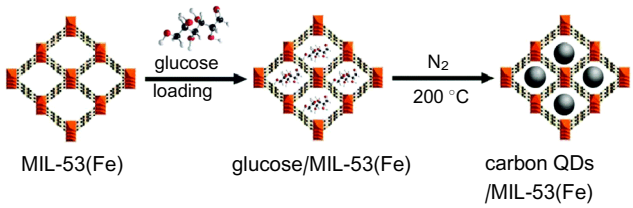


Figure 10. Scheme of the synthesis of the carbon QD/MIL-53(Fe) composite including loading and carbonization of glucose molecules.[224] Published with permission from the Chinese Chemical Society (CCS), Peking University (PKU) and the Royal Society of Chemistry (RSC).

In the nano-CuS/HKUST-1 composite, the metal-organic framework structure acted as the host for nano-CuS and also as a sacrificial template, *i.e.*, it served as a source of copper ions for the formation of CuS.[223] The octahedral shape of MOF crystals was retained upon formation of the composite.

Lin *et al.*[224] developed a preparation method for the carbon QD/MOF composite by *in situ* generation of carbon QDs, which were electron acceptors. The carbon QD/MIL-53(Fe) composite was obtained by encapsulation of glucose as a carbon source into the pores of activated MIL-53(Fe) and the subsequent heat treatment of the glucose/MIL-53(Fe) composite (Fig. 10).

Table 1 gives examples of MOF composites with 0D materials.

Table 1. Conditions of synthesis, morphology and applications of some composites of MOFs with 0D materials.

Composite	Reagents	Conditions of synthesis			Morphology	Application	Ref.
		medium	*T*, °C	τ, h			
Pt/UiO-66	$ZrCl_4$, terephthalic acid, platinum NPs	Water, acetic acid	120	24	MOF spheres with encapsulated Pt NPs	Catalysis (hydrogenation of hex-1-ene, cyclooctene, *trans*-stilbene, *cis*-stilbene, triphenylethylene)	189
Pt/ZIF-8	ZnO, platinum NPs, 2MI	DMF, water	70	24	Core/shell	Catalysis (hydrogenation of alkenes)	201
Cu_2O/ZIF-8	Cu_2O/SiO_2, $Zn(NO_3)_2 \cdot 6H_2O$, 2MI	NaOH, N_2 atmosphere	–	–	Yolk/shell	Catalysis (hydrogenation of 4-nitrophenol)	207

Table 1 (continued).

Composite	Reagents	Conditions of synthesis			Morphology	Application	Ref.
		medium	T, °C	τ, h			
Pt/UiO-66	$ZrCl_4$, terephthalic acid, $H_2PtCl_6 \cdot 6\,H_2O$	DMF	120	24	Core/shell	Catalysis (aerobic oxidation of cinnamic alcohol)	211
N-TiO_2/ MIL-100(Fe)	N-TiO_2, MIL-100(Fe)	Water	RT [a]	3	N-TiO_2 in MOF pores	Photodecomposition of methylene blue and rhodamine B dyes	222
CuS/HKUST-1 nanoparticles	HKUST-1, thioacetamide	Ethanol	30	12	NPs inside MOFs and on the surface	Oxygen reduction reaction	223
Carbon QD/MIL-53(Fe)	MIL-53(Fe), glucose	Ethanol, water	RT [a]	24	QDs inside MOFs	Photocatalytic reduction of Cr^{VI}	224
Au/Ni-MOF	Ni-MOF nanosheets, $HAuCl_4$, $NaBH_4$	Water	RT [a]	1/40	Gold NPs in MOF pores	Catalysis (reduction of nitroaromatic compounds)	225
Au/UiO-66	UiO-66, $HAuCl_4$, $NaBH_4$	n-Hexane	RT [a]	1/3	Gold NPs in MOF pores	Catalysis (oxidation of benzyl alcohol)	226
Pd nanocubes/ MIL-101(Fe)	Pd nanocubes, $FeCl_3$, terephthalic acid	DMF	120	12	MOFs on the surface of Pd nanocubes	Catalysis (hydrogenation of α,β-unsaturated carbonyl compounds)	227
Fe_3O_4/MIL-100	Fe_3O_4, mercaptoacetic acid, $FeCl_3$, trimesic acid	Ethanol	70	1/2	Core/shell	Photocatalytic decomposition of methylene blue	228
Fe_3O_4/GO/ MIL-100(Fe)	Fe_3O_4, GO, $FeCl_3$, trimesic acid	Water	70	24	Core/shell	Photocatalytic decomposition of 2,4-dichlorophenol	229
TiO_2/UiO-68, modified with a chiral ionic liquid	UiO-68, modified with a chiral ionic liquid, $Ti(OPr^i)_4$	Toluene	—	—	Core/shell	Catalysis (Baylis – Hillman – Morita reaction)	230
Pd/UiO-66/ PDMS [b]	$Pd(NO_3)_2 \cdot 2\,H_2O$, UiO-66, PDMS [b]	DMF, then reduction in $H_2 - Ar$ flow	RT, [a] 200	24 4	Core/shell	Catalysis (hydrogenation of styrene)	231

[a] Room temperature (RT); [b] polydimethylsiloxane.

3. Composites of metal-organic frameworks with 1D materials

1D materials include nanotubes, nanofibres (NFs), nanoribbons, nanowires (NWs) and nanorods (NRs). The useful properties of the 1D materials (for example, carbon nanotubes possess high conductivity, while nanoribbons may serve as bridges for electron transfer both in the external circuit and inside MOFs) improve the properties of composites.[132] The following types of MOF composites with 1D materials are considered:

— MOFs are wrapped around the 1D material,

— 1D materials are located on the external surface of MOFs,

— MOFs with 1D nanoribbon materials are grown on a carbon cloth.

Among methods of synthesis of MOF composites with 1D materials, noteworthy are polymerization *in situ* and the template method where 1D materials are used as templates for the dissolution of metal ions, thus initiating the formation of MOFs.[155] A facile hydrothermal process was proposed to prepare a composite of CNTs with MOF based on manganese and terephthalic acid, which could overcome the limitations of usual manganese-based electrode materials.[232] Most of the composites are formed by carbon nanotubes combined with MOFs. The composites such as S/S-ZIF-8/CNTs [233] and PCN-224 / MWCNTs (MWCNTs are multi-walled CNTs) [234] possess excellent properties, including large specific surface area, medium porosity, heat conductivity, mechanical strength and corrosion resistance.[69] Various amounts of CNTs were used to decorate hollow MIL-101 in order to obtain porous hollow MIL-101/CNT composite.[235] By integrating a conductive water-stable copper complex based on hexahydroxytriphenylene with single-walled carbon nanotubes (SWCNTs), White *et al.*[236] obtained a composite that was used in field effect transistor-based sensors to separate carbohydrate molecules according to their size.[236] Nano-sized zinc oxide precursors and MWCNTs were used to synthesize a composite of ZIF-8 with MWCNTs (Fig. 11 *a*).[237] The ZIF-8 crystals were nucleated *in situ* and grew around entangled MWCNTs, which had ZnO precursor NPs on the surface. The process can be divided into two stages, adsorption of ZnO particles on the MWCNT surface and reaction of protonated 2MI with the adsorbed ZnO nanoparticles to form MOF crystals. The MWCNTs/ZIF-8 material was additionally treated with sulfur to give the MWCNT/ZIF-8/S composite, which was used in lithium

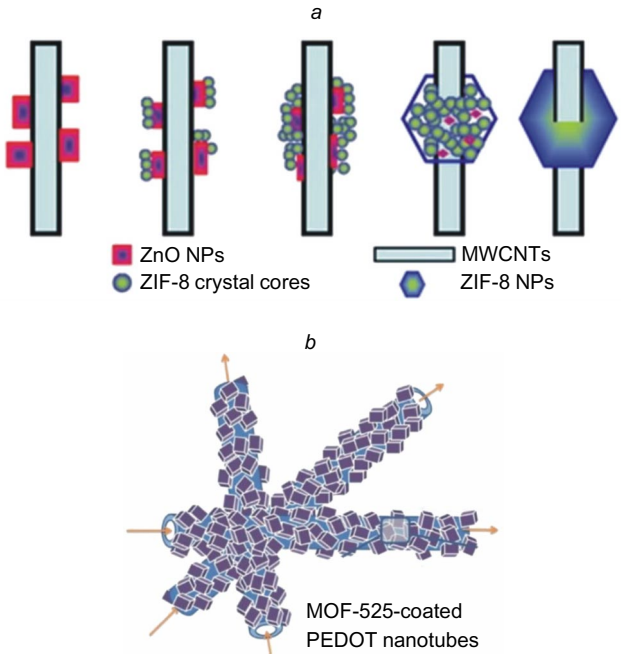


Figure 11. Hypothetical mechanism of the synthesis of the MWCNT/ZIF-8 composite with ZnO nanoparticles gradually absorbed by organic ligands (*a*),[237] and structure of the MOF-525-coated PEDOT nanotube composite (*b*).[238] PEDOT is poly(3,4-ethylenedioxythiophene). Figure 11 *a* is published with permission from Elsevier, Fig. 11 *b* is published in accordance with the Creative Commons Attribution license (CC BY 4.0).

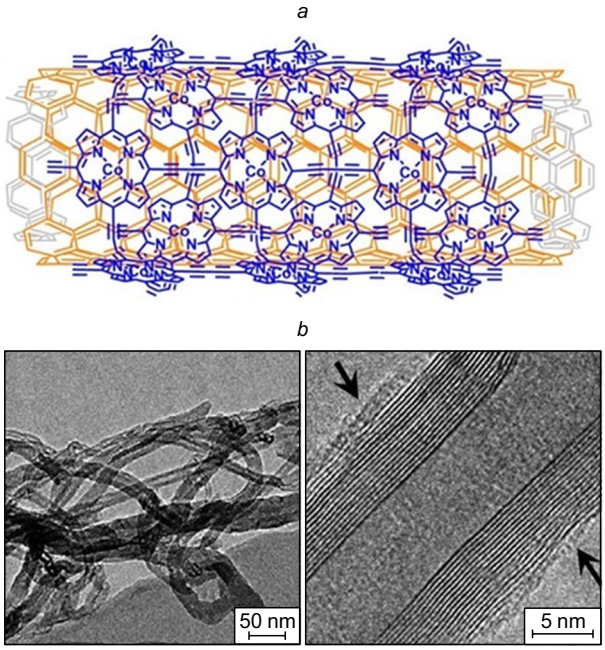


Figure 12. Molecular structure (*a*) and TEM images (*b*) of $(CoP)_n$ and MWCNT composites.[245] TEM is transmission electron microscopy. The arrows point to a thin nanoshell layer (1.5 nm). Published with permission from the American Chemical Society.

sulfur batteries.[226] The MOF-525/PEDOT composites were obtained *in situ* (Fig. 11 *b*). Poly(3,4-ethylenedioxythiophene) nanotubes were coated by porphyrin-based MOF-525 nanocrystals.[238]

A dense membrane of amino acid-based MOF was synthesized. This membrane attached to the porous CNT-based buckypaper (paper with increased elasticity) serves for efficient and selective removal of Pb^{2+} ions from multicomponent aqueous systems.[239] Similarly to one-pot synthesis, the encapsulation of CNTs with a large surface area gives rise to more nucleation sites per unit volume and facilitates the growth of MOFs. Kong *et al.*[240] described a continuous and low-defect ZIF-8 membrane built on CNTs by dipcoating–rubbing technique. First, a thin layer of the composite of graphite and ZIF-8 nanoparticles was deposited on the surface of macroporous CNTs, and then the composite was rubbed for the formation of a stable seed layer. Graphite in the seed layer served as the binding agent for anchoring and stabilizing ZIF-8 nanoparticles on a carbon support and for filling the pores and smoothing the CNT surface. Rudolph and co-workers[241–243] synthesized ZIF-8/CNT, HKUST-1/VA CNT (VA CNTs are vertically aligned carbon nanotubes) and NH_2-MIL-101(Al)/CNT composites using a method according to which CNTs were pretreated with hydrogen peroxide in order to increase their dispersibility in polar solvents *via* increasing the number of functional (for example, carboxyl) groups on their surface.

The MOF/CNT and MOF/MWCNT composites are in demand in various fields: electrocatalysis, water splitting, sorption of greenhouse gases and pollutants, removal of dyes and separation of low-molecular-weight gases.[244] One of the goals of the preparation of MOF composites with CNTs and MWCNTs is to increase mechanical strength, which would expand the scope of applicability of these composites.

Jia *et al.*[245] carried out polymerization of cobalt(II) 5,10,15,20-tetraethynylporphyrin (CoP) *in situ* on the surface of oxidized MWCNTs in order to obtain the composite of MWCNTs with a multilayer porphyrin shell (Fig. 12).

Metal-organic frameworks UiO-66-NH_2 were grown *in situ* on the surface of carbon nanofibres using oxidation with nitric acid.[58] This simple method can be used simultaneously to obtain carbon fibres with enhanced interlaminar shear strength characteristics and also tensile strength.

Wee *et al.*[246] applied spontaneous phase segregation to prepare composites of MOFs (*e.g.*, ZIF-8) and semiconductor 1D materials. In particular, encapsulation of ZnO nanorods into ZIF-8 matrix using this method improved their UV absorption and photocatalytic activity. Using the bottle-around-the-ship method, Zhan *et al.*[247] prepared core/shell MOF composites and metal oxide semiconductor/MOF composites in which ZnO nanorods acted as not

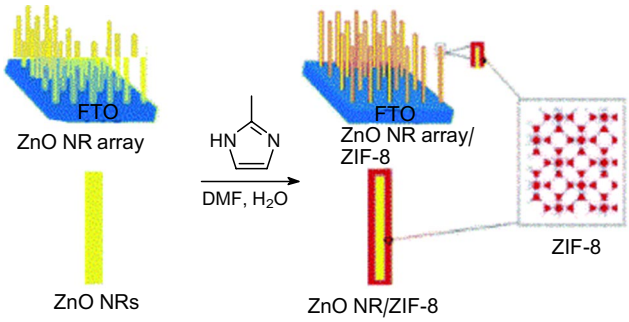


Figure 13. Fabrication of ZnO nanorods/ZIF-8 composite by the bottle-around-the-ship method.[247] Published with permission from the Royal Society of Chemistry.

only the template, but also as the source of zinc ions to form ZIF shells (Fig. 13).[198, 247] ZnO nanorod arrays were implanted into fluorine-doped tin oxide-coated glass and subjected to galvanostatic electrodeposition. This facilitated the synthesis of core/shell composites of MOFs. The bottle-around-the-ship method proved to be convenient for manufacturing some devices based on MOF composite films for sensor or catalytic applications.[248–250] For example, gas sensor based on ZnO/ZIF-CoZn composite [ZIF-CoZn is isostructural to ZIF-8(Zn) or ZIF-67(Co)] was fabricated by deposition of a ZIF-CoZn thin film on the array of ZnO nanowires. Apart from the Zn^{2+} ions dissolved from ZnO nanorods, the introduced Co^{2+} cations also participated in the synthesis of the ZnO/ZIF-CoZn composite, which resulted in the formation of a two-layer metal thin film of MOF on the ZnO nanowire array.[251]

4. Composites of metal-organic frameworks with 2D materials

The 2D materials promising for the design of MOF composites and possessing useful physicochemical properties such as electrical conductivity and high mechanical, chemical and thermal stability can exist as powders, fibres, foams, cloths and so on.[45, 252] Composites of MOFs with 2D materials can be obtained by growing MOFs on nanosheets and by encapsulation of 2D materials into MOFs.[253–255] Nanosheet materials (*e.g.*, GO) are usually combined with MOFs by the solvothermal method. In addition, facile ultrasonic synthesis can also be used; in this case, the target products are formed over a shorter period of time than in the solvothermal method.[256, 257]

A method for deposition of conductive polyaniline (PANI) on the crystals of MOFs to obtain high-performance supercapacitors has been developed (Fig. 14).[258] The ZIF-67 crystals of $\sim$300 nm size were chosen as the material for electrical charge storage; the crystals were attached to the surface of carbon fibre cloth. Polyaniline is easily processed and has high capacitance, chemical stability, unique mechanism of protic acid doping and low cost. The PANI/ZIF-67/carbon cloth electrode obtained in this way showed high mechanical strength and flexible characteristics. SEM images of this electrode showed that the PANI chains coated the MOF surface and the interconnected single crystals of MOFs served as links.

Electrode materials with enhanced characteristics to be used in supercapacitors were manufactured by carbonization of MOF composites based on zinc and 8-hydroxyquinoline with PANI.[259]

Almost all types of MOF composites with 2D materials were prepared by one-pot synthesis. Usually, 2D materials are added to a solution containing readily soluble MOF precursors and then hydrothermal reactions are carried out under the same conditions as in the synthesis of MOFs.[86] This method was used to prepare a series of composites of MOFs [MOF-5, MIL-100(Fe), HKUST-1] with graphite and GO.[260–263] It was shown that functional groups and defects of carbon components may serve as nucleation centres during the MOF synthesis *in situ*, which favours the formation of MOF crystals and gives rise to synergistic effects. A similar process was used to prepare other MOF/2D material composites such as HKUST-1/macroporous carbon, MOF-2/FCNF (FCNF is functionalized carbon nanofibre) and ZIF-8/branched polyethyleneimine/carbon QDs.[264–267]

One-pot synthesis proved to be promising for the fabrication of some specific systems, *e.g.*, mixed-matrix membrane based on MOF/2D material composites.[121, 268]

The layer-by-layer assembly was successfully used to grow ZIF-8 and MIL-53-NH_2 crystals on polyacrylonitrile nanofibre mats[269] or on carbon fibres[270, 271] and to fabricate a core/shell structure, particularly, FCNF/HKUST-1 supported on Al_2O_3. This structure was characterized by high uniformity and high quality of the coating and also smooth surface texture at low temperature (< 70 °C).[272] Using a similar approach, HKUST-1 was grown on electrospun cellulose nanofibres.[273] A two-component ZIF-8/GO membrane was developed by layer-by-layer deposition of a suspension of graphene oxide on ZIF-8 (Fig. 15).[274] Although the hydroxyl groups on the polydopamine

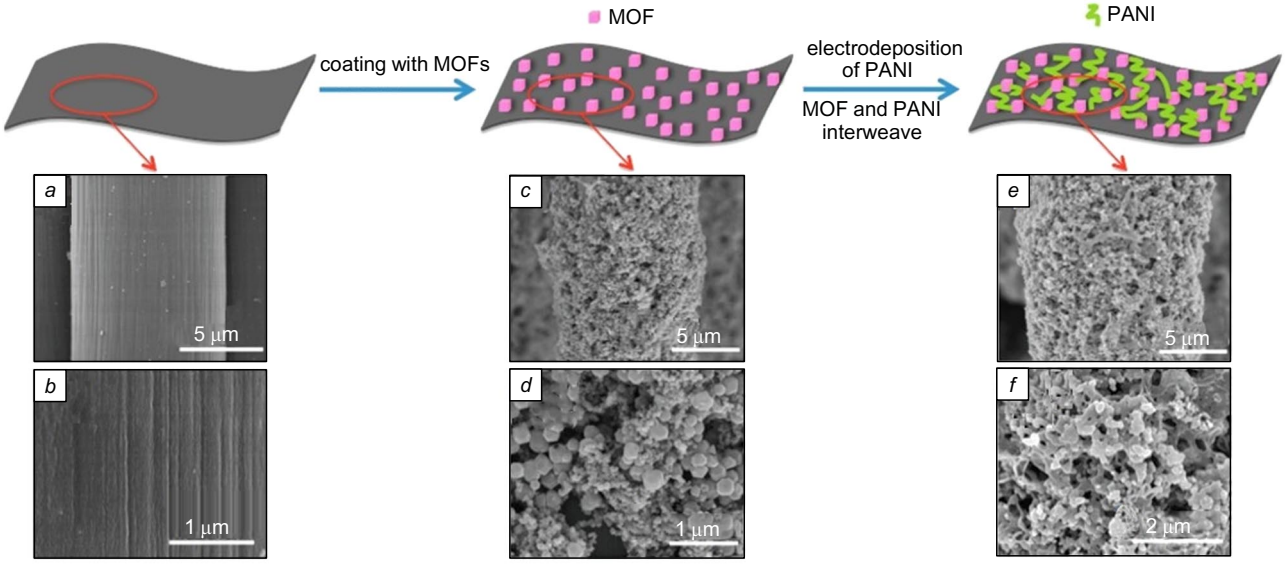


Figure 14. SEM images of carbon fibre cloth (*a*, *b*), ZIF-67 coating (*c*, *d*) and PANI (*e*, *f*).[258] SEM is scanning electron microscopy. Published with permission from the American Chemical Society.

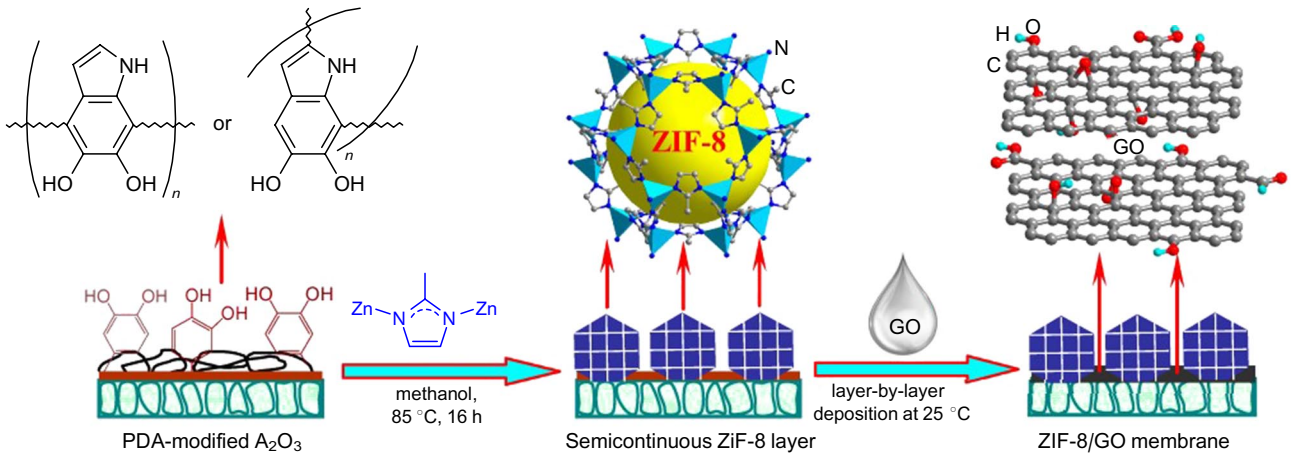


Figure 15. Layer-by-layer assembly of the ZIF-8/GO membrane.[274] Designations in the right-hand part of the picture: the light-blue tetrahedra correspond to zinc clusters, the yellow sphere shows the theoretical pore volume inside MOF. Published with permission from the American Chemical Society.

(PDA)-modified Al_2O_3 support surface facilitated the reactions between MOF precursors and the support, there were still numerous gaps that decreased the total gas permeability of the obtained membrane.

The above-mentioned methods reflect several approaches to the *in situ* synthesis of MOF/2D material composites (synthesis of MOFs in the presence of 2D materials). However, the excessive amount of 2D materials formed *in situ* may hamper the formation of MOF and lead to unsatisfactory characteristics or even destruction of the composite.[263, 275] Therefore, in some cases, ideal MOF/2D material composites are formed by *ex situ* syntheses (integration of pre-synthesized MOFs with 2D materials) such as direct mixing, self-assembly and mechanochemical synthesis. For example, a series of MOFs were doped with graphene by dispersing MOF nanocrystals in a graphene–hexane dispersion followed by deposition of the dispersion of composites on titanium substrates.[276] These composites were utilized for the fabrication of efficient supercapacitors. A material for a supercapacitor electrode containing 10 wt.% RGO/HKUST-1 composite (RGO is reduced graphene oxide) was obrained.[277] First, ultrasonic treatment of RGO and HKUST-1 was carried out, then the RGO/HKUST composite was mixed with conductive carbon black and a water-immiscible binder and, finally, the mixture was sprayed onto flexible carbon fibre paper. A MIL-101-modified carbon paste electrode was fabricated by a similar procedure.[278] The MIL-101/RGO composite was manufactured by dispersing a MOF powder in a GO suspension in water and subjected to reductive treatment with hydrazine hydrate.[279] The MIL-101/RGO/S multicomponent composite was obtained by infiltration of the sulfur-containing liquid phase.

As a rule, the textural properties (in particular, specific surface area and pore volume) and the crystal structure, which depend on not only thermal, but also mechanical treatment of porous solids, considerably affect the gas storage performance.[280] Therefore, mechanical processes (ball milling, compression, *etc.*) are sometimes used to control the textural properties of MOF/2D material composites, especially platinum-doped MOF–carbon mixtures. Blanita *et al.*[281] studied the effect of ball milling and compression on the textural properties, crystal structure and hydrogen uptake of HKUST-1 and Pt/AC mixtures (AC is activated carbon). It was found that after ball milling or compression, the surface area and pore volume of the samples significantly decreased.

Highly dispersed and stable MOF/GO composites were obtained in two stages: first, the self-assembly of Cu-MOFs and graphene sheets took place *via* cooperative π–π interactions, hydrogen bonding and copper coordination to oxygen atoms under continuous exposure to ultrasound, and then the resulting composite was subjected to hydrothermal reduction to be converted into a highly conductive form.[282] The MIL-101(Cr)/S composite wrapped into graphene was obtained from the MIL-101/S crystals and reduced graphene sheets as a result of electrostatic attraction.[156] The self-assembly method was also used to obtain ZIF-67/GO nanocomposites.[283]

Pickering emulsions, discovered by Ramsden and Pickering, are intensively studied by specialists in various fields, mainly because these emulsions provide a large interfacial area, which intensifies the occurring processes [see Ref. 284 and M.Yu.Koroleva, E.V.Yutrov. *Russ. Chem. Rev.*, **91**, RCR5024 (2022)]. Pickering emulsions are dispersions stabilized by solid particles located at the oil/water interface. Highly exfoliated GO can act as a stabilizer for a Pickering emulsion in the preparation of various composites, *e.g.*, HKUST-1/GO (Fig. 16).[285] During the reaction, GO not only stabilized the Pickering emulsions, but markedly modified the morphology and surface porosity and increased water resistance of the resulting HKUST-1/GO composite.

The encapsulation of 2D nanomaterials into MOFs may extend the potential applications of composites to fields such as chemical analysis, energy conversion and data storage. For example, ultrathin graphene nanosheets are stabilized in the presence of MOFs, which increases the accessibility of their surface and active sites. In addition, low electrical conductivity of MOFs increases upon blending with GO owing to improved electron transfer in the composite.[286] In the preparation of composites based on MOFs and GO, synergistic effects are observed. In particular, ultrasmall MOFs with an average size <10 nm were grown on GO, with the growth being controlled *via* electrostatic and coordination interactions of excess metal ions.[287]

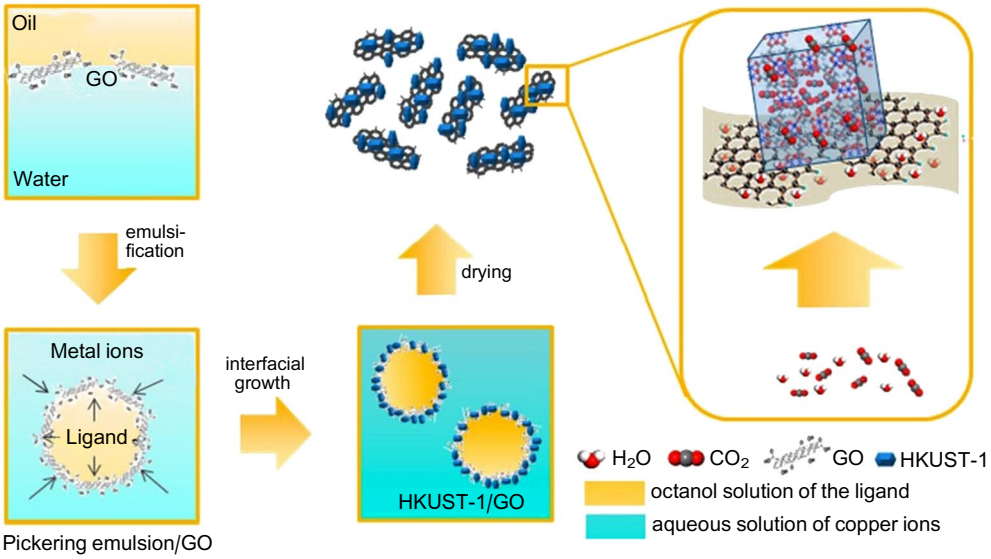


Figure 16. Scheme of the synthesis of the HKUST-1/GO composite by the Pickering emulsion-induced growth method.[285] Published with permission from the American Chemical Society.

The interaction of MOFs with GO changes both the electronic structure and the spatial arrangement of the adsorption sites in the composites, which makes it possible to markedly increase the energy of their binding to guest molecules.[288] The presence of oxygenated groups (hydroxyl, carboxyl, *etc.*) on the GO surface is favourable for the heterogeneous nucleation of MOF crystals on nanosheets.[289, 290]

The MOF/GO and MOF/RGO composites are usually prepared by *in situ* and post-synthesis methods. The *in situ* methods are preferable due to the availability, versatility and mild conditions [that is, the possibility of using water as a solvent and low temperature (in some cases, room temperature)]. Jahan *et al.*[291] used pyridine-functionalized GO as a building block in the assembly of Fe-containing MOF based on 5,10,15,20-tetrakis(4-carboxyphenyl)-21*H*,23*H*-porphyrin.

Graphene oxide and reduced graphene oxide showed high potential for improving some characteristics such as electron transfer and stability of MOFs, the increase of which is a key problem of catalysis and electrocatalysis. Ultrathin nanolayers of several MOFs, such as Co-ZIF, Ni-ZIF, Co,Cu-ZIF and Co,Fe-ZIF, were obtained for the same purpose. The layers were deposited on the RGO surface, with their direction being controlled using the heterogeneous nucleation strategy.[292] Methods for attaching ZIF-8 on both sides of GO nanolayer and deposition of the composite on a porous support were developed, in particular, spin coating in the early stage and secondary growth using the contra-diffusion method (also called interfacial synthesis) in the final stage (Fig. 17).[293]

The Fe-MOF/RGO nanosheet composites, characterized by high theoretical capacitance of MOFs and electrical conductivity of RGO nanolayers, was obtained by solvothermal method.[294] The enhanced electrochemical characteristics of this composite are due to the synergistic effect of Ni-MOFs and GO nanolayers with a unique nanoflower morphology. [295]

Using a combination of density functional theory (DFT) and force field molecular dynamic calculations, an atomistic model of the interface in the ZIF-8/GO composite was generated.[296] It was shown that the composite structure is stabilized at the interface by uniform interactions between the hydrogen atoms of the terminal NH and OH groups of

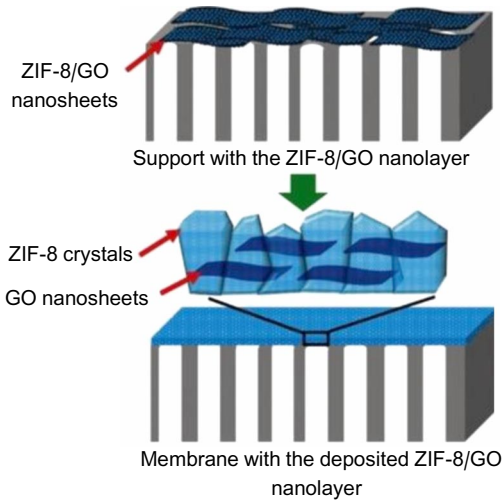


Figure 17. Scheme of the fabrication of an ultrathin membrane with ZIF-8/GO nanolayer deposited by interfacial synthesis.[293] Published with permission from John Wiley and Sons.

ZIF-8 and the oxygen atoms of the epoxy, hydroxyl, and carboxyl groups on the GO surface, which results in the optimal surface coverage with MOF particles.

There are detailed studies of MOF composites with nanosheets of carbon materials such as MIL-100(Fe)/mesoporous carbon,[297] graphene aerogel/MOF(Fe^{3+}),[298] Pd/partially reduced GO/Ce-MOF,[299] TMU-16/GO (Ref. 300) and MIL-68(Al)/GO.[301]

Table 2 gives examples of composites of MOFs with 2D materials.

5. Composites of metal-organic frameworks with 3D-materials

Typical examples of MOF composites with 3D materials are systems with a cubic structure and a core/shell structure. These composites are often obtained using melt diffusion [306] or layer-by-layer assembly, which provides accurate control over the thickness of MOF shell. In the core/shell composites, chemical reactions occur on the core surface, while the

Table 2. Conditions of synthesis, morphology and applications of some composites of MOFs with 2D materials.

Composite	Reagents	Conditions of synthesis			Morphology	Application	Ref.
		medium	T, °C	τ, h			
Ultrathin MOF nanosheets (Co-ZIF, Ni-ZIF, Co,Cu-ZIF or Co,Fe-ZIF)/RGO	RGO, 2MI, metal salt	Methanol, water	RT	1/120	Three-dimensional foam-like hierarchical MOF architecture on RGO sheets	Oxygen evolution reaction	292
Ag nanoparticles/ RGO/MIL-88B(Fe)	Terephthalic acid, $FeCl_3$, RGO, $AgNO_3$	Methanol, $NaBH_4$	RT	3	RGO nanosheets with MOF and Ag nanoparticles on the surface	Oxygen evolution reaction	302
NiFe-MOFs/ graphene nanoplates	$Ni(NO_3)_2 \cdot 6H_2O$, $Fe(NO_3)_3 \cdot 9H_2O$, graphene nanoplates, trimesic acid	H_2O, DMF, ethanol,	85	24	MOFs on graphene nanoplates	Oxygen evolution reaction	303
GO/Cu-MOFs	GO, terephthalic acid, triethylenediamine, $Cu(NO_3)_2 \cdot 3H_2O$	DMF	120	36	MOFs on GO nanoplates	Hydrogen evolution, oxygen reduction and oxygen evolution reactions	304
$FeNi_3-Fe_3O_4$ nanoparticles/MOFs/ CNTs	$FeNi_3-Fe_3O_4$ nanoparticles, MOF based on terephthalic acid, CNTs	Water	100	36	Ultrathin $FeNi_3-Fe_3O_4$ nanoparticles on MOF nanosheets in 1D CNT matrix	Hydrogen and oxygen evolution reactions	305

porous shell prevents the aggregation with neihgbouring cores during the reaction.[307] In the yolk/shell composites, owing to the cavity between the core and the shell, the metal surface exposed to reactants increases and the interaction becomes more uniform.[195]

An important place among the MOF/3D material composites belongs to the POM/MOF composites in which POMs are either a part of the proper metal-organic framework or are encapsulated in the MOF cavity *via* host–guest interactions. The POM/MOF composites are prepared by three main methods:

— growth of MOFs around POMs,

— encapsulation of POM clusters into MOF pores,

— formation of POMs in the pores of pre-synthesized MOFs.

MOF composites obtained by the synthesis of HKUST-1 in the presence of POMs were called NENU.[308, 309] The NENU-11 composite (porous sodalite-type MOF with POM template) showed good adsorption capacity and degrading properties towards dimethyl methylphosphonate.[310] If the solubility of POMs does not pose a problem for the composite synthesis, the composite can be prepared by modification after the synthesis of MOFs. In addition, simple impregnation is also widely used to obtain POM/MOF composites.[311]

The presence of phosphotungstic acid (PTA) as POM in the MIL-101/PTA composite can increase the acidity and catalytic activity of MOF, especially in ring opening reactions.[312, 313] Without using any modulators, NENU-3a with cuboctahedron-shaped crystals was synthesized. The use of this MOF for the production of biodiesel resulted in fatty acid ($C_{12}-C_{22}$) conversion of more than 90% *versus* < 22% attained by using a composite with the octahedral crystal configuration.[314] Keggin type heteropolyacids $H_3PW_{12}O_{40}$ and $H_3PMo_{12}O_{40}$ were immobilized into NU-1000 to catalyze the Biginelli reaction.[315–324] The rhodium complex based on 2,2′-bipyridine-5,5′-dicarboxylic acid was used to facilitate the encapsulation of $PW_{12}O_{40}^{3-}$. Both components were co-immobilized into UiO-67:[325] first, POM was encapsulated into MOF cavities and then the catalytic rhodium complex was introduced by post-synthetic ligand exchange to obtain the composite. Various methods, including the *in situ* synthesis of MIL-100(Fe), were used to prepare the POM/MIL-100(Fe) composite, which showed high stability in water.[326]

Composites of enzymes with MOFs are considered to be valuable materials for medical and biochemical industry; they not only retain high activity of enzymes, especially in catalytic reactions,[327–330] but also compensate for enzyme drawbacks such as incompatibility with organic solvents, narrow pH range of operation and low electrical resistance at high temperatures.[53, 94, 331, 332] Depending on the MOF nature, pore size and shape, enzymes of different molecular sizes can be encapsulated into MOFs without leaching or aggregation.[19] The mismatch between the size of the pores and enzyme molecules leads to aggregation of the latter before diffusion into MOFs and, consequently, to low enzyme loading. In addition, enzymes are able to interact with a vacant metal site or linker of MOFs.[333] The enzyme/MOF composites are obtained using four methods: adsorption, covalent bonding, co-precipitation and encapsulation into pores. Unlike free enzymes, many composites of MOFs with enzymes show high catalytic activity, because immobilization of enzymes in host MOFs prevents them from self-aggregation.[53, 334, 335] Modification of MOFs after the synthesis can also enhance interaction and binding between MOFs and enzymes and increase the catalytic activity of the composite.[336, 337] In addition, the presence of enzymes in

MOFs can affect the selectivity of the composite in catalytic reactions.[338]

According to the requirements imposed on MOF composites with SiO_2, they are obtained by three main methods: *in situ* synthesis, sol–gel process and impregnation. These composites not only increase the hydrophilicity of MOFs owing to the presence of silanol groups in silica, but also facilitate the formation and processing of strong MOF crystals. The MOF composites with silica show excellent productivity for various applications. In particular, when used as the stationary phase of a chromatographic column, the silica/MOF core/shell composite has a narrower size distribution of MOF crystals, which substantially increases the efficiency of separation.[339] Silica has a directing effect on the growth of MOF crystals, and this allows efficient design and control of their morphology. The interaction of the silanol groups on the silica precursor with MOF metal sites can induce structural changes in the composite and increase its surface area and volume of micropores.[340] In addition, silica/MOF composites containing various open metal sites can act as not only catalysts, but also promoters for bimetallic catalysts.[341] MOF composites with silica are used in biomedicine for targeted drug delivery, angiography, diagnosis and treatment of some diseases,[342, 343] and for special purposes.[98, 132, 344–346]

Owing to chemical stability and good mechanical properties, silica not only reinforces the structures of MOF materials, but also increases their stability due to hydrophobic interactions and covalent bonding.[347]

The layers of MOFs are deposited on silica particles *in situ* using single-layer or layer-by-layer assembly techniques. First, silica modified with carboxylate groups was obtained and then Zr^{4+} ions were adsorbed on its surface for the reaction with terephthalic acid, thus giving the SiO_2/UiO-66 composite (Fig. 18).[348] Silica particles of similar size were used as the support in this process. This afforded regularly shaped MOF crystals with a narrow size distribution, which is very important for biomedical applications.

According to the sol–gel process, first, MOF crystals are synthesized, and then silica precursors are hydrolyzed and condensed in the presence of these crystals to form a

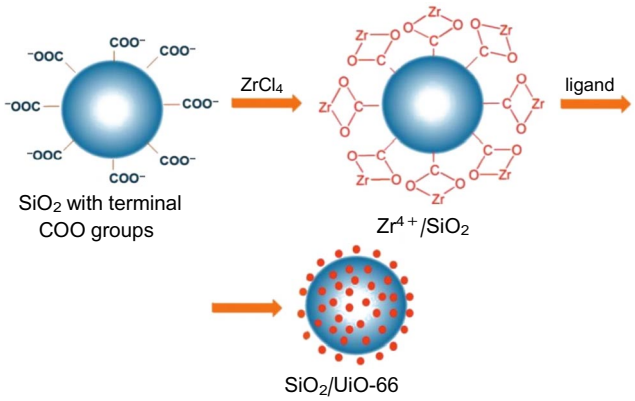


Figure 18. Scheme of the synthesis of the core/shell SiO_2/UiO-66 composite by *in situ* coating.[348] Published with permission from Elsevier.

SiO_2 gel.[349, 350] Silica coatings obtained using this strategy not only preserve the initial structure of MOFs, but also increase the stability and the mechanical properties of composites.

The impregnation method can be used to grow MOFs in the pores of silica materials, which enables the control over the morphology of MOFs/silica composites.[351, 352] Abolghasemi *et al.*[353] prepared the mesoporous silica SBA-15 with uniform large pores, which was then impregnated with a solution of MOF-5 precursor to grow MOFs only on the pore surface (Fig. 19). The MOF-5/SBA-15 nanocomposite obtained in this way demonstrated enhanced adsorption capacity towards small molecules.

Mention should be made of the use of PDMS coating to increase the hydrophobicity of MOF-5 and HKUST-1 without the loss of their own properties, including the crystallinity, specific surface area and pore characteristics.[354] A comparison of HKUST-1/PDMS and the initial HKUST-1 showed good catalytic activity for the coated composite, whereas the initial MOF accelerated the reaction only in the first minutes, and then the activity decreased due to saturation of the active sites with water (Fig. 20 *a*). The use of silica composites leads to a greater surface area,

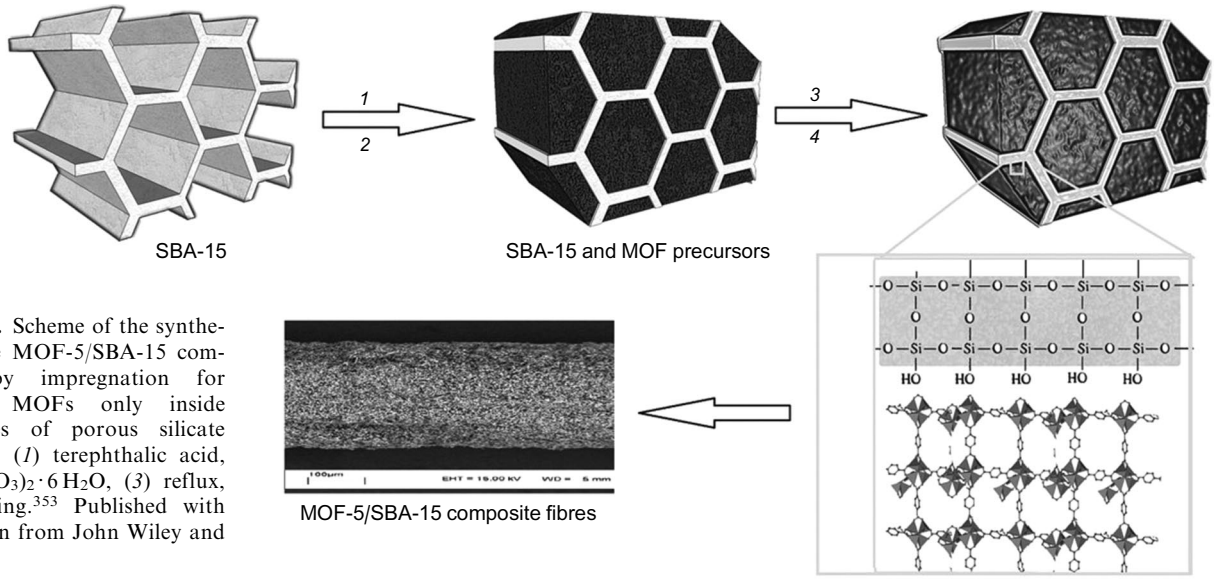


Figure 19. Scheme of the synthesis of the MOF-5/SBA-15 composite by impregnation for growing MOFs only inside the pores of porous silicate materials. (*1*) terephthalic acid, (*2*) $Zn(NO_3)_2 \cdot 6H_2O$, (*3*) reflux, (*4*) washing.[353] Published with permission from John Wiley and Sons.

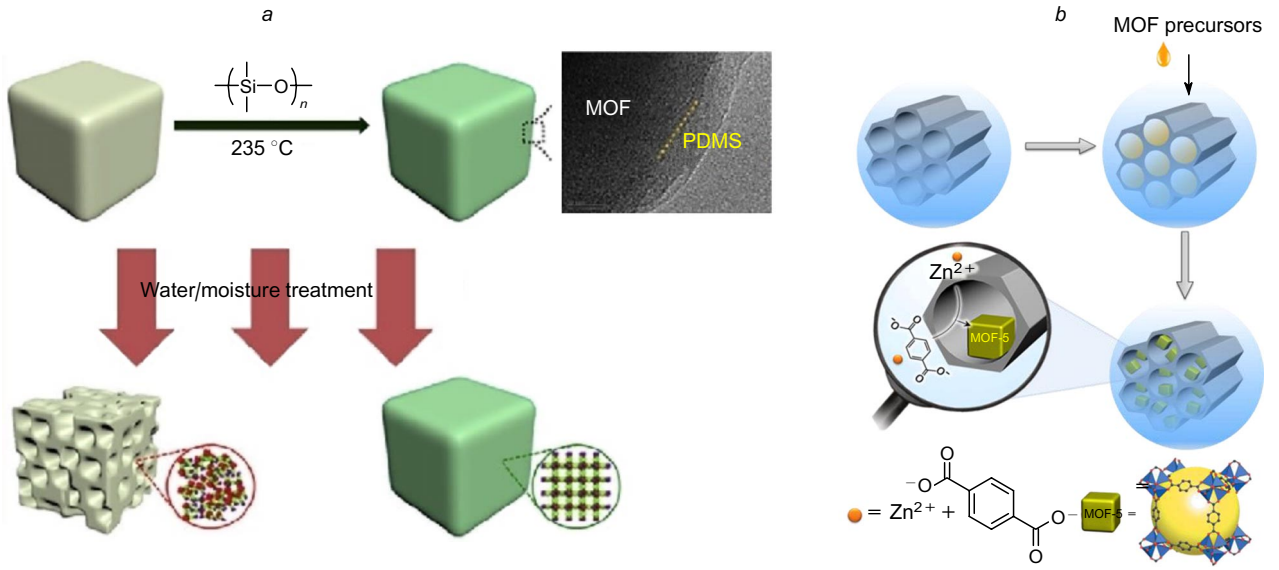


Figure 20. Scheme illustrating polydimethylsiloxane coating of MOF to increase water stability (*a*)[354] and formation of MOF at 120 °C in 24 h by dispersion of SBA-15 (*b*).[355] Published with permission from the American Chemical Society.

which expands the scope of catalytic applications of the materials.[355]

In the first experiment, a solution of MOF-5 precursors was injected into the hydrophilic pores of SBA-15. Then MOF-5 was formed in the pores of SBA-15, although conducting the reaction in a single solvent resulted in the formation of MOF on the surface of silica (Fig. 20 *b*). It is evident that the size of MOF particles and the size of silica pores are the key factors for this process.

Table 3 gives examples of MOF composites with SiO_2.

Polymers possessing high thermal, chemical and mechanical stability and good formability are used most often as matrices for incorporating MOFs.[50] MOFs and polymers may interact *via* electrostatic attraction, covalent binding to linkers or to open coordination sites (metal ions) on the particle surface. The methods used to prepare MOFs/polymer composites developed to date are surveyed in Fig. 21.[374]

In most cases, MOF/polymer composites are obtained by post-synthesis, which includes, depending on the starting point of polymerization, grafting-to and grafting-from methods. The interactions may be covalent and/or non-covalent, which is determined by the nature of functional groups located both on the MOF and on the polymer. For

Table 3. Conditions of synthesis, morphology and applications of some composites of MOFs with SiO_2.

Composite	Reagents	Conditions of synthesis			Morphology	Application	Ref.
		medium	*T*, °C	*τ*, h			
SiO_2/UiO-66	$ZrCl_4$, SiO_2 modified with carboxyl groups, terephthalic acid	DMF, AcOH	120	24	UiO-66 coating on a silica core	HPLC stationary phase [a]	348
MOF-5/SBA-15	MOF-5, SBA-15	Double solvent method			MOF-5 in SBA-15 channels	Catalyst of the Friedel–Crafts alkylation	355
ZIF-8/SiO_2	$Zn(NO_3)_2 \cdot 6H_2O$, SiO_2 modified with carboxyl groups, 2MI	DMF, methanol	RT	24	Core/shell	HPLC stationary phase	356
UiO-66-NH_2/SiO_2	$ZrCl_4$, SiO_2, 2-amino-terephthalic acid	DMF	80	12	Core/shell	HPLC stationary phase	357
HKUST-1/SiO_2	$Cu(NO_3)_2$, trimesic acid, TEOS	Water	120	24	MOFs are incorporated into mesoporous silica pores	HPLC stationary phase	358
Cu-MOFs/SiO_2	$Cu(NO_3)_2 \cdot 3H_2O$, terephthalic acid, MCM-41	–	See [b]	1/2	MOF nanocrystals are incorporated into mesoporous silica pores	Adsorption of CO_2	359
MIL-101(Cr)/SiO_2	$Cr(NO_3)_3 \cdot 9H_2O$, terephthalic acid, MCM-41	Water	120	8	MOFs are incorporated into mesoporous silica pores	Adsorption of CO_2	360

Table 3 (continued).

Composite	Reagents	Conditions of synthesis			Morphology	Application	Ref.
		medium	T, °C	τ, h			
HKUST-1/SiO_2	HKUST-1 and TEOS	Sol–gel process, water, ethanol	–	–	Uniform distribution of HKUST-1 in silica gel matrix	Adsorption of N_2	361
MIL-101(Cr)/SiO_2	$Cr(NO_3)_3 \cdot 9\,H_2O$, terephthalic acid, TEOS	Water, 1 M NH_4F, HCl	–	–	Uniform distribution of MIL-101(Cr) in silica gel matrix	Adsorption of water vapour	362
ZIF-8/MCM-41	$Zn(NO_3)_2 \cdot 4\,H_2O$, MCM-41, 2MI	Water	120	24	Uniform distribution of ZIF-8 in MCM-41 matrix	Absorption of H_2S	363
HKUST-1/SiO_2	Terephthalic acid, $Cu(NO_3)_2$, SiO_2	DMSO	–	2	MOFs in porous monolithic silica gel	Catalyst of oxidation of alkylbenzenes	364
ZIF-8/SiO_2, ZIF-7/SiO_2, UiO-66/SiO_2, HKUST-1/SiO_2	MOFs and TEOS	Water, methanol	–	2	Core/shell	Catalyst of reduction of 4-nitrophenol	365
Pd/MIL-88B-NH_2/SiO_2	Pd/MIL-88B-NH_2, TEOS	Ethanol	40	2	Core/shell/shell	Catalyst of aerobic oxidation of benzyl alcohol	366
HKUST-1/SiO_2, ZIF-8/SiO_2	$Cu(CH_3COO) \cdot 2.5\,H_2O$, trimesic acid or $Zn(NO_3)_2$ and 2MI, SiO_2	Ethanol	–	1/12	MOFs on silica foam	Separation of gas mixtures	367
SiO_2/Eu(2,6-dipicolinate)	2,6-Dipicolinic acid, $Eu(NO_3)_3 \cdot 6\,H_2O$, SiO_2 modified by carboxyl groups	DMF	120	72	MOFs on silica gel spheres	Fluorescence probing	368
SiO_2/MIL-68(Al)	$AlCl_3 \cdot 6\,H_2O$, terephthalic acid, SiO_2	DMF	130	18.5	MIL-68(Al) on the surface of silica particles	Removal of pollutants (aniline, nitrobenzene and phenol)	369
HKUST-1/SiO_2	SiO_2, HKUST-1	Water, ethanol, pentadecane	–	–	Physically dispersed HKUST-1 domains of micrometre size in silica aerogel granules	Catalysis (isomerization of styrene oxide)	370
Catalase/ZIF-8/SiO_2	Catalase/ZIF-8, TEOS	Phosphate buffer	–	16	Mesoporous silica layer around catalase particles/ZIF-8	Enzymatic activity	371
HKUST-1/ silica monolith	$Cu(NO_3)_2$, trimesic acid, silica monolith	DMSO	100	3	MOF nanocrystals inside mesopores of silica monolith	Catalysis (Friedländer reaction)	372
UiO-66(NH_2)/ SBA-15	$ZrOCl_2 \cdot 8\,H_2O$, 2-aminoterephthalic acid, SBA-15	Water	–	–	MOF nanocrystals inside SBA-15 pores	Transformation of steroids	373

[a] HPLC is high-performance liquid chromatography. [b] Microwave heating for 30 min, a 300 W heater.

example, the UiO-66-NH_2/PMAA composite (PMAA is polymethacrylic acid) was obtained using simultaneously atom transfer radical polymerization, click chemistry and post-synthetic modification.[375] PMAA is often used as a coating for MOFs, since it contains a large number of functional groups, including alkynyl moieties, which are potentially able to react with the amino groups of UiO-66-NH_2, and a carboxylic acid groups for electrostatic interaction with the NH_2 function of enzymes.

Apart from conjugated organic polymers, covalent organic frameworks can also be used for coating and protection of MOFs; this gives rise to photoactive molecular blocks that can be used in biomedicine. Actually, MOFs can function as templates for the synthesis of COFs; strong interaction between MOFs and COFs results in the formation of core/shell nanocomposites. A photoactive porphyrin COF was grown epitaxially on the outer surface of UiO-NH_2 (UiO-66) by polymerization of terephthalaldehyde and porphyrin taken in various ratios.[376]

Composites in which a metal-organic framework is used as a shell on the crystal surface of another MOF showed improved properties (*e.g.*, higher porosity, surface area,

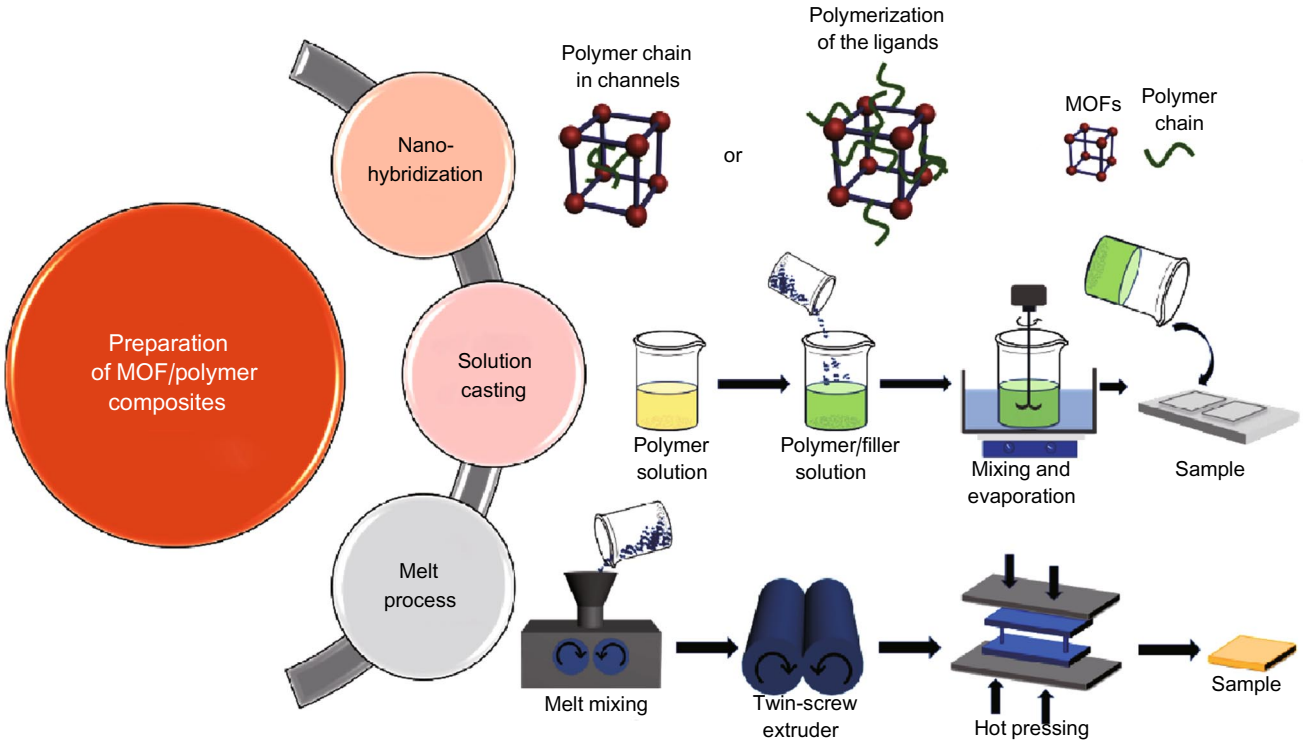


Figure 21. Possible methods for the preparation of MOF/polymer composites.[374] Encapsulation of polymer chains into regulated and adjustable nanochannels provides control over the polymer chain distribution. The main synthetic methods include polymerization in MOF channels and polymerization of MOF ligands. Solution casting is a widely used method for the fabrication of composites. As a rule, MOF particles are first dispersed in the solvent by stirring or sonication and then mixed with a polymer solution to prepare the final MOF/polymer solution. The melt compounding method is more suitable for commercial use, as it is versatile and environmentally benign. This method includes physical mixing of both thermoplastic and thermosetting polymers: MOFs are directly mixed with the melted polymer in a chamber, which is followed by physical mixing using a twin-screw extruder. The next stage is hot pressing to obtain required samples. Published in accordance with the Creative Commons Attribution license (CC BY 4.0).

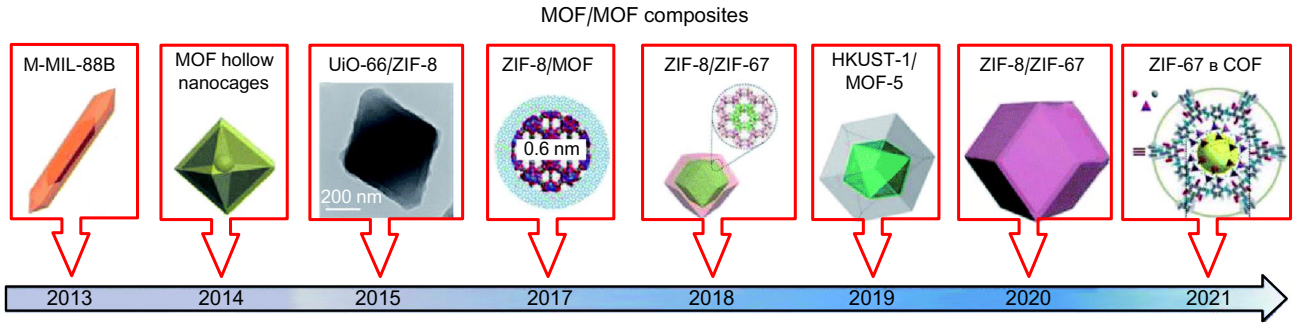


Figure 22. Key dates of significant publications on studying MOF/MOF composites.[377] Published with permission from the Royal Society of Chemistry.

crystallinity, mechanical strength and structural stability) that cannot be attained for a single MOF. The key dates for significant publications on MOF/MOF composites are depicted in Fig. 22.

A method for mixing of two different MOFs for the preparation of zirconium porphyrin framework with embedded Cu^{II}-MOF has been developed. The material designated as MOF-525(Cu) can serve as a host for sulfur in a lithium sulfur battery.[306] 3D MOF composites are usually fabricated by a layer-by-layer assembly method, which makes it possible to precisely control the thickness of MOF shell. For example, in core/shell 3D composites, the core surface can serve for the reaction, while the porous shell acts as the barrier layer that hampers surface activation towards aggregation with the neighbouring cores during the reaction. These types of composites are obtained by several methods and can have several structures such as core/shell, yolk/shell, *etc*. In Fig. 23, the MOF/MOF core/shell composite structure is depicted as a peach with an hierarchically ordered exocarp–mesocarp–endocarp system of layers.[378] These complex composites have shells of carboxylate MOFs based on low-valent metals, which are synthesized under mild conditions, and cores made of carboxylate MOFs based on high-valent metals, which are presynthesized under more drastic conditions. In addition, functional groups of both MOFs and their reactions play an important role in the formation of these structures.

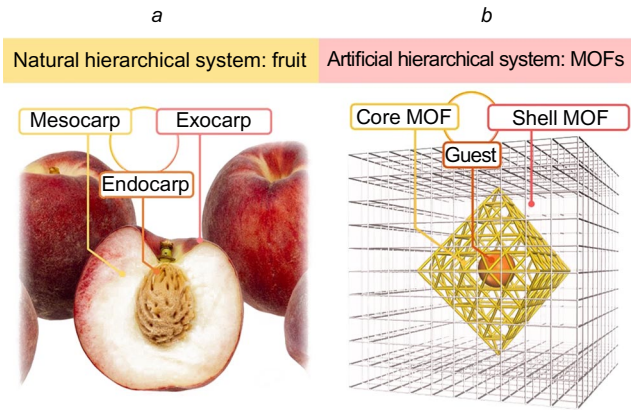


Figure 23. Examples of natural (*a*) and artificial (*b*) hierarchical systems. (*a*) peach structure with hierarchically ordered exocarp–mesocarp–endocarp system; (*b*) structure of MOF/MOF composite.[378] Published in accordance with the Creative Commons Attribution license (CC BY 4.0) (CC BY 4.0).

It should be emphasized that lattice parameters considerably affect the epitaxial growth of MOFs on different MOFs. For the formation of the MOF/MOF composite, the lattice mismatch should not exceed 15%.[95] When ZIF-8 precursors were added to ZIF-67, the epitaxial growth afforded the ZIF-67/ZIF-8 core/shell composite.[379] It is of interest that in the presence of methanol and Co^{2+} ions, a different type of coordination was implemented, which converted the core/shell structure of ZIF-67/ZIF-8 into a hollow rhombic dodecahedron, Zn/Co-ZIF. This crystal can encapsulate palladium NPs; the Pd/Zn/Co-ZIF yolk/shell composite was used as a heterogeneous catalyst for acetylene hydrogenation and was highly stable in the reaction medium. Lu *et al.*[380] reported the epitaxial growth of the Ni-MOF shell on the UiO-67 surface using PVP as a regulator.

The MOF plus ZIF strategy ensured a uniform growth of a ZIF-67 coating on MOF-74:[381] activated MOF-74 nanowires and 2MI powders were placed into a common system and treated at 120 °C at a reduced pressure, then 2MI was converted from the solid to gaseous state; and the gas-phase 2MI ligands reacted with MOF-74 to give a ZIF-67 shell *in situ*.

Examples of MOF composites with 3D materials are given in Table 4.

Table 4. Conditions of synthesis, morphology and applications of some composites of MOFs with 3D materials.

Composite	Reagents	Conditions of synthesis			Morphology	Application	Ref.
		medium	*T*, °C	τ, h			
			MOF composites with polymers				
UiO-66-NH_2/PMAA	UiO-66-NH_2, PMAA	Water	25	4	PMAA is attached to the MOF surface	Enzymatic activity	375
UiO-66-NH_2/ porous organic polymer	UiO-66-NH_2, monomer of the porous organic polymer	DMF	75	48	Porous organic polymer grown on the MOF surface	Generation of singlet oxygen $^1O_2$	376
NU-1000/poly-ethyleneimine	NU-1000, polyethylene-imine	Water (a cotton ball was treated with a mixture of MOFs and polyethyleneimine in water)		1/60	MOFs and polyethylene-imine are attached to a cotton ball	Catalysis (hydrolysis of dimethyl 4-nitro-phenylphosphate)	382
ZIF-8/polyimide	$Zn(NO_3)_2 \cdot 6H_2O$, 2MI, polyimide	Methanol	RT	24	MOFs is attached to polyimide fibres or membrane	Catalysis (Knövenagel condensation)	383
PDA/glucose oxidase/ZIF-8	$Zn(NO_3)_2 \cdot 6H_2O$, 2MI, glucose oxidase, dopamine	Water	RT	24	PDA and glucose oxidase are anchored to the MOF surface	Enzymatic activity	384
Polyvinylidene fluoride/HKUST-1	Polyvinylidene fluoride, HKUST-1	Acetone, DMF	–	1/2	Mixed-matrix membrane (includes polymer and MOFs)	Catalysis (Knövenagel condensation)	385
			MOF/MOF composites				
ZIF-67/ZIF-8	ZIF-67, 2MI, $Zn(NO_3)_2 \cdot 6H_2O$	Methanol	120	4	Core/shell	Catalysis (acetylene hydrogenation)	379
UiO-67/Ni-MOF	$NiCl_2 \cdot 6H_2O$, terephthalic acid, UiO-67	DMF, ethanol, water	RT	8	Core/shell	Catalysis (glucose oxidation)	380
HKUST-1/ZIF-8	HKUST-1, 2MI, $Zn(NO_3)_2 \cdot 6H_2O$	Methanol	RT	3	Core/shell	Precursor of nano-materials	386

Table 4 (continued).

Composite	Reagents	Conditions of synthesis			Morphology	Application	Ref.
		medium	T, °C	τ, h			
			POM/MOF composites				
PTA/MIL-101	$Cr(NO_3)_3 \cdot 9\,H_2O$, terephthalic acid, PTA	Water	210	2/3	MOFs with encapsulated PTA	Catalysis (styrene oxide ring opening)	313
PTA/HKUST-1 (c-NENU-3a)	$Cu(NO_3)_2 \cdot 3\,H_2O$, *p*-methylbenzoic acid, PTA	Ethanol	80	1.5	MOFs with encapsulated PTA	Production of biodiesel	315
Phosphomolybdic acid hydrate/HKUST-1 (c-NENU-5)	Trimesic acid, phosphomolybdic acid hydrate, $Cu(OAc)_2 \cdot H_2O$	Water, ethanol	RT	12	Phosphomolybdic acid is anchored to MOF surface	Biomass conversion	387
PTA/MIL-100(Cr)	PTA, trimesic acid, HF, CrO_3	Water	220	96	MOFs with encapsulated PTA	Conversion of cellobiose to sorbitol	388
$H_3PW_{12}O_{40}$/MFM-300(In) (MFM is Manchester framework material)	$In(NO_3)_3 \cdot 5\,H_2O$, diphenyl-3,3′,5,5′-tetracarboxylic acid, $H_3PW_{12}O_{40}$	See [a]	80	1/2	Core/shell	Decomposition of pharmaceutically active compounds	389

[a] Milling and hot pressing without a solvent.

6. Properties of composites of metal-organic frameworks

The main goal of the synthesis of MOF composites is to overcome the drawbacks of MOFs and provide for new functional properties of the obtained composites, including a change in the structure, template effects, *etc*.

An important drawback of MOFs is low stability; therefore, specialists should find reagents (precursors, solvents, redox agents) and conditions (temperature, pressure) for the composite synthesis that would preserve the initial metal-organic framework.[21,41] To minimize the risk of MOF degradation during the synthesis of the composite, functional materials should be thoroughly selected on the basis of published and/or experimental data on MOF stability, since this characteristics affects the subsequent applications of the composite. In addition, it is necessary to carry out various investigations (*e.g.*, powder X-ray diffraction) to confirm the presence of MOF after formation of the composite.

The metal nodes in MOFs are considered to be hydrophilic; they can easily react with water molecules.[390–394] Therefore, the crucial factor in the improvement of MOF water resistance *via* the integration with FMs is to prevent contacts between MOF and water molecules. For example, MOF-5/NH_2-GO composite was synthesized and tested for stability in a moist environment.[395] Due to the presence of polar functional groups on the surface, graphene oxide can be regarded as hydrophilic; however, it still contains distorted graphene-like layers with a relatively high level of aromaticity; therefore, it is more hydrophobic than pure MOFs and can repel water molecules.[396] In comparison with the X-ray diffraction patterns of MOF-5, those of the composites occurring in a moist environment did not markedly change with time, which was indicative of their higher water resistance in comparison with the starting materials.

Zu *et al.* [397] obtained the HKUST-1/graphite oxide composite and studied the modulation of the hydrophilicity/hydrophobicity of MOFs. The results showed that the adsorption capacity of MOFs towards polar solvent (water) clearly decreases, while that towards non-polar solvent (benzene) increases after incorporation of graphite oxide (Fig. 24). Hence, more hydrophobic medium surrounding the copper sites can be created owing to the presence of carbon-containing component, which may help to block the adsorption of water molecules in order to avoid their attack on the coordination bonds. This accounts for the increase in the hydrothermal stability of HKUST-1/graphite oxide composites.

Bian *et al.*[285] also obtained HKUST-1/GO composites by the interfacial growth induced by a Pickering emulsion. According to the special strategy of interfacial growth, GO nanosheets surrounded the surface of composites and functioned as sponges preventing water molecules from incorporation into the core, which markedly improved the surface water resistance and hydrothermal stability of the composites.

One more effective strategy for increasing water stability is to cover MOFs with carbon compounds, as they can prevent direct contact with water. This strategy can be

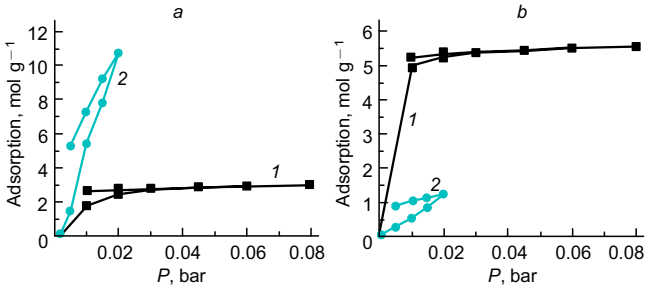


Figure 24. Adsorption–desorption isotherms of water vapour and benzene by HKUST-1 (*a*) and HKUST-1/GO composite (*b*):[397] (*1*) benzene, (*2*) water. Published in accordance with the Creative Commons Attribution license (CC BY 4.0).

implemented *via* controlled carbonization under an inert gas. Lately, this approach has become popular for the design of carbon materials with a hierarchical pore structure using MOFs as precursors.[398, 399] The carbonization develops gradually from the surface of the crystal towards the core; therefore, by controlling the time and temperature of carbonization, it is possible to fabricate MOF/carbon composites with the required thickness and structure of carbon shells. Using carbonization, MOF-5 with an amorphous carbon coating was obtained;[400] this material showed an exceptional stability under wet conditions and could even retain the intact crystal structure after being kept in water for two hours.[398] An increase in the MOF stability with respect to water (steam) after formation of a composite was also reported by other authors.[242, 401]

Apart from low water stability, one more drawback hampering the practical application of MOFs is low thermal stability (see above). Composites that integrate MOFs and FMs have an enhanced thermal stability compared to the starting components. For example, interpenetrating MOF-5/MWCNT composite with micro(meso)pores, which was obtained by one-pot synthesis, showed higher water resistance and thermal stability than the constituents.[242] The thermal stability of MIL-101 considerably increased after incorporation of MWCNTs.[225] Analogous results were obtained in other studies.[234, 240] The USTA-16/GO composite with a core/shell structure has higher decomposition and collapse temperatures than the components.[402] The increase in the thermal stability is due to strong interactions between MOF and GO, increase in the thermal conductivity after addition of graphene oxide, restricted movement of elements of the crystal structure and a decrease in the input of thermal energy due to the GO film. The MOF-2/CNF also demonstrated enhanced thermal stability.[280]

It is noteworthy that after integration with FMs, the MOF structure can be stable to electron beam irradiation, since FMs can efficiently scatter electrostatic charges, thus protecting the structure.[3, 144, 155, 403] For example, the MOF-5/MWCNT composite was obtained, for which a high-resolution image of the MOF-5 crystals was recorded even under electron-beam irradiation or in the presence of atmospheric moisture.[54] The structural stability was attributed to the ability of incorporated MWCNTs to scatter electrostatic charges accumulated upon the electron beam dosing. Similar effects were observed[255, 404] for the MOF-5/MWCNT composites and nano-sized HKUST-1/GO.

The combination of MOFs and FMs may increase the mechanical strength of the composite. After incorporation of MWCNTs into MOF-5, the porosity of MOF can be retained upon mechanical treatment (polishing, shaping or other sample preparation procedures). Xin *et al.*[405] reported that the composite based on platinum-loaded MWCNTs and MOF-5 showed a sharp (2.3-fold) increase in the hydrogen storage capacity compared to that for Pt/MWCNTs. However, the authors did not explain why the porosity of MOF was retained during mechanical processes after integration with platinum-loaded MWCNTs.

Apart from the given examples of increasing MOF stability, mention should be made of a ZIF-8-based membrane with a high resistance to high pressure, which was made of porous CNT paper by secondary growth.[237] Experiments confirmed that this membrane can retain robust structure and excellent hydrothermal stability at pressures of up to 500 kPa; this opens up prospects for using the membrane in gas adsorption and separation.

Actually, the integration of MOFs with FMs may improve simultaneously their stability characteristics.[54, 237, 242, 252, 404, 405] This would markedly expand the scope of industrial applications of MOF composites.

The barrier properties of organic ligands and overlap of the p- and d-orbitals of central metal ions make MOFs poor conductors; [406] therefore, they cannot be used in the fields related to electricity.[407] However, this situation can change upon the introduction of conductive FMs, as they can generate new paths for electric charge transfer in the composite and thus increase the conductivity.[406, 408] In particular, it was shown[409] that in the composite of MOF-5 with benzoic acid-functionalized graphene, FM servers as both a structure-directing template and the framework linker during the assembly of MOFs. The main issue is that the insertion of graphene changes the insulating character of MOF-5 and increases its conductivity, which provides for the potential use of this composite in the CO_2 and N_2 gas separation sensors.

A graphene/metal porphyrin MOF composite with various amounts of pyridine-functionalized dye loaded in RGO sheets was obtained.[294] The modified RGO acted as a building block in the synthesis of MOFs and a reinforcing filler; this increased the charge transfer rate and opened up paths for the four-electron oxygen reduction reaction. It was found that the dielectric constant of the IRMOF-8/AC composite gradually increases with increasing carbon concentration.[410] As the carbon content was increased from 17.77 to 22.2 mass %, the composite turned from an insulator into a conductor.[397] Similar changes took place in Ni-MOF-5/RGO and HKUST-1/graphene.[411, 412]

A comparison of the electrical conductivity of HKUST-1 and nano-CuS/HKUST-1 showed that the initial MOF had a considerably lower specific conductivity (1.6×10^{-9} S cm^{-1}) than the composite (4.7×10^{-8}–1.8 S cm^{-1}). In view of the importance of the conductivity (apart from maintaining the porosity), the optimal content of nano-CuS (28 mass %) for applicaqtion of the composite as a catalyst in the electrocatalytic oxygen reduction was determined.[273]

An improvement of the electrochemical characteristics of MOFs upon the formation of composites with 2D materials such as RGO was established; this may be due to the synergistic effect of functional MOFs with a high theoretical capacity and highly conductive RGO.[413, 414]

While using MOFs as adsorbents, one should bear in mind that their enormous internal space is often not completely used because in their pore structure, weak dispersion interactions are generated to retain small adsorbate molecule.[413, 415, 416] The integration of MOFs and FMs may considerably enhance these dispersion interactions. Often, MOF composites are manufactured using materials such as graphene and GO (see above), which have numerous oxygenated (hydroxyl, carbonyl and epoxide) groups on the basal planes of the carbon sheets and have carboxyl groups at the periphery. These functional groups provide additional forces of attraction to adsorbate molecules. Hence, functional materials that can serve as fillers, building blocks, templates, *etc.*, when present in appropriate amounts, promote crystallization of MOFs by functioning as nucleation centres; they also affect the coordination number of inorganic nodes (metal ions) of the framework; increase dispersion forces; and give rise to additional

adsorption sites by forming new pores at the interface between MOF and FM.[393, 416–418] These factors are favourable for the physical adsorption of small molecules (such as ammonia and hydrogen).[393, 416–419]

7. Template effects in the composites of metal-organic frameworks

The template effects that arise upon the incorporation of FMs into MOFs open up attractive functional opportunities. In the synthesis of composites, FMs can act as structure-directing, crystal size-controlling and reaction-accelerating agents. In order to obtain MOF crystals of various size and morphology and to reduce the time of composite synthesis, various amounts of diverse FMs are used. Template effects are of considerable interest, since they can significantly affect the properties and subsequent applications of MOFs,[420, 421] while reduction of the time of composite synthesis decreases the cost of their subsequent processing to advanced materials. Thus, varying MOF properties may constitute an effective strategy for the development of new MOFs or their composites tailored to solve specific problems.[422]

One of the consequences of the template effect is a change in the morphology of initial MOF. For example, the $CoFe_2O_4/TiO_2$/HKUST-1 composite had a polyhedral morphology, which differed from the rod-like morphology of initial HKUST-1.[423] The average particle size in this composite was 30 ± 2 nm.

Cha *et al.*[424] reported *in situ* synthesis of fully inorganic perovskite $CsPbX_3$ (X = I, Br, Cl) inside a MIL-101 crystal at room temperature (Fig. 25). The unusually bright contrast observed in the HAADF-STEM image (HAADF-STEM is high-angle annular dark-field scanning transmission electron microscopy) was attributed to the $CsPbI_3$ quantum dots located in the mesoporous cages of MIL-101. According to the authors, MIL-101 not only functioned as a nanoreactor for the formation of uniform perovskite QDs, but also increased their stability.

An interesting half core/shell structure was found for the g-C_3N_4/Fe_3O_4/ZIF-8 composite.[425] In comparison with the particles of the initial ZIF-8, which had a dodecahedral crystal structure and a ~350 nm particle size, the ZIF-8 nanoparticles in the composite had relatively smooth edges and a smaller size (~140 nm), which may be due to the effect of g-C_3N_4 nanosheets, which restricted their growth. It should be noted that Fe_3O_4 nanoparticles cannot be seen in the TEM images, which confirms incorporation of Fe_3O_4 into ZIF-8 and the half core/shell structure of the composite.

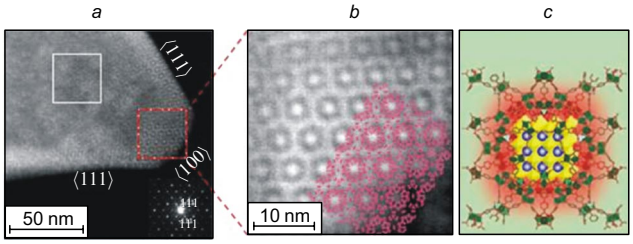


Figure 25. HAADF-STEM images at different magnifications (*a*, *b*) and structure of the MIL-101 crystal with embedded perovskite $CsPbX_3$ QDs (*c*).[424] The insets in Fig. *a* show the areas of $CsPbX_3$/MIL-101 chosen for HAADF-STEM examination. Figure *b* shows the image of MIL-101 model overlapped along the [110] direction. The dark green colour in Fig. *c* designates chromium atoms; yellow colour shows the pore space inside MOFs, light green are benzene rings of the ligands, violet shows cerium atoms; the pink colour symbolizes bright photoluminescence of QDs. Published with permission from the American Chemical Society.

Huo *et al.*[426] demonstrated that the Fe_3O_4 morphology is formed by aggregations of irregularly shaped NPs of various sizes, while the ZIF-8 crystals are regularly shaped rhombic dodecahedra of equal size. However, the morphology of the Fe_3O_4/ZIF-8 composite differs from those of both Fe_3O_4 and ZIF-8. The composite has a unique architecture in which NPs are embedded in irregular polyhedra. In turn, the mere appearance of this structure, probably caused by steric hindrance and interpenetration of different crystals during the growth, confirms the possibility of one-pot preparation of MOF composite.

Prasanth *et al.*[427] reported the MIL-101/SWCNT composite with a clear-cut change in the morphology. Layers of the MIL-101 composite with a cubic structure, arising due to the growth of this MOF on the functionalized surface of SWCNTs, are clearly detectable in the TEM image (Fig. 26).

The MOF-5/GO composite has a sandwich-like structure with alternating MOF layers and GO sheets at appropriate GO contents. This interesting effect was explained [399] by the fact that the assembly was based on the attachment of MOF blocks to the graphene layer *via* chemical bonds between the MOF metal sites and epoxide groups in the basal planes of GO. However, since the affinity of ZnO_4 tetrahedra to carboxyl groups (mainly at GO edges) is higher than the affinity to epoxide groups, and at high GO loadings, more carboxyl groups are added, the preferable reactions at the ends of GO form a worm-like structure.

The HKUST-1 composites with aminated (urea-modified) GO was found to have a loose lace pattern of the surface (unlike the smooth surface of primary MOFs), the appearance of which was attributed to the amino groups at the edges of graphene sheets.[428] The carboxyl groups were also involved in MOF crystallization; however, their influ-

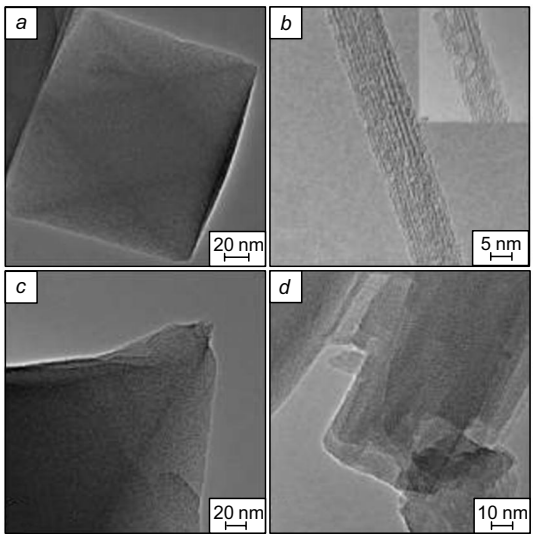


Figure 26. TEM images of MIL-101 (*a*), SWCNTs (*b*), MIL-101/8 mass % SWCNTs (*c*) and MIL-101/10 mass % SWCNTs (*d*).[427] Published with permission from Elsevier.

ence was minor compared to that of the amino groups. Diazonium grafting was used [409] for a threefold increase in the number of carboxyl groups in the basal planes of RGO and the subsequent preparation of the MOF-5/graphene composite functionalized with benzoic acid. When the content of functionalized graphene was 1 mass %, the composite had a sandwich structure similar to the structure of MOF-5/GO containing 5 mass % GO.[365] When the amount of functionalized graphene was increased to 5 mass %, the composite showed a nanowire morphology: the MOF-5 nanowire grew along the [220] direction, and its diameter equal to ~300 nm was close to the lateral size of functionalized graphene.[408]

Jin *et al.*[294] obtained a composite from Fe-containing MOF based on 5,10,15,20-tetrakis(4-carboxyphenyl)-21*H*,23*H*-porphyrin with RGO functionalized with a 4-styrylpyridine-based dye. Upon the addition of 5–10 mass % of the dye, the shape of composite crystals gradually changed from plates (initial Fe-MOF) to rods, and the MOF lattice was distorted. As the amount of the dye increased to 50 mass %, the resulting composite was amorphous.

The morphology of La-MOF nanocrystals changed upon the formation of composites with GO quantum dots: when the QD content was below 5 mass %, the La-MOF crystals were shaped like spindly rectangular rods, which became shorter with increasing amount of GO; further increase in the GO content (> 5 mass %) resulted in conversion of the crystals into irregular large-size thick blocks.[290] The hypothetical mechanism of formation of La-MOF/GO composites is shown in Fig. 27. In the initial La-MOF crystals, the La^{3+} ions are coordinated by six water molecules and three oxygen atoms of carboxyl groups of the organic linkers. The spindly rectangular structure of La-MOF is due to stretching of the parallel ribbon-like molecular layers along one axis and their stacking through phenyl groups of the organic linkers along the other axis. Initially, La^{3+} ions were bound to the functional groups of GO (for example, carboxyl, hydroxyl or epoxy groups); therefore, the introduction of GO decreased the number of free La^{3+} ions, which formed the extending MOF crystals.[281] When the content of GO was relatively high, the number of oxygen-containing groups increased, and stacking and extension of MOFs were significantly restricted because of the lack of free La^{3+} ions and the effects caused by the formed GO–La complexes. Simultaneously, MOF crystals were formed between the GO–La layers, and the morphology gradually changed from thin rectangular La-MOF rods towards composite blocks of an irregular shape.

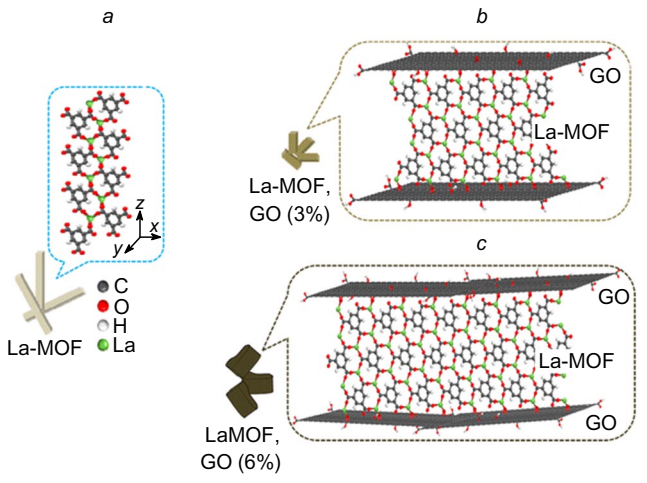


Figure 27. Mechanism of formation of La-MOFs (*a*) and La-MOFs/GO composites with GO contents below (*b*) and above 5% (*c*). The six water molecules coordinated to La^{3+} cations are omitted.[290] Published with permission from the American Chemical Society.

It should be noted that the content of FMs is significant for the formation of morphology and structure of the resulting composites. When present in low amounts, FMs can act as efficient nucleation centres and/or auxiliary materials, change the coordination chemistry of MOFs and improve the existing or bring about new functional properties (such as stability, electrical conductivity and emergence of non-specific dispersion forces). Thus, the synergism of the two components has a beneficial effect on the subsequent use of the composites. However, when the FM content is too high, the number of functional groups on the surface considerably increases, and the number of accessible MOF sites becomes too low to interact with these groups.[125] Hence, a part of FMs remains as agglomerates and can even play a role of physical barriers that prevent crystallization; this would lead to MOF distortion (or even destruction).[260, 387, 428, 429]

For the formation of composites, it is necessary to control the amount of FMs that would define their location (distribution) relative to MOFs and the exact composition (identity and purity), structure (crystalline or amorphous) or morphology of the composite.[21, 41, 430] There are two main problems related to the control of location (distribution) of FMs: it is necessary to attain a uniform distribution of FMs and ensure that they can be located only inside MOFs, but should not be attached to the surface. Chemical grafting of FMs (or FM precursors) can efficiently solve the distribution problem; however, this strategy is applicable only to MOFs with additional functions.

In many cases, apart from the change in the morphology, the size of the composite crystal becomes smaller than the crystal size of the initial MOFs, since the introduction of FMs prevents MOF crystallization.[293] Upon the introduction of FMs, metal ions first bind to functional groups on the FM surface, which reduces the number of free metal ions and gives rise to additional extended MOF crystals. In addition, FMs act as termination agents, in particular, they cleave the bonds between isolated small MOF particles and prevent their growth to form large crystals. Therefore, the crystal size in the composite is usually smaller than the crystal size of initial MOFs. Yang *et al.*[242] showed that high content of CNTs leads to larger numbers of ZIF-8 growth centres on their surface (Fig. 28); this leads to a decrease in the size of MOF crystals from 25–35 to 15–25 nm.

The incorporation of graphene QDs into ZIF-8 changed both the crystal shape (from rhombic dodecahedron inherent in the initial MOF to sphere for the composite) and size (decreased from 70–80 nm characteristic of the initial ZIF-8 to 25–30 and 36 nm in the composite containing 1.2 and 0.4 mass % QDs, respectively).[431] The crystal size and morphology of MOFs and composites vary depending on the conditions of synthesis and the nature of FMs.[251] For example, the initially hexagonal shape of ZIF-8 crystal of 100–150 nm size gradually changed to uniform nanospheres of ~4 nm diameter for the 20 mass % GO/ZIF-8 composite.[251] The ~10 μm crystal size of the initial

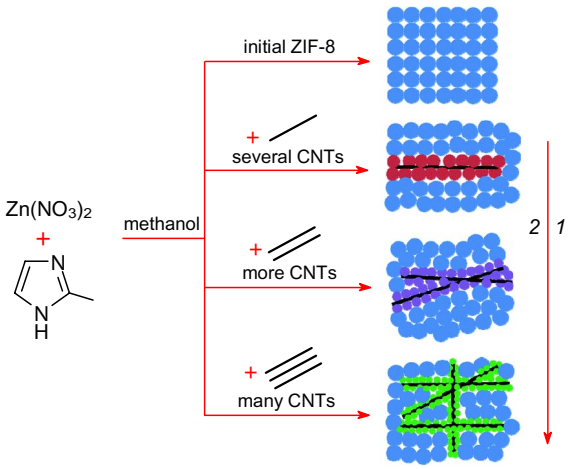


Figure 28. Decrease in the ZIF-8 crystal size with increasing the amount of CNTs. (*1*) decrease in the crystal size on the CNT surface, (*2*) increase in the number of ZIF-8 nucleation centres.[242] Published with permission from the Royal Society of Chemistry.

HKUST-1 was shown[252] to decrease to 10–40 nm for 9 mass % GO/HKUST-1 composite.

Also, metal-organic framework structure can be embedded *in situ* into FM pores, which accounts for smaller size MOFs in comparison with the large initial MOFs.[261, 262, 404, 432] In this case, the carbon skeleton of FMs actually acts as an agent restricting the growth of MOF crystals; the crystallite size of the obtained composites is in good agreement with the size of the carbon-containing matrix.[262, 408]

Quite a few procedures have been developed to accelerate the synthesis of MOFs, including microwave and sonochemical synthesis and so on.[26, 123, 433–435] The rate of crystallization of MOFs can be considerably increased using functionalized self-assembled monolayers[436, 437] or by introduction of GO into the system during MOF synthesis.[438] The introduction of GO reduces the time of crystallization since MOF cores are linked to GO sheets, which promotes faster crystallization. This effect was attributed to chemical affinity between MOFs and GO, since the functional groups present in GO can coordinate the metal sites of MOFs, thus accelerating the synthesis.

The POM/HKUST-1 composite can considerably improve the kinetics of synthesis. In aqueous solutions, Cu^{2+} cations are complexed with POMs. The copper cations are arranged around the POM structure, so that binding *via* benzenetricarboxylate groups gives rise to the HKUST-1 structure. This is a unique example in which the template mechanism based on a certain correspondence at the molecular level and resulting in the formation of nanosized building blocks can be observed *in situ* during the formation of a synthetic nanoporous material. The interaction between two materials even reduces the energy requirements of the process, which is indicated by the fact that the synthesis at room temperature is accomplished over a short period of time.[312, 439, 440]

Apart from the incorporated amount of FMs, other factors such as geometry of MOF particles, the chemistry of FM surface and even the size of GO flakes considerably influence the template effects and the properties of the resulting composites. Indeed, not any MOF is suitable for the fabrication of composites. Since composites are formed *via* binding of accessible active sites on GO and MOFs, the specific geometry of MOF particles can affect the synthesis.[120] The cubic unit cells of MOF-5 and HKUST-1 are suitable for the attachment of GO layers to the metal coordination nodes of MOFs along the parallel and/or perpendicular directions, which in turn facilitates the subsequent growth of MOFs (Fig. 29).[416] In the case of MIL-100(Fe) with an octahedral morphology, the nucleation of crystals develops along several directions, while the usual crystallization of MOF is retarded. Therefore, MIL-100(Fe) cannot be considered to be a perfect candidate for the fabrication of MOF/GO composites.

The surface chemistry of FMs (in particular, the number of functional groups) is also important for varying the structure and properties of the composite. The MOF-818/CNF composites were obtained by *in situ* synthesis.[261] Using ultrasonic treatment, it was possible to inject the precursor solution into the inner cavity of CNFs; therefore, the growth of nanosized particles of MOFs is restricted by the inner diameter of CNFs. The initial CNF sample was activated with hydrogen peroxide, which thus gave functionalized CNFs with a large number of functional groups on the external surface. It is important that using the same method of synthesis, uniform MOF distribution on the external walls of nanofibres and MOF laying in the cavities of functionalized nanofibres were observed. In addition, the introduction of functionalized CNFs also played a structure directing role, resulting in the synthesis of MOF-2 instead of predicted MOF-5.

Gardian *et al.*[439] showed that in the absence of functional groups, only physical mixtures of HKUST-1 and graphite can be formed, whereas the incorporation of GO leads to the formation of highly ordered HKUST-1/GO composites. This is due to the fact that the amount of oxygenated groups on a typical GO is $\sim$2.5 mmol g^{-1}, while that on graphite is $<$0.2 mmol g^{-1}; therefore, the limited reactions between MOFs and graphite do not finally give a composite.[416]

A specific feature of the surface chemistry of GO is related to the presence of various types of oxygenated groups, most often epoxy and carboxyl groups. According

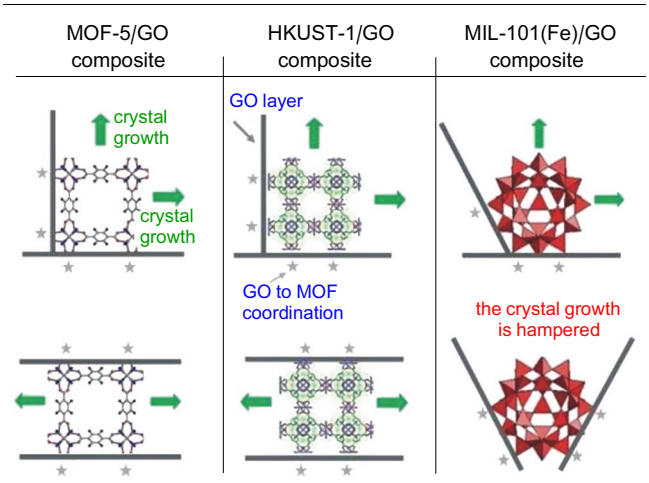


Figure 29. Coordination between the carbon layers of GO and MOF blocks for MOF-5, HKUST-1 and MIL-100(Fe). For MIL-100(Fe), red pyramids designate the supertetrahedral structures obtained from trimers of iron octahedra linked by ligand molecules.[416] Published with permission from Elsevier.

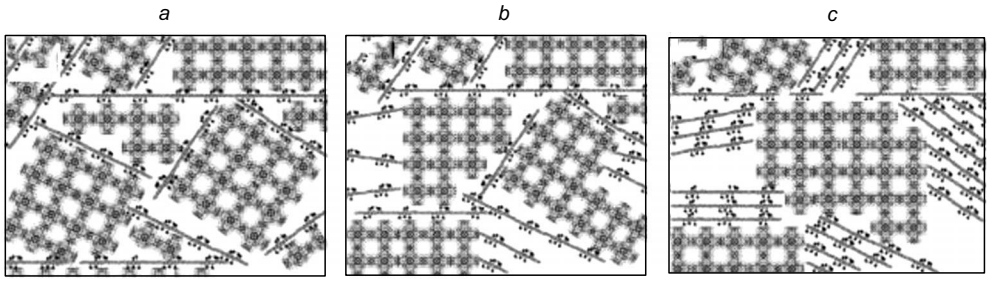


Figure 30. Structure of the HKUST-1/GO composite with low (*a*), medium (*b*) and high (*c*) contents of GO.[86] Continuous lines designate GO, and lattices correspond to HRUST-1. Published with permission from Royal Society of Chemistry.

to the Lerf–Klinowski model, carboxyl groups are mainly located along the edges, while epoxy groups are in the basal planes of GO.[441] Both types of groups are involved in interactions with metal sites and act as nucleation centres for the growth of MOFs. The use of GO obtained by the Hummers method resulted in a higher porosity of HKUST-1/GO, than the use of GO obtained by the Brodie's method.[413, 442] Most MOF crystals were located at the edges of GO surface. Saad *et al.*[409] observed the structure-directing effect upon increase in the number of carboxyl groups on the GO surface. This effect induced the formation of nanowires consisting of MOF-5 and boric acid-modified GO. When GO was modified by other specific groups, the formation of composites with new functional properties was possible.[294, 443–445]

It was found that the size of GO flakes affects the structure of the resulting MOF/GO composites. Composites are predominantly formed with GO flakes the size of which is close to or smaller than the MOF crystal size.[410, 440, 442]

Porosity is a key characteristic of MOFs, which determines the possibility of their application for gas storage, separation of gas mixtures, catalysis, *etc*. As a rule, small pore size is favourable for gas storage even at room temperature [413, 446] and (with allowance for the shape effect) it is also favourable for catalysis.[447, 448] Indeed, when the amount of FMs is low, new pores in composites are formed mainly at the interface between FM and MOF, where some of the primary nucleation centres (namely, FM functional groups) are located. At high contents of FMs, additional pores may appear, because the number of functional groups exceeds the number of accessible sites of MOFs they can react with, while remaining in the FMs (Fig. 30).[86] Apparently, the decrease in pore size of MOFs is caused by their partial filling, since well-dispersed FMs in composites can occupy some of the space and block some of the pore channels.

Quite a few publications, especially those addressing gas adsorption, report the formation of new pores and decrease in the pore size after the integration of MOFs and FMs, while the increase in gas storage capacity is attributed to extension of the functional properties of composites.[54, 429, 445, 449–451] The MOF-5/CNT composite had a stable network structure of pores, which was retained after removal of the solvent (DMF, diethylformamide or chloroform).[54] Additional ultramicropores of 0.4–0.7 nm in diameter appeared at the interface between MOFs and FMs where heteronucleation takes place. This increased the volume of micropores (< 1 nm) in the composite by ~150% and increased the specific surface area by ~65% compared with that in the primary MOFs. The increase in the micropore volume and the corresponding small pore size (1 nm or less) are favourable for high uptake of hydrogen.[452–454] A 50% increase in the hydrogen storage capacity was attained (from 1.2 to 1.52 mass % at 77 K and 1 bar and from 0.3 to 0.61 mass % at 298 K and 95 bar).[54]

Sohrabi *et al.*[234] synthesized the MIL-101/SWCNT composite with decreased pore size, increased volume of micropores and additionally formed ultramicropores (6.7 Å). These properties significantly increased the storage capacity of hydrogen at temperatures of 77 and 298 K and pressures up to 60 bar.[182] In the synthesis of MIL-101/AC composites, large particles of activated carbon were crushed into smaller particles, which occupied a part of MOF micro- and mesopores (cavities); therefore, the formation of additional micropores (0.45–0.61 nm), increase in the total volume of pores and decrease in the pore size were observed.[450]

Unsaturated metal sites inside MOFs can react with gas molecules; therefore, gas adsorption capacity may markedly increase.[455, 456] Nevertheless, in the original MOFs (before the formation of composites), these vacant Lewis metal sites are easily poisoned *via* coordination of excess organic linkers located in the pores. Apart from the decrease in the pore size, one more result of incorporation of FMs is protection of the unsaturated metal sites by blocking the channels (steric hindrance effect) and/or competing occupation of these sites. This mitigates poisoning of unsaturated metal sites and makes them accessible for better interaction with adsorbate molecules.[449] For example, this promoted the adsorption uptake of CO_2 by the MIL-101/CMK-3 composite (CMK-3 is mesoporous carbon) and increased the hydrogen storage capacity of MIL-101/AC and MIL-101/Li-AC.[449, 457]

However, the incorporation level of functional materials must be controlled, since in the excess of FMs, surplus functional groups can react with most unsaturated metal centres and thus reduce the number of active sites for binding to adsorbate molecules, which will eventually lead to relatively low gas adsorption.[442]

Thus, by integration of MOFs with FMs, it is possible to considerably increase the stability and electrical conductivity of initial MOFs. Furthermore, the introduction of FMs ensures a required relationship between the high porosity and weak dispersion forces. Metal-organic frameworks are usually obtained as powders, and MOF composites can be designed as hierarchically structured materials (*e,g*., membrane composites, MOF/COF, MOF/hierarchical porous carbon monoliths),[269, 356, 404, 455–461] which are more easily treated and processed.

8. Conclusion

Composites of metal-organic frameworks represent a new class of materials that are obtained and analyzed using the full potential of modern science. According to published sources considered in this review, the current stage of

research into MOF composites is characterized by accumulation of experimental facts and their theoretical interpretation and generalization. Composites of MOFs demonstrated a great potential as promising materials owing to their unique optical, electrochemical, magnetic and other properties. The formation of composites is a way to extend the scope of applications of MOFs from scavenging of organic pollutants,[462–466] detection and separation of gases[467–469] and catalysis[115,470,471] to the design of new innovative materials for supercapacitors,[79,472–474] targeted drug delivery,[475] fuel cells,[452,476,477] *etc*.

The authors view on the progress in the research into MOFs and composites based on them is stated below.

First of all, note that the range of MOFs used for this purpose is rather broad and is not limited to the examples described here. A great choice of MOFs with a broad inventory of synthetic strategies for their preparation, simplicity of many approaches, scalability and appropriate cost-to-quality ratio provide the methodological platform for the design of promising MOF composites. It is important to develop composites in which the framework structures include unusual heteroatoms, such as selenium and tellurium. Over the last decade, several new approaches to the fabrication of these composites have been proposed. It can be expected that their development would be continued at a higher level. There are numerous methods for the preparation of composites of MOFs: encapsulation, impregnation, infiltration, grinding in the solid state, co-precipitation, *etc*. The use of different methods may result in different properties of the MOF composites; hence, new applications are expected to appear.

All synthetic approaches and strategies have great potential for the research carried out in various fields related to the production of composites of MOFs and functional materials. In the synthesis of composites, it is especially difficult to exactly control the size and position of functional materials relative to MOFs. Most of synthetic methods include several stages and have some limitations; furthermore, they imply the use of expensive organic solvents. Hence, the development of new synthetic approaches free from the listed drawbacks is a relevant task.

Despite the huge potential of MOF composites, their commercialization cannot be called successful. Therefore, it would be pertinent to obtain composites based on commercially available MOFs.

In this review, MOF composites are classified in terms of the dimensionality of the used functional materials. The composite properties and template effects are considered. By combining MOFs with appropriate 0D, 1D, 2D or 3D materials, it is possible not only to facilitate the synthesis, but also to improve functionality, porosity and thermal, magnetic and electrical properties of composites, according to particular requirements.[478,479] Most of the composites described in the review are combinations of MOFs and separate functional materials. Also, it is of considerable interest to combine several materials with MOFs (or even to combine MOFs with other MOFs).

Among the challenges that should be overcome in order to start efficient engineering development of MOF composites, worthy of note is the development of a standard protocol for their characterization: each sample is tested in a different way; therefore, it is difficult to compare the types of MOF composites.

Computer simulation is becoming an indispensable tool for the development and application of MOFs owing to fast computations using modern computers, which rapidly provide new results.[480] Currently, the simulation mainly concerns the adsorption of gases such as methane, hydrogen and acetylene in pristine MOFs. In view of the rapid development of studies on the fabrication of MOF composites for the storage and separation of molecules, more attention should be paid to simulation in order to guide the design and optimize the properties of composite materials.

Thus, despite the fact that the studies of composites of metal-organic frameworks started not long ago, this promising class of compounds has already found application in various fields. It is evident that the number of new MOF composites would increase from year to year and new applications would appear.

This study was prepared with the financial support of the Russian Science Foundation (Project No. 22-13-00260).

9. List of abbreviations and symbols

AC — activated carbon,
ADF-STEM — annular dark-field scanning transmission electron microscopy,
CNF — carbon nanofibre,
CNT — carbon nanotube,
COF — covalent organic frameworks,
CoP — cobalt(II) 5,10,15,20-tetraethynylporphyrin,
FMs — functional materials,
FCNF — functionalized carbon nanofibre,
FTO — fluorine-doped tin oxide,
g-C_3N_4 — graphitic carbon nitride,
GO — graphene oxide,
HAADF-STEM — high-angle annular dark-field scanning transmission electron microscopy,
HER — hydrogen evolution reaction,
HKUST — Hong Kong University of Science and Technology,
HPLC — high-performance liquid chromatography,
2MI — 2-methylimidazole,
MAA — mercaptoacetic acid,
MFM — Manchester Framework Material,
MMM — mixed matrix membrane,
MIL — Materials Institute Lavoisier,
MOF — metal-organic framework,
MXene — two-dimensional inorganic compounds,
MWCNTs — multiwalled carbon nanotubes,
NENU — Northeast Normal University,
NU — Northwestern University,
NPs — nanoparticles,
NRs — nanorods,
NWs — nanowires,
OER — oxygen evolution reaction,
ORR — oxygen reduction reaction,
PANI — polyaniline,
PCN — porous coordination network,
PDA — polydopamine,
PDMS — polydimethylsiloxane,
PEDOT — poly(3,4-ethylenedioxythiophene),
PMAA — polymethacrylic acid,
POM — polyoxometalate,
PTA — phosphotungstic acid,
PVP — polyvinylpyrrolidone,
PXRD — powder X-ray diffraction,
QDs — quantum dots,
RGO — reduced graphene oxide,

RT — room temperature,
SEM — scanning electron microscopy,
SWCNTs — single-walled carbon nanotubes,
TEM — transmission electron microscopy,
TEOS — tetraethoxysilane,
TMU — Tarbiat Modares University,
UiO — Universiteteti Oslo,
UTSA — University of Texas at San Antonio,
VA CNTs — vertically aligned carbon nanotubes,
ZIF — Zeolitic Imidazolate Frameworks.

References

1. G.I.Dzhardimalieva, I.E.Uflyand. In *Chemistry of Polymeric Metal Chelates*. (Cham: Springer, 2018). P. 633
2. G.I.Dzhardimalieva, I.E.Uflyand. *RSC Adv.*, **7**, 42242 (2017)
3. V.V.Butova, M.A.Soldatov, A.A.Guda, K.A.Lomachenko, C.Lamberti. *Russ. Chem. Rev.*, **85**, 280 (2016)
4. A.Yu.Tsivadze, M.K.Knyazeva, O.V.Solovtsova, I.E.Men'shchikov, A.A.Fomkin, A.V.Shkolin, E.V.Khozina, V.A.Grachev, O.E.Aksyutin, A.G.Ishkov. *Russ. Chem. Rev.*, **88**, 925 (2019)
5. V.V.Arslanov, M.A.Kalinina, E.V.Ermakova, O.A.Raitman, Yu.G.Gorbunova, O.E.Aksyutin, A.G.Ishkov, V.A.Grachev, A.Yu.Tsivadze. *Russ. Chem. Rev.*, **88**, 775 (2019)
6. D.N.Dybtsev, D.G.Samsonenko, V.P.Fedin. *Russ. J. Coord. Chem.*, **42**, 557 (2016)
7. V.I.Isaeva, L.M.Kustov. *Petrol. Chem.*, **50**, 167 (2010)
8. L.M.Kustov. *Russ. J. Phys. Chem. A*, **89**, 2006 (2015)
9. I.S.Antipin, M.V.Alfimov, V.V.Arslanov, V.A.Burilov, S.Z.Vatsadze, Ya.Z.Voloshin, K.P.Volcho, V.V.Gorbatchuk, Yu.G.Gorbunova, S.P.Gromov, S.V.Dudkin, S.Yu.Zaitsev, L.Ya.Zakharova, M.A.Ziganshin, A.V.Zolotukhina, M.A.Kalinina, E.A.Karakhanov, R.R.Kashapov, O.I.Koifman, A.I.Konovalov, V.S.Korenev, A.L.Maksimov, N.Zh.Mamardashvili, G.M.Mamardashvili, A.G.Martynov, A.R.Mustafina, R.I.Nugmanov, A.S.Ovsyannikov, P.L.Padnya, A.S.Potapov, S.L.Selektor, M.N.Sokolov, S.E.Solovieva, I.I.Stoikov, P.A.Stuzhin, E.V.Suslov, E.N.Ushakov, V.P.Fedin, S.V.Fedorenko, O.A.Fedorova, Yu.V.Fedorov, S.N.Chvalun, A.Yu.Tsivadze, S.N.Shtykov, D.N.Shurpik, M.A.Shcherbina, L.S.Yakimova. *Russ. Chem. Rev.*, **90**, 895 (2021)
10. A.A.Pribylov, K.O.Murdmaa. *Russ. Chem. Bull., Int Ed.*, **71**, 240 (2022)
11. M.N.Timofeeva, I.A.Lukoyanov, V.N.Panchenko, S.H.Jhung. *Russ. Chem. Bull., Int. Ed.*, **71**, 599 (2022)
12. E.V.Alexandrov, A.P.Shevchenko, N.A.Nekrasova, V.A.Blatov. *Russ. Chem. Rev.*, **91**, RCR5032 (2022)
13. Yu.G.Gorbunova, Yu.Yu.Enakieva, M.V.Volostnykh, A.A.Sinelshchikova, I.A.Abdulaeva, K.P.Birin, A.Yu.Tsivadze. *Russ. Chem. Rev.*, **91**, RCR5038 (2022)
14. K.A.Kovalenko, A.S.Potapov, V.P.Fedin. *Russ. Chem. Rev.*, **91**, RCR5026 (2022)
15. L.Fu, Q.Yang, D.Li, J.Y.Lu. *Mendeleev Commun.*, **30**, 589 (2020)
16. I.K.Rubtsova, S.N.Melnikov, M.A.Shmelev, S.A.Nikolaevskii, I.A.Yakushev, J.K.Voronina, E.D.Barabanova, M.A.Kiskin, A.A.Sidorova, I.L.Eremenko. *Mendeleev Commun.*, **30**, 722 (2020)
17. C.M.Oliva González, A.de Monserrat Navarro Tellez, B.I.Kharisov, O.V.Kharissova, T.E.Serrano Quezada, L.T.González. *Mendeleev Commun.*, **31**, 91 (2021)
18. M.A.Agafonov, E.V.Alexandrov, N.A.Artyukhova, G.E.Bekmukhamedov, V.A.Blatov, V.V.Butova, Y.M.Gayfulin, A.A.Garibyan, Z.N.Gafurov, Yu.G.Gorbunova, L.G.Gordeeva, M.S.Gruzdev, A.N.Gusev, G.L.Denisov, D.N.Dybtsev, Yu.Yu.Enakieva, A.A.Kagilev, A.O.Kantyukov, M.A.Kiskin, K.A.Kovalenko, A.M.Kolker, D.I.Kolokolov, Y.M.Litvinova, A.A.Lysova, N.V.Maksimchuk, Y.V.Mironov, Yu.V.Nelyubina, V.V.Novikov, V.I.Ovcharenko, A.V.Piskunov, D.M.Polyukhov, V.A.Polyakov, V.G.Ponomareva, A.S.Poryvaev, G.V.Romanenko, A.V.Soldatov, M.V.Solovyeva, A.G.Stepanov, I.V.Terekhova, O.Yu.Trofimova, V.P.Fedin, M.V.Fedin, O.A.Kholdeeva, A.Yu.Tsivadze, U.V.Chervonova, A.I.Cherevko, V.F.Shul'gin, E.S.Shutova, D.G.Yakhvarov. *J. Struct. Chem.*, **63**, 671 (2022)
19. L.Feng, K.-Y.Wang, X.-L.Lv, T.-H.Yan, H.-C.Zhou. *Nat. Sci. Rev.*, **7**, 1743 (2020)
20. B.Halford. *C&EN Global Enterprise*, **95**, 6 (2017)
21. I.M.Hönicke, I.Senkovska, V.Bon, I.A.Baburin, N.Bönisch, S.Raschke, J.D.Evans, S.Kaskel. *Angew. Chem., Int. Ed.*, **57**, 13780 (2018)
22. S.Salimi, K.Akhbari, S.M.F.Farnia, J.M.White. *Cryst. Growth Des.*, **22**, 1654 (2022)
23. L.Ma, J.Gao, C.Huang, X.Xu, L.Xu, R.Ding, H.Bao, Z.Wang, G.Xu, Q.Li, P.Deng, H.Ma. *ACS Appl. Mater. Interfaces*, **13**, 57831 (2021)
24. P.Salcedo-Abraira, S.M.F.Vilela, N.Ureña, F.Salles, A.Várez, P.Horcajada. *Inorg. Chem.*, **60**, 11803 (2021)
25. Y.Quan, W.Shi, Y.Song, X.Jiang, C.Wang, W.Lin. *J. Am. Chem. Soc.*, **143**, 3075 (2021)
26. S.Lee, D.Kim, J.Kim, O.-S.Jung. *Cryst. Growth Des.*, **20**, 3601 (2020)
27. H.Yang, B.Liu, J.Bright, S.Kasani, J.Yang, X.Zhang, N.Wu. *ACS Appl. Energy Mater.*, **3**, 4007 (2020)
28. M.Zhang, Q.Lin, W.Wu, Y.Ye, Z.Yao, X.Ma, S.Xiang, Z.Zhang. *ACS Appl. Mater. Interfaces*, **12**, 16367 (2020)
29. R.K.Baimuratova, G.I.Dzhardimalieva, N.D.Golubeva, N.N.Dremova, A.V.Ivanov. *Pure Appl. Chem.*, **92**, 859 (2020)
30. R.K.Baimuratova, N.D.Golubeva, G.I.Dzhardimalieva, G.I.Davydova, E.I.Knerelman. *Key Eng. Mater.*, **816**, 108 (2019)
31. G.I.Dzhardimalieva, A.D.Pomogailo. *Russ. Chem. Rev.*, **77**, 259 (2008)
32. O.V.Kharissova, V.A.Zhinzhilo, M.A.Chernomorova, I.E.Uflyand, I.Gómez de la Fuente, B.I.Kharisov. *Mendeleev Commun.*, **31**, 893 (2021)
33. I.E.Uflyand, V.A.Zhinzhilo, J.D.Bryantseva. *J. Inorg. Organomet. Polym. Mater.*, **31**, 4710 (2021)
34. I.E.Uflyand, V.A.Zhinzhilo, G.I.Dzhardimalieva, E.I.Knerelman, G.I.Davydova, I.G.Shunina. *Russ. J. Gen. Chem.*, **90**, 1884 (2020)
35. G.I.Dzhardimalieva, R.K.Baimuratova, E.I.Knerelman, G.I.Davydova, S.E.Kudaibergenov, O.V.Kharissova, V.A.Zhinzhilo, I.E.Uflyand. *Polymers*, **12**, 1024 (2020)
36. I.E.Uflyand, V.A.Zhinzhilo, G.I.Dzhardimalieva. *J. Inorg. Organomet. Polym. Mater.*, **30**, 965 (2020)
37. I.E.Uflyand, V.A.Zhinzhilo, V.O.Nikolaevskaya, B.I.Kharisov, C.M.Oliva González, O.V.Kharissova. *Microchem. J.*, **168**, 106387 (2021)
38. E.Moisés Cedeño Morales, M.A.Méndez-Rojas, L.M.Torres-Martínez, L.F.Garay-Rodríguez, I.López, I.E.Uflyand, B.I.Kharisov. *Polyhedron*, **210**, 115517 (2021)
39. A.Kirchon, L.Feng, H.F.Drake, E.A.Joseph, H.-C.Zhou. *Chem. Soc. Rev.*, **47**, 8611 (2018)
40. U.Ryu, S.Jee, P.C.Rao, J.Shin, C.Ko, M.Yoon, K.S.Park, K.M.Choi. *Coord. Chem. Rev.*, **426**, 213544 (2021)
41. L.Chen, R.Luque, Y.Li. *Chem. Soc. Rev.*, **46**, 4614 (2017)
42. L.Feng, K.-Y.Wang, G.S.Day, M.R.Ryder, H.-C.Zhou. *Chem. Rev.*, **120**, 13087 (2020)
43. X.Liu, X.Wang, F.Kapteijn. *Chem. Rev.*, **120**, 8303 (2020)
44. A.J.Howarth, Y.Liu, P.Li, Z.Li, T.C.Wang, J.T.Hupp, O.K.Farha. *Nat. Rev. Mater.*, **1**, 15018 (2016)
45. P.Falcaro, R.Ricco, A.Yazdi, I.Imaz, S.Furukawa, D.Maspoch, R.Ameloot, J.D.Evans, C.J. Doonan. *Coord. Chem. Rev.*, **307**, 237 (2016)

46. M.E.Mahmoud, S.M.Elsayed, S.E.M.E.Mahmoud, R.O.Aljedaani, M.A.Salam. *J. Mol. Liq.*, **347**, 118274 (2022)
47. X.Wang, L.Li, K.Li, R.Su, Y.Zhao, S.Gao, W.Guo, Z.Luan, G.Liang, H.Xi, R.Zou. *J. Colloid Interface Sci.*, **606**, 272 (2022)
48. Y.Liu, S.Wang, B.Yu, Y.Zhang, X.Kong, Y.Mi, J.Zhang, Z.Guo, W.Xu, X.Chen. *Inorg. Chem.*, **59**, 13184 (2020)
49. P.Railey, Y.Song, T.Liu, Y.Li. *Mater. Res. Bull.*, **96**, 385 (2017)
50. S.Li, F.Huo. *Nanoscale*, **7**, 7482 (2015)
51. W.Cai, X.Liu, L.Wang, B.Wang. *Mater. Today Nano*, **17**, 100144 (2022)
52. G.Avci, S.Velioglu, S.Keskin. *ACS Appl. Mater. Interfaces*, **10**, 33693 (2018)
53. A.N.V.Azar, S.Velioglu, S.Keskin. *ACS Sustain. Chem. Eng.*, **7**, 9525 (2019)
54. M.Xu, Z.Liu, X.Huai, L.Lou, J.Guo. *RSC Adv.*, **10**, 34621 (2020)
55. Y.Pramudya, S.Bonakala, D.Antypov, P.M.Bhatt, A.Shkurenko, M.Eddaoudi, M.J.Rosseinsky, M.S.Dyer. *Phys. Chem. Chem. Phys.*, **22**, 23073 (2020)
56. Z.Liu, X.Wang, Y.Liu, L.Li, S.Li. *Microporous Mesoporous Mater.*, **331**, 111659 (2022)
57. J.Rogacka, A.Seremak, A.Luna-Triguero, F.Formalik, I.Matito-Martos, L.Firlej, S.Calero, B.Kuchta. *Chem. Eng. J.*, **403**, 126392 (2021)
58. X.Yang, X.Jiang, Y.Huang, Z.Guo, L.Shao. *ACS Appl. Mater. Interfaces*, **9**, 5590 (2017)
59. H.Ning, Z.Yang, Z.Yin, D.Wang, Z.Meng, C.Wang, Y.Zhang, Z.Chen. *ACS Appl. Mater. Interfaces*, **13**, 17781 (2021)
60. T.Rodenas, I.Luz, G.Prieto, B.Seoane, H.Miro, A.Corma, F.Kapteijn, F.X.Llabrés i Xamena, J.Gascon. *Nature Mater.*, **14**, 48 (2015)
61. A.Hinokimoto, J.-S.M.Lee, H.Izu, L.Chen, M.Tsujimoto, S.Horike. *ACS Appl. Energy Mater.*, **3**, 11529 (2020)
62. M.A.Nasalevich, R.Becker, E.V.Ramos-Fernandez, S.Castellanos, S.L.Veber, M.V.Fedin, F.Kapteijn, J.N.H.Reek, J.I.van der Vlugt, J.Gascon. *Energy Environ. Sci.*, **8**, 364 (2015)
63. M.Zhong, S.Zhang, A.Dong, Z.Sui, L.Feng, Q.Chen. *J. Mater. Sci.*, **55**, 10388 (2020)
64. G.H.Ning, B.Tian, L.M.Tan, Z.Ding, T.S. Herng, J.Ding, K.P.Loh. *Inorg. Chem.*, **55**, 9892 (2016)
65. T.Zhang, W.Lin. *Chem. Soc. Rev.*, **43**, 5982 (2014)
66. S.Zheng, H.Xue, H.Pang. *Coord. Chem. Rev.*, **373**, 2 (2018)
67. Q.-L.Zhu, Q.Xu. *Chem. Soc. Rev.*, **43**, 5468 (2014)
68. L.Chen, X.Zhang, X.Cheng, Z.Xie, Q.Kuang, L.Zheng. *Nanoscale Adv.*, **2**, 2628 **(**2020**)**
69. P.Kumar, K.Vellingiri, K.H.Kim, R.J.C.Brown, M.J.Manos. *Microporous Mesoporous Mater.*, **253**, 251 (2017)
70. M.Aghayi-Anaraki, V.Safarifard. *Eur. J. Inorg. Chem.*, 1916 (2020)
71. B.E.Meteku, J.Huang, J.Zeng, F.Subhan, F.Feng, Y.Zhang, Z.Qiu, S.Aslam, G.Li, Z.Yan. *Coord. Chem. Rev.*, **413**, 213261 (2020)
72. S.S.Nadar, N.Varadan O, S.Suresh, P.Rao, D.J.Ahirrao, S.Adsare. *J. Taiwan Inst. Chem. Eng.*, **91**, 653 (2018).
73. R.Y.Wang, C.Y.Zhang, S.P.Wang, Y.Y.Zhou. *Prog. Chem.*, **27**, 945 (2015)
74. S.Yadav, R.Dixit, S.Sharma, S.Dutta, K.Solanki, R.K.Sharma. *Mater. Adv.*, **2**, 2153 (2021)
75. I.E.Uflyand, V.N.Naumkina, V.A.Zhinzhilo. *Russ. J. Appl. Chem.*, **94**, 1453 (2021)
76. M.Muschi, C.Serre. *Coord. Chem. Rev.*, **387**, 262 (2019)
77. H.Qu, L.Huang, Z.Han, Y.Wang, Z.Zhang, Y.Wang, Q.Chang, N.Wei, M.J.Kipper, J.Tang. *J. Porous Mater.*, **28**, 1837 (2021)
78. J.Aguilera-Sigalat, D.Bradshaw. *Coord. Chem. Rev.*, **307**, 267 (2016)
79. R.B.Choudhary, S.Ansari, M.Majumder. *Renew. Sustain. Energy Rev.*, **145**, 110854 (2021)
80. M.Kalaj, K.C.Bentz, S.Ayala Jr., J.M.Palomba, K.S.Barcus, Y.Katayama, S.M.Cohen. *Chem. Rev.*, **120**, 8267 (2020)
81. G.W.Peterson, D.T.Lee, H.F.Barton, T.H.Epps, G.N.Parsons. *Nat. Rev. Mater.*, **6**, 605 (2021)
82. B.V.K.J.Schmidt. *Macromol. Rapid Commun.*, **41**, 1900333 (2020)
83. D.D.Chronopoulos, H.Saini, I.Tantis, R.Zbořil, K.Jayaramulu, M.Otyepka. *Small*, **18**, 2104628 (2022)
84. S.El Hankari, M.Bousmina, A.El Kadib. *Prog. Mater. Sci.*, **106**, 100579 (2019)
85. N.S.K.Gowthaman. *Mater. Res. Foundations*, **82**, 276 (2020)
86. X.-W.Liu, T.-J.Sun, J.-L.Hu, S.-D.Wang. *J. Mater. Chem. A*, **4**, 3584 (2016)
87. R.Sule, A.K.Mishra. *Environ. Sci. Pollut. Res.*, **27**, 16004 (2020)
88. K.Wang, K.N.Hui, K.S.Hui, S.Peng, Y.Xu. *Chem. Sci.*, **12**, 5737 (2021).
89. Y.Zheng, S.Zheng, H.Xue, H.Pang. *Adv. Funct. Mater.*, **28**, 1804950 (2018)
90. X.Zhang, S.Zhang, Y.Tang, X.Huang, H.Pang. *Composites, Part B: Eng.*, **230**, 109532 (2022)
91. L.Zhu, L.Meng, J.Shi, J.Li, X.Zhang, M.Feng. *J. Environ.*, **232**, 964 (2019)
92. S.Li, K.Yang, C.Tan, X.Huang, W.Huang, H.Zhang. *Chem. Commun.*, **52**, 1555 (2016)
93. Z.Li, J.Guo, Y.Wan, Y.Qin, M.Zhao. *Nano Res.*, **15**, 3514 (2022)
94. X.Lian, Y.Fang, E.Joseph, Q.Wang, J.Li, S.Banerjee, C.Lollar, X.Wang, H.C.Zhou. *Chem. Soc. Rev.*, **46**, 3386 **(**2017)
95. C.Liu, J.Wang, J.Wan, C.Yu. *Coord. Chem. Rev.*, **432**, 213743 (2021)
96. M.Ma, L.Lu, H.Li, Y.Xiong, F.Dong. *Polymers*, **11**, 1823 (2019)
97. N.Yuan, X.Zhang, L.Wang. *Coord. Chem. Rev.*, **421**, 213442 (2020)
98. G.Zhan, H.C.Zeng. *Coord. Chem. Rev.*, **320**, 181 (2016)
99. W.Xiang, Y.Zhang, H.Lin, C.Liu. *Molecules*, **22**, 2103 (2017)
100. Q.Yang, Q.Xu, H.L.Jiang. *Chem. Soc. Rev.*, **46**, 4774 **(**2017)
101. J.Yu, C.Mu, B.Yan, X.Qin, C.Shen, H.Xue, H.Pang. *Mater. Horiz.*, **4**, 557 **(**2017)
102. H.Saini, N.Srinivasan, V.Šedajová, M.Majumder, D.P.Dubal, M.Otyepka, R.Zbořil, N.Kurra, R.A.Fischer, K.Jayaramulu. *ACS Nano*, **15**, 18742 (2021)
103. J.Sun, S.Abednatanzi, P.V.D.Voort, Y.Y.Liu, K.Leus. *Catalysts*, **10**, 578 (2020).
104. G.Zhang, D.Huang, M.Cheng, L.Lei, S.Chen, R.Wang, W.Xue, Y.Liu, Y.Chen, Z.Li. *J. Mater. Chem. A*, **8**, 17883 (2020)
105. I.Ahmed, S.H.Jhung. *Mater. Today*, **17**, 136 (2014)
106. H.Dai, X.Yuan, L.Jiang, H.Wang, J.Zhang, J.Zhang, T.Xiong. *Coord. Chem. Rev.*, **441**, 213985 (2021)
107. J.Li, T.Lan, Y.Chen, J.Yang, L.Li, J.Li. *Huagong Xuebao/ CIESC J.*, **72**, 167 (2021)
108. Z.U.Zango, K.Jumbri, N.S.Sambudi, A.Ramli, N.H.H.A.Bakar, B.Saad, M.N.H.Rozaini, H.A.Isiyaka, A.H.Jagaba, O.Aldaghri, A.Sulieman. *Polymers*, **12**, 2648 (2020)
109. A.Bieniek, A.P.Terzyk, M.Wiśniewski, K.Roszek, P.Kowalczyk, L.Sarkisov, S.Keskin, K.Kaneko. *Prog. Mater. Sci.*, **117**, 100743 (2021)
110. X.Ge, R.Wong, A.Anisa, S.Ma. *Biomaterials*, **281**, 121322 (2022)
111. M.Liu, X.Ren, X.Meng, H.Li. *Chin. J. Chem.*, **39**, 473 (2021)
112. M.Oggianu, N.Monni, V.Mameli, C.Cannas, S.A.Sahadevan, M.L.Mercuri. *Magnetochemistry*, **6**, 39 (2020)
113. J.W.M.Osterrieth, D.Fairen-Jimenez. *Biotechnol. J.*, **16**, 2000005 (2021)

114. L.Chen, Q.Xu. *Matter*, **1**, 57 (2019)
115. K.-G.Liu, Z.Sharifzadeh, F.Rouhani, M.Ghorbanloo, A.Morsali. *Coord. Chem. Rev.*, **436**, 213827 (2021)
116. T.Wu, X.Liu, Y.Liu, M.Cheng, Z.Liu, G.Zeng, B.Shao, Q.Liang, W.Zhang, Q.He, W.Zhang. *Coord. Chem. Rev.*, **403**, 213097 (2020)
117. Z.Liang, C.Qu, W.Guo, R.Zou, Q.Xu. *Adv. Mater.*, **30**, 1702891 **(**2018**)**
118. S.Sundriyal, H.Kaur, S.K.Bhardwaj, S.Mishra, K.-H.Kim, A.Deep. *Coord. Chem. Rev.*, **369**, 15 (2018)
119. Y.Xue, S.Zheng, H.Xue, H.Pang. *J. Mater. Chem. A*, **7**, 7301 (2019)
120. F.-Y.Yi, R.Zhang, H.Wang, L.-F.Chen, L.Han, H.-L.Jiang, Q.Xu. *Small Methods*, **1**, 1700187 (2017)
121. T.Yue, C.Xia, X.Liu, Z.Wang, K.Qi, B.Y.Xia. *ChemElectroChem*, **8**, 1021 (2021)
122. N.F.H.N.Zaiman, N.Shaari, N.A.M.Harun. *Int. J. Energy Res.*, **46**, 471 (2022)
123. J.Lei, R.Qian, P.Ling, L.Cui, H.Ju. *Trends Anal. Chem.*, **58**, 71 (2014)
124. A.Amini, S.Kazemi, V.Safarifard. *Polyhedron*, **177**, 114260 (2020)
125. B.Huang, Y.Li, W.Zeng. *Chemosensors*, **9**, 226 (2021)
126. S.Kempahanumakkagari, K.Vellingiri, A.Deep, E.E.Kwon, N.Bolan, K.H.Kim. *Coord. Chem. Rev.*, **357**, 105 (2018)
127. S.S.Alneyadi. *Heterocycles*, **102**, 622 (2021)
128. M.Shen, F.Forghani, X.Kong, D.Liu, X.Ye, S.Chen, T.Ding. *Compr. Rev. Food Sci. Food Saf.*, **19**, 1397 (2020)
129. H.Kaur, S.Sundriyal, V.Pachauri, S.Ingebrandt, K.-H.Kim, A.L.Sharma, A.Deep. *Coord. Chem. Rev.*, **401**, 213077 (2019)
130. P.Cheng, C.Wang, Y.V.Kaneti, M.Eguchi, J.Lin, Y.Yamauchi, J.Na. *Langmuir*, **36**, 4231 (2020)
131. J.Yao, H.Wang. *Chem. Soc. Rev.*, **43**, 4470 (2014)
132. A.Elrasheedy, N.Nady, M.Bassyouni, A.El-Shazly. *Membranes*, **9**, 88 (2019)
133. S.Yu, H.Pang, S.Huang, H.Tang, S.Wang, M.Qiu, Z.Chen, H.Yang, G.Song, D.Fu, B.Hu, X.Wang. *Sci. Total Environ.*, **800**, 149662 (2021)
134. Y.Xue, C.Liu, G.Andrews, J.Wang, Y.Ge. *Nano Convergence*, **9**, 15 (2022)
135. W.Pan, Z.Li, S.Qiu, C.Dai, S.Wu, X.Zheng, M.Guan, F.Gao. *Mater. Today Bio*, **13**, 100214 (2022)
136. T.Guo, Y.Huang, N.Zhang, T.Chen, C.Wang, X.Xing, Z.Lu, L.Wen. *Inorg. Chem.*, **61**, 2538 (2022)
137. X.Xiao, X.Li, S.Zheng, J.Shao, H.Xue, H.Pang. *Adv. Mater. Interfaces*, **4**, 1600798 (2017)
138. Y.Xu, Q.Li, H.Xue, H.Pang. *Coord. Chem. Rev.*, **376**, 292 (2018)
139. Y.Yan, P.Gu, S.Zheng, M.Zheng, H.Pang, H.Xue. *J. Mater. Chem. A*, **4**, 19078 (2016)
140. T.Mondal, D.Haldar, A.Ghosh, U.K.Ghorai, S.K.Saha. *New J. Chem.*, **44**, 55 (2020)
141. Y.Lu, S.Wang, K.Yu, J.Yu, D.Zhao, C.Li. *Microporous Mesoporous Mater.*, **319**, 111062 (2021)
142. M.Zhang, L.Vojtech, Z.Ye, F.Hladik, E.Nance. *ACS Appl. Nano Mater.*, **3**, 7211 (2020)
143. D.Xiao, H.Qi, Y.Teng, D.Pierre, P.T.Kutoka, D.Liu. *Nanoscale Res. Lett.*, **16**, 167 (2021)
144. W.S.Lee, S.Jeon, S.J.Oh. *Nano Converg.*, **6**, 10 (2019)
145. H.Lee, S.Lee. *ACS Appl. Nano Mater.*, **4**, 11573 (2021)
146. A.D.Pomogailo, A.S.Rozenberg, I.E.Uflyand. *Nanochastisty Metallov v Polimerakh. (Metal Nanoparticles in Polymers)*. (Moscow: Khimiya, 2000)
147. T.Sadhukha, T.S.Wiedmann, J.Panyam. *Biomaterials*, **35**, 7860 (2014)
148. R.Tao, X.Ma, X.Wei, Y.Jin, L.Qiu, W.Zhang. *J. Mater. Chem. A*, **8**, 17360 (2020)
149. L.Guo, Y.Xu, A.R.Ferhan, G.Chen, D.H.Kim. *J. Am. Chem. Soc.*, **135**, 12338 (2013)
150. Y.Xu, S.Zheng, H.Tang, X.Guo, H.Xue, H.Pang. *Energy Storage Mater.*, **9**, 11 (2017)
151. J.Zong, X.Song, R.Wang, W.Xu, W.Zhou, S.Li, Y.Feng, H.Chen. *Chem. Mater.*, **33**, 8460 (2021)
152. R.H.Alshammari, U.C.Rajesh, D.G.Morgan, J.M.Zaleski. *ACS Appl. Bio Mater.*, **3**, 7631 (2020)
153. H.Fu, S.Sun, X.Yang, W.Li, X.An, H.Zhang, Y.Dong, X.Jiang, A.Yu. *Powder Technol.*, **328**, 389 (2018)
154. C.Dulgerbaki, N.N.Maslakci, A.I.Komur, A.U.Oksuz. *Eur. Polym. J.*, **107**, 173 (2018)
155. P.Lamagni, B.L.Pedersen, A.Godiksen, S.Mossin, X.-M.Hu, S.U.Pedersen, K.Daasbjerg, N.Lock. *RSC Adv.*, **8**, 13921 (2018)
156. K.K.Gangu, S.B.Jonnalagadda. *Front. Chem.*, **9**, 747615 (2021)
157. X.Liu, H.Li, L.-P.Xiao, R.-C.Sun, G.Song. *Green Chem.*, **21**, 1498 (2019)
158. C.Rösler, R.A.Fischer. *CrystEngComm*, **17**, 199 (2015)
159. Y.Mitsuka, N.Ogiwara, M.Mukoyoshi, H.Kitagawa, T.Yamamoto, T.Toriyama, S.Matsumura, M.Haneda, S.Kawaguchi, Y.Kubota, H.Kobayashi. *Angew. Chem., Int. Ed.*, **60**, 22283 (2021)
160. Z.Huang, L.Fan, B.Chen, S.Zhou, J.Huang, Q.Li, G.Zhan. *J. Mater. Chem. A*, **9**, 3976 (2021)
161. F.-F.Wang, Q.Wang, X.Chen, D.-L.Chen, W.Zhu. *J. Phys. Chem. C*, **124**, 23738 (2020)
162. W.Xia, A.Mahmood, R.Zou, Q.Xu. *Energy Environ. Sci.*, **8**, 1837 (2015)
163. F.Chen, K.Shen, J.Chen, X.Yang, J.Cui, Y.Li. *ACS Cent. Sci.*, **5**, 176 (2019)
164. R.Ding, D.Li, Y.Li, J.Yu, M.Jia, J.Xu. *ACS Appl. Nano Mater.*, **4**, 4632 (2021)
165. M.Duan, L.Jiang, G.Zeng, D.Wang, W.Tang, J.Liang, H.Wang, D.He, Z.Liu, L.Tang. *Appl. Mater. Today*, **19**, 100564 (2020)
166. L.Chen, B.Huang, X.Qiu, X.Wang, R.Luque, Y.Li. *Chem. Sci.*, **7**, 228 (2016)
167. C.Chen, Q.Mo, J.Fu, O.Yang, L.Zhang, C.-Y.Su. *ACS Catal.*, **12**, 3604 (2022)
168. J.R.Varghese, C.Wendt, F.B.Dix, D.Aulakh, U.Sazama, A.A.Yakovenko, M.Fröba, J.Wochnowski, D.V.Goia, M.Wriedt. *Inorg. Chem.*, **60**, 13000 (2021)
169. M.Rivera-Torrente, M.Filez, R.Hardian, E.Reynolds, B.Seoane, M.V.Coulet, F.E.Oropeza Palacio, J.P.Hofmann, R.A.Fischer, A.L.Goodwin, P.L.Llewellyn, B.M.Weckhuysen. *Chem. – Eur. J.*, **24**, 7498 (2018)
170. D.Cartagenova, S.Bachmann, K.Püntener, M.Scalone, M.A.Newton, F.A.Peixoto Esteves, T.Rohrbach, P.P.Zimmermann, J.A.van Bokhoven, M.Ranocchiari. *Catal. Sci. Technol.*, **12**, 954 (2022)
171. J.Yang, H.Ye, F.Zhao, B.Zeng. *ACS Appl. Mater. Interfaces*, **8**, 20407 (2016)
172. Z.Zhang, X.Cui, W.Yuan, Q.Yang, H.Liu, H.Xu, H.-L.Jiang. *Inorg. Chem. Front.*, **5**, 29 (2018)
173. G.I.Dzhardimalieva, I.E.Uflyand. *J. Polym. Res.*, **25**, 255 (2018)
174. N.Goyal, R.K.Rai. In *Metal-Organic Frameworks (MOFs) as Catalysts*. (Ed. N.Goyal). (Singapore: Springer, 2022). P. 731
175. A.Aijaz, Q.Xu. *J. Phys. Chem. Lett.*, **5**, 1400 (2014)
176. Y.P.Zhang, Y.Zhou, Y.Zhao, C.J.Liu. *Catal. Today*, **263**, 61 (2016)
177. A.Aijaz, A.Karkamkar, Y.J.Choi, N.Tsumori, E.Rönnebro, T.Autrey, H.Shioyama, Q.Xu. *J. Am. Chem. Soc.*, **134**, 13926 (2012)
178. H.Pang, Y.Zhang, T.Cheng, W.Y.Lai, W.Huang. *Nanoscale*, **7**, 16012 (2015)
179. L.Peng, S.Yang, D.T.Sun, M.Asgari, W.L.Queen. *Chem. Commun.*, **54**, 10602 (2018)
180. Q.L.Zhu, J.Li, Q.Xu. *J. Am. Chem. Soc.*, **135**, 10210 (2013)

181. Y.-Z.Chen, Q.Xu, S.-H.Yu, H.-L.Jiang. *Small*, **11**, 71 (2015)
182. Y.H.Zhou, Q.Yang, Y.Z.Chen, H.L.Jiang. *Chem. Commun.*, **53**, 12361 (2017)
183. L.Chen, X.Chen, H.Liu, Y.Li. *Small*, **11**, 2642 (2015)
184. Y.Z.Chen, Y.X.Zhou, H.Wang, J.Lu, T.Uchida, Q.Xu, S.H.Yu, H.L.Jiang. *ACS Catal.*, **5**, 2062 (2015)
185. M.Meledina, S.Turner, M.Filippousi, K.Leus, I.Lobato, R.K.Ramachandran, J.Dendooven, C.Detavernier, P.Van Der Voort, G.Van Tendeloo. *Part. Part. Syst. Charact.*, **33**, 382 (2016)
186. N.R.Habib, E.Asedegbega-Nieto, A.M.Taddesse, I.Diaz. *Dalton Trans.*, **50**, 10340 (2021)
187. L.Ma, Y.He, Y.Wang, Y.Wang, R.Li, Z.Huang, Y.Jiang, J.Gao. *Electrochim. Acta*, **318**, 525 (2019)
188. M.Deng, X.Bo, L.Guo. *J. Electroanal. Chem.*, **815**, 198 (2018)
189. Q.Wang, X.-S.Wang, C.-H.Chen, X.Yang, Y.-B.Huang, R.Cao. *Chem. Commun.*, **54**, 8822 (2018)
190. A.W.Augustyniak, W.Zawartka, J.A.R.Navarro, A.M.Trzeciak. *Dalton Trans.*, **45**, 13525 (2016)
191. G.Lu, S.Li, Z.Guo, O.K.Farha, B.G.Hauser, X.Qi, Y.Wang, X.Wang, S.Han, X.Liu, J.S.DuChene, H.Zhang, Q.Zhang, X.Chen, J.Ma, S.C.J.Loo, W.D.Wei, Y.Yang, J.T.Hupp, F.Huo. *Nat. Chem.*, **4**, 310 (2012)
192. W.Zhang, Y.Liu, G.Lu, Y.Wang, S.Li, C.Cui, J.Wu, Z.Xu, D.Tian, W.Huang, J.S.DuCheneu, W.D.Wei, H.Chen, Y.Yang, F.Huo. *Adv. Mater.*, **27**, 2923 (2015)
193. C.S.L.Koh, H.Y.F.Sim, S.X.Leong, S.K.Boong, C.Chong, X.Y.Ling. *ACS Mater. Lett.*, **3**, 557 (2021)
194. X.Jiang, H.-Y.Chen, L.-L.Liu, L.-G.Qiu, X.Jiang. *J. Alloys Compd.*, **646**, 1075 (2015)
195. Y.Liu, T.Liu, L.Tian, L.Zhang, L.Yao, T.Tan, J.Xu, X.Han, D.Liu, C.Wang. *Nanoscale*, **8**, 19075 (2016)
196. C.H.Kuo, Y.Tang, L.Y.Chou, B.T.Sneed, C.N.Brodsky, Z.Zhao, C.K.Tsung. *J. Am. Chem. Soc.*, **134**, 14345 (2012)
197. N.Qin, A.Pan, J.Yuan, F.Ke, X.Wu, J.Zhu, J.Liu, J.Zhu. *ACS Appl. Mater. Interfaces*, **13**, 12463 (2021)
198. Y.Zhao, N.Kornienko, Z.Liu, C.Zhu, S.Asahina, T.-R.Kuo, W.Bao, C.Xie, A.Hexemer, O.Terasaki, P.Yang, O.M.Yaghi. *J. Am. Chem. Soc.*, **137**, 2199 (2015)
199. X.Huang, S.Yan, D.Deng, L.Zhang, R.Liu, Y.Lv. *ACS Appl. Mater. Interfaces*, **13**, 3471 (2021)
200. Z.Li, R.Yu, J.Huang, Y.Shi, D.Zhang, X.Zhong, D.Wang, Y.Wu, Y.Li. *Nat. Commun.*, **6**, 8248 (2015)
201. Q.Yang, W.Liu, B.Wang, W.Zhang, X.Zeng, C.Zhang, Y.Qin, X.Sun, T.Wu, J.Liu, F.Huo, J.Lu. *Nat. Commun.*, **8**, 14429 (2017)
202. R.Riccò, O.Linder-Patton, K.Sumida, M.J.Styles, K.Liang, H.Amenitsch, C.J.Doonan, P.Falcaro. *Chem. Mater.*, **30**, 5630 (2018)
203. L.Chen, H.Li, W.Zhan, Z.Cao, J.Chen, Q.Jiang, Y.Jiang, Z.Xie, Q.Kuang, L.Zheng. *ACS Appl. Mater. Interfaces*, **8**, 31059 (2016).
204. L.N.Chen, H.Q.Li, M.W.Yan, C.F.Yuan, W.W.Zhan, Y.Q.Jiang, Z.X.Xie, Q.Kuang, L.S.Zheng. *Small*, **13**, 1700683 (2017)
205. G.Cai, W.Zhang, L.Jiao, S.H.Yu, H.L.Jiang. *Chem*, **2**, 791 (2017)
206. N.Zhang, Q.Shao, P.Wang, X.Zhu, X.Huang. *Small*, **14**, 1704318 (2018)
207. B.Li, J.-G.Ma, P.Cheng. *Angew. Chem., Int. Ed.*, **57**, 6834 (2018)
208. S.Wang, Y.Fan, J.Teng, Y.-Z.Fan, J.-J.Jiang, H.-P.Wang, H.Grützmacher, D.Wang, C.-Y.Su. *Small*, **12**, 5702 (2016)
209. Q.Zhou, L.Xu, Z.Kan, L.Yang, Z.Chang, B.Dong, X.Bai, G.Lu, H.Song. *J. Hazard. Mater.*, **426**, 128075 (2022)
210. L.Chen, X.Chen, H.Liu, C.Bai, Y.Li. *J. Mater. Chem. A*, **3**, 15259 (2015)
211. H.Liu, L.Chang, C.Bai, L.Chen, R.Luque, Y.Li. *Angew. Chem., Int. Ed.*, **55**, 5019 (2016)
212. H.Liu, L.Chang, L.Chen, Y.Li. *J. Mater. Chem. A*, **3**, 8028 (2015)
213. M.Zhao, K.Yuan, Y.Wang, G.Li, J.Guo, L.Gu, W.Hu, H.Zhao, Z.Tang. *Nature (London)*, **539**, 76 (2016)
214. J.Zhuang, L.Y.Chou, B.T.Sneed, Y.Cao, P.Hu, L.Feng, C.K.Tsung. *Small*, **11**, 5551 (2015)
215. L.Chen, W.Zhan, H.Fang, Z.Cao, C.Yuan, Z.Xie, Q.Kuang, L.Zheng. *Chem.–Eur. J.*, **23**, 11397 (2017)
216. D.Buso, J.Jasieniak, M.D.H.Lay, P.Schiavuta, P.Scopece, J.Laird, H.Amenitsch, A.J.Hill, P.Falcaro. *Small*, **8**, 80 (2012)
217. S.J.Qin, B.Yan. *Sens. Actuators, B*, **272**, 510 (2018)
218. Y.Gao, J.Wu, W.Zhang, Y.Tan, J.Zhao, B.Tang. *Mater. Lett.*, **128**, 208 (2014)
219. R.Li, J.Hu, M.Deng, H.Wang, X.Wang, Y.Hu, H.L.Jiang, J.Jiang, Q.Zhang, Y.Xie, Y.Xiong. *Adv. Mater.*, **26**, 4783 (2014)
220. D.Esken, S.Turner, C.Wiktor, S.B.Kalidindi, G.Van Tendeloo, R.A.Fischer. *J. Am. Chem. Soc.*, **133**, 16370 (2011)
221. S.Saha, G.Das, J.Thote, R.Banerjee. *J. Am. Chem. Soc.*, **136**, 14845 (2014)
222. J.Huang, H.Song, C.Chen, Y.Yang, N.Xu, X.Ji, C.Li, J.-A.You. *J. Environ. Chem. Eng.*, **5**, 2579 (2017)
223. K.Cho, S.-H.Han, M.P.Suh. *Angew. Chem., Int. Ed.*, **55**, 15301 (2016)
224. R.Lin, S.Li, J.Wang, J.Xu, C.Xu, J.Wang, C.Li, Z.Li. *Inorg. Chem. Front.*, **5**, 3170 (2018)
225. R.Yan, Y.Zhao, H.Yang, X.-J.Kang, C.Wang, L.-L.Wen, Z.-D.Lu. *Adv. Funct. Mater.*, **28**, 1802021 (2018)
226. J.Zhu, P.C.Wang, M.Lu. *Appl. Catal. A: Gen.*, **477**, 125 (2014)
227. V.R.Bakuru, S.B.Kalidindi. *Chem.–Eur. J.*, **23**, 16456 (2017)
228. H.Zhao, L.Qian, H.Lv, Y.Wang, G.Zhao. *ChemCatChem*, **7**, 4148 (2015)
229. Q.Gong, Y.Liu, Z.Dang. *J. Hazard. Mater.*, **371**, 677 (2019)
230. Y.-H.Hu, C.-X.Liu, J.-C.Wang, X.-H.Ren, X.Kan, Y.-B.Dong. *Inorg. Chem.*, **58**, 4722 (2019)
231. G.Huang, Q.Yang, Q.Xu, S.Yu, H.Jiang. *Angew. Chem., Int. Ed.*, **55**, 7379 (2016)
232. Y.Zhang, B.Lin, Y.Sun, X.Zhang, H.Yang, J.Wang. *RSC Adv.*, **5**, 58100 (2015)
233. H.Zhang, W.Zhao, M.Zou, Y.Wang, Y.Chen, L.Xu, H.Wu, A.Cao. *Adv. Energy Mater.*, **8**, 1800013 (2018)
234. S.Sohrabi, S.Dehghanpour, M.Ghalkhani. *J. Mater. Sci.*, **53**, 3624 (2018)
235. Y.Hu, Z.Fang, X.Wan, X.Ma, S.Wang, S.Fan, M.Dong, Z.Ye, X.Peng. *Chem. Eng. J.*, **430**, 133086 (2022)
236. D.L.White, B.A.Day, Z.Zeng, Z.M.Schulte, N.R.Borland, N.L.Rosi, C.E.Wilmer, A.Star. *J. Am. Chem. Soc.*, **143**, 8022 (2021)
237. Y.Yue, B.Guo, Z.A.Qiao, P.F.Fulvio, J.Chen, A.J.Binder, C.Tian, S.Dai. *Microporous Mesoporous Mater.*, **198**, 139 (2014)
238. T.Y.Huang, C.W.Kung, Y.T.Liao, S.Y.Kao, M.Cheng, T.H.Chang, J.Henzie, H.R.Alamri, Z.A.Alothman, Y.Yamauchi, K.C.Ho, K.C.Wu. *Adv. Sci.*, **4**, 1700261 (2017)
239. M.Baratta, T.F.Mastropietro, R.Bruno, A.Tursi, C.Negro, J.Ferrando-Soria, A.I.Mashin, A.Nezhdanov, F.P.Nicoletta, G.De Filpo, E.Pardo, D.Armentano. *ACS Appl. Nano Mater.*, **5**, 5223 (2022)
240. L.Kong, X.Zhang, H.Liu, T.Wang, J.Qiu. *J. Phys. Chem. Solids*, **77**, 23 (2015)
241. L.Ge, L.Wang, V.Rudolph, Z.Zhu. *RSC Adv.*, **3**, 25360 (2013)
242. Y.Yang, L.Ge, V.Rudolph, Z.Zhu. *Dalton Trans.*, **43**, 7028 (2014)
243. R.Lin, L.Ge, S.Liu, V.Rudolph, Z.Zhu. *ACS Appl. Mater. Interfaces*, **7**, 14750 (2015)
244. H.Jiang, Y.Feng, M.Chen, Y.Wang. *Int. J. Hydrogen Energy*, **38**, 10950 (2013)
245. H.Jia, Z.Sun, D.Jiang, P.Du. *Chem. Mater.*, **27**, 4586 (2015)

246. L.H.Wee, N.Janssens, S.P.Sree, C.Wiktor, E.Gobechiya, R.A.Fischer, C.E.A.Kirschhock, J.A.Martens. *Nanoscale*, **6**, 2056 (2014)
247. W.Zhan, Y.He, J.Guo, L.Chen, X.Kong, H.Zhao, Q.Kuang, Z.Xie, L.Zheng. *Nanoscale*, **8**, 13181 (2016)
248. W.T.Koo, S.J.Kim, J.S.Jang, D.H.Kim, I.D.Kim. *Adv. Sci.*, **6**, 1970126 (2019)
249. M.Drobek, J.H.Kim, M.Bechelany, C.Vallicari, A.Julbe, S.S.Kim. *ACS Appl. Mater. Interfaces*, **8**, 8323 (2016)
250. H.Tian, H.Fan, M.Li, L.Ma. *ACS Sens.*, **1**, 243 (2016)
251. M.S.Yao, W.X.Tang, G.E.Wang, B.Nath, G.Xu. *Adv. Mater.*, **28**, 5229 (2016)
252. Y.Luan, Y.Qi, H.Gao, N.Zheng, G.Wang. *J. Mater. Chem. A*, **2**, 20588 (2014)
253. X.Huang, B.Zheng, Z.Liu, C.Tan, J.Liu, B.Chen, H.Li, J.Chen, X.Zhang, Z.Fan, W.Zhang, Z.Guo, F.Huo, Y.Yang, L.Xie, W.Huang, H.Zhang. *ACS Nano*, **8**, 8695 (2014)
254. R.Kumar, K.Jayaramulu, T.K.Maji, C.N.R.Rao. *Chem. Commun.*, **49**, 4947 (2013)
255. S.Liu, L.Sun, F.Xu, J.Zhang, C.Jiao, F.Li, Z.Li, S.Wang, Z.Wang, X.Jiang, H.Zhou, L.Yang, C.Schick. *Energy Environ. Sci.*, **6**, 818 (2013)
256. W.Zhang, Y.Tan, Y.Gao, J.Wu, J.Hu, A.Stein, B.Tang. *J. Appl. Electrochem.*, **46**, 441 (2016)
257. L.R.Redfern, Z.Li, X.Zhang, O.K.Farha. *ACS Appl. Nano Mater.*, **1**, 4413 (2018)
258. L.Wang, X.Feng, L.Ren, Q.Piao, J.Zhong, Y.Wang, H.Li, Y.Chen, B.Wang. *J. Am. Chem. Soc.*, **137**, 4920 (2015)
259. S.N.Guo, Y.Zhu, Y.Y.Yan, Y.L.Min, J.C.Fan, Q.J.Xu, H.Yun. *J. Power Sources*, **316**, 176 (2016)
260. S.Luo, J.Wang. *Environ. Sci. Pollut. Res.*, **25**, 5521 (2018)
261. Y.Yan, X.Bo, L.Guo. *Talanta*, **218**, 121123 (2020).
262. Y.Xiao, B.Guo, J.Zhang, C.Hu, R.Ma, D.Wang, J.Wang. *Dalton Trans.*, **49**, 5730 (2020)
263. R.Abazari, S.Sanati, A.Morsali. *Inorg. Chem.*, **61**, 3396 (2022)
264. P.Pachfule, B.K.Balan, S.Kurungot, R.Banerjee. *Chem. Commun.*, **48**, 2009 (2012)
265. Y.Shu, Q.Lu, F.Yuan, Q.Tao, D.Jin, H.Yao, Q.Xu, X.Hu. *ACS Appl. Mater. Interfaces*, **12**, 49480 (2020)
266. Y.Zhang, A.Nsabimana, L.Zhu, X.Bo, C.Han, M.Li, L.Guo. *Talanta*, **129**, 55 (2014)
267. X.Lin, G.Gao, L.Zheng, Y.Chi, G.Chen. *Anal. Chem.*, **86**, 1223 (2014)
268. S.Qiu, M.Xue, G.Zhu. *Chem. Soc. Rev.*, **43**, 6116 (2014)
269. M.Bechelany, M.Drobek, C.Vallicari, A.Abou Chaaya, A.Julbe, P.Miele. *Nanoscale*, **7**, 5794 (2015)
270. X.-J.Yu, Y.-M.Xian, C.Wang, H.-L.Mao, M.Kind, T.Abu-Husein, Z.Chen, S.-B.Zhu, B.Ren, A.Terfort, J.-L.Zhuang. *J. Am. Chem. Soc.*, **141**, 18984 (2019)
271. A.L.Semrau, Z.Zhou, S.Mukherjee, M.Tu, W.Li, R.A.Fischer. *Langmuir*, **37**, 6847 (2021)
272. J.Zhao, B.Gong, W.T.Nunn, P.C.Lemaire, E.C.Stevens, F.I.Sidi, P.S.Williams, C.J.Oldham, H.J.Walls, S.D.Shepherd, M.A.Browe, G.W.Peterson, M.D.Losego, G.N.Parsons. *J. Mater. Chem. A*, **3**, 1458 (2015)
273. E.Laurila, J.Thunberg, S.P.Argent, N.R.Champness, S.Zacharias, G.Westman, L.Öhrström**.** *Adv. Eng. Mater.*, **17**, 1282 (2015)
274. A.Huang, Q.Liu, N.Wang, Y.Zhu, J.Caro. *J. Am. Chem. Soc.*, **136**, 14686 (2014)
275. L.J.Shen, L.J.Huang, S.J.Liang, R.W.Liang, N.Qin, L.Wu. *RSC Adv.*, **4**, 2546 (2014)
276. K.M.Choi, H.M.Jeong, J.H.Park, Y.B.Zhang, J.K.Kang, O.M.Yaghi. *ACS Nano*, **8**, 7451 (2014)
277. P.Srimuk, S.Luanwuthi, A.Krittayavathananon, M.Sawangphruk. *Electrochim. Acta*, **157**, 69 (2015)
278. Y.Z.Li, H.F.Chao, H.J.Du, W.B.Liu, Y.W.Li, J.S.Ye. *J. Electroanal. Chem.*, **709**, 65 (2013)
279. W.Z.Bao, Z.A.Zhang, Y.H.Qu, C.K.Zhou, X.W.Wang, J.Li. *J. Alloys Compd.*, **582**, 334 (2014)
280. B.Yeskendir, J.-P.Dacquin, Y.Lorgouilloux, C.Courtois, S.Royer, J.Dhainaut. *Mater. Adv.*, **2**, 7139 (2021)
281. G.Blanita, M.Mihet, G.Borodi, I.Misan, I.Coldea, D.Lupu. *Microporous Mesoporous Mater.*, **203**, 195 (2015)
282. X.Wang, Q.X.Wang, Q.H.Wang, F.Gao, F.Gao, Y.Z.Yang, H.X.Guo. *ACS Appl. Mater. Interfaces*, **6**, 11573 (2014)
283. K.Y.A.Lin, F.K.Hsu, W.D.Lee. *J. Mater. Chem. A*, **3**, 9480 (2015)
284. A.G.Nugmanova, M.A.Kalinina. *Colloid J.*, **83**, 614 (2021)
285. Z.Bian, J.Xu, S.Zhang, X.Zhu, H.Liu, J.Hu. *Langmuir*, **31**, 7410 (2015)
286. F.Bu, X.Feng, T.Jiang, I.Shakir, Y.Xu.*Chem. – Eur. J.*, **23**, 8358 (2017)
287. M.Fan, D.Liao, M.F.Aly Aboud, I.Shakir, Y.Xu. *Angew. Chem., Int. Ed.*, **59**, 8247 (2020)
288. V.A.Zhinzhilo, E.A.Lebedintseva, V.N.Naumkina, I.E.Uflyand. *Russ. J. Appl. Chem.*, **94**, 1059 (2021)
289. Z.Bian, X.Zhu, T.Jin, J.Gao, J.Hu, H.Liu. *Microporous Mesoporous Mater.*, **200**, 159 (2014)
290. J.-W.Liu, Y.Zhang, X.-W.Chen, J.-H.Wang. *ACS Appl. Mater. Interfaces*, **6**, 10196 (2014)
291. M.Jahan, Q.Bao, K.P.Loh. *J. Am. Chem. Soc.*, **134**, 6707 (2012)
292. C.Liu, X.Huang, J.Liu, J.Wang, Z.Chen, R.Luo, C.Wang, J.Li, L.Wang, J.Wan. *Adv. Sci.*, **7**, 1901480 (2020)
293. Y.Hu, J.Wei, Y.Liang, H.Zhang, X.Zhang, W.Shen, H.Wang. *Angew. Chem., Int. Ed.*, **55**, 2048 (2016)
294. Y.Jin, C.Zhao, Z.Sun, Y.Lin, L.Chen, D.Wang, C.Shen. *RSC Adv.*, **6**, 30763 (2016)
295. Y.Zhou, Z.Mao, W.Wang, Z.Yang, X.Liu. *ACS Appl. Mater. Interfaces*, **8**, 28904 (2016)
296. S.Bonakala, A.Lalitha, J.E.Shin, F.Moghadam, R.Semino, H.B.Park, G.Maurin. *ACS Appl. Mater. Interfaces*, **10**, 33619 (2018)
297. J.Lin, M.Hassan, X.Bo, L.Guo. *J. Electroanal. Chem.*, **801**, 373 (2017)
298. L.Liu, Y.Yan, Z.Cai, S.Lin, X.Hu. *Adv. Mater. Interfaces*, **5**, 1701548 (2018)
299. A.A.Ibrahim, A.Lin, F.Zhang, K.M.AbouZeid, M.S.El Shall. *ChemCatChem*, **9**, 469 (2017)
300. M.Tanhaei, A.R.Mahjoub, V.Safarifard. *Mater. Lett.*, **227**, 318 (2018)
301. S.Wu, L.Yu, F.Xiao, X.You, C.Yang, J.Cheng. *J. Alloys Compd.*, **724**, 625 (2017)
302. D.A.Islam, K.Barman, S.Jasimuddin, H.Acharya. *ChemElectroChem*, **4**, 3110 (2017)
303. P.Thangavel, M.Ha, S.Kumaraguru, A.Meena, A.N.Singh, A.M.Harzandi, K.S.Kim. *Energy Environ. Sci.*, **13**, 3447 (2020)
304. M.Jahan, Z.Liu, K.P.Loh. *Adv. Funct. Mater.*, **23**, 5363 (2013)
305. K.Srinivas, Y.Lu, Y.Chen, W.Zhang, D.Yang. *ACS Sustain. Chem. Eng.*, **8**, 3820 (2020)
306. Z.Wang, B.Wang, Y.Yang, Y.Cui, Z.Wang, B.Chen, G.Qian. *ACS Appl. Mater. Interfaces*, **7**, 20999 (2015)
307. S.Zhang, J.Ye, Z.Liu, H.Lu, S.Shi, Y.Qi, G.Ning. *Dalton Trans.*, **49**, 13044 (2020)
308. P.Mialane, C.Mellot-Draznieks, P.Gairola, M.Duguet, Y.Benseghir, O.Oms, A.Dolbecq. *Chem. Soc. Rev.*, **50**, 6152 (2021)
309. W.A.Shah, S.Ibrahim, S.Abbas, L.Naureen, M.Batool, M.Imran, M.A.Nadeem, *J. Environ. Chem. Eng.*, **9**, 106004 (2021)
310. Z.Zhang, Y.Liu, H.Tian, X.Ma, Q.Yue, Z.Sun, Y.Lu, S.Liu. *ACS Nano*, **15**, 16581 (2021)
311. J.Zhu, Z.Wang, X.Song, B.Zhao, Y.Li, Y.Wang. *Micro Nano Lett.*, **16**, 90 (2021)
312. I.Ahmed, N.A.Khan, Z.Hasan, S.H.Jhung. *J. Hazard. Mater.*, **250**–**251**, 37 (2013)
313. L.H.Wee, F.Bonino, C.Lamberti, S.Bordiga, J.A.Martens. *Green Chem.*, **16**, 1351 (2014)

314. Y.Liu, S.Liu, D.He, N.Li, Y.Ji, Z.Zheng, F.Luo, S.Liu, Z.Shi, C.Hu. *J. Am. Chem. Soc.*, **137**, 12697 (2015)
315. Z.Zhang, Y.-W.Liu, H.-R.Tian, X.-H.Li, S.-M.Liu, Y.Lu, Z.-X.Sun, T.Liu, S.-X.Liu. *Matter*, **2**, 250 (2020)
316. S.Liu, Y.Ma, L.Gao, J.Pan. *Chem. Eng. J.*, **341**, 198 (2018)
317. Y.Wu, B.Li, X.Wang, S.Yu, H.Pang, Y.Liu, X.Liu, X.Wang. *Chem. Eng. J.*, **378**, 122105 (2019)
318. Y.Hu, Z.Huang, J.Liao, G.Li. *Anal. Chem.*, **85**, 6885 (2013)
319. E.M.Peña-Méndez, R.M.Mawale, J.E.Conde-González, B.Socas-Rodríguez, J.Havel, C.Ruiz-Pérez. *Talanta*, **207**, 120275 (2020)
320. J.Liu, F.Yang, Q.Zhang, W.Chen, Y.Gu, Q.Chen. *Inorg. Chem.*, **58**, 3564 (2019)
321. J.Zhu, M.Shen, X.Zhao, P.Wang, M.Lu. *ChemPlusChem*, **79**, 872 (2014)
322. J.Zhu, P.Wang, M.Lu. *Catal. Sci. Technol.*, **5**, 3383 (2015)
323. X.Zhao, Y.Duan, F.Yang, W.Wei, Y.Xu, C.Hu. *Inorg. Chem.*, **56**, 14506 (2017)
324. C.T.Buru, M.C.Wasson, O.K.Farha. *ACS Appl. Nano Mater.*, **3**, 658 (2020)
325. Y.Benseghir, A.Lemarchand, M.Duguet, P.Mialane, M.Gomez-Mingot, C.Roch-Marchal, T.Pino, M.-H.Ha-Thi, M.Haouas, M.Fontecave, A.Dolbecq, C.Sassoye, C.Mellot-Draznieks. *J. Am. Chem. Soc.*, **142**, 9428 (2020)
326. Y.Xin, Y.Bai, J.Liu, L.Ma, G.Li. *Chem. – Asian J.*, **16**, 3363 (2021)
327. S.S.Nadar, V.K.Rathod. *Int. J. Biol. Macromol.*, **152**, 1108 (2020)
328. J.Mehta, S.Dhaka, N.Bhardwaj, A.K.Paul, S.Dayananda, S.-E.Lee, K.-H.Kim, A.Deep. *Sens. Actuators, B: Chem.*, **290**, 267 (2019)
329. Y.Pan, H.Li, J.Farmakes, F.Xiao, B.Chen, S.Ma, Z.Yang. *J. Am. Chem. Soc.*, **140**, 16032 (2018)
330. L.Qi, Z.Luo, X.Lu. *ACS Sustain. Chem. Eng.*, **7**, 7127 (2019)
331. R.J.Drout, L.Robison, O.K.Farha. *Coord. Chem. Rev.*, **381**, 151 (2019)
332. C.Doonan, R.Riccò, K.Liang, D.Bradshaw, P.Falcaro. *Acc. Chem. Res.*, **50**, 1423 (2017)
333. D.Feng, T.-F.Liu, J.Su, M.Bosch, Z.Wei, W.Wan, D.Yuan, Y.-P.Chen, X.Wang, K.Wang, X.Lian, Z.-Y.Gu, J.Park, X.Zou, H.-C.Zhou. *Nat. Commun.*, **6**, 5979 (2015)
334. W.Duan, Z.Zhao, H.An, Z.Zhang, P.Cheng, Y.Chen, H.Huang. *Top. Curr. Chem.*, **377**, 34 (2019)
335. Y.Cao, Z.Wu, T.Wang, Y.Xiao, Q.Huo, Y.Liu. *Dalton Trans.*, **45**, 6998 (2016)
336. W.-L.Liu, N.-S.Yang, Y.-T.Chen, S.Lirio, C.-Y.Wu, C.-H.Lin, H.-Y.Huang. *Chem. – Eur. J.*, **21**, 115 (2015)
337. Y.Du, X.Jia, L.Zhong, Y.Jiao, Z.Zhang, Z.Wang, Y.Feng, M.Bilal, J.Cui, S.Jia. *Coord. Chem. Rev.*, **454**, 214327 (2022)
338. C.Wang, K.Liao. *ACS Appl. Mater. Interfaces*, **13**, 56752 (2021)
339. R.D.Arrua, A.Peristyy, P.N.Nesterenko, A.Das, D.M.D'Alessandro, E.F.Hilder. *Analyst*, **142**, 517 (2017)
340. C.Chen, B.Li, L.Zhou, Z.Xia, N.Feng, J.Ding, L.Wang, H.Wan, G.Guan. *ACS Appl. Mater. Interfaces*. **9**, 23060 (2017)
341. H.Yang, J.Li, H.Zhang, Y.Lv, S.Gao. *Microporous Mesoporous Mater.*, **195**, 87 (2014)
342. H.Li, M.M.Sadiq, K.Suzuki, R.Ricco, C.Doblin, A.J.Hill, S.Lim, P.Falcaro, M.R.Hill. *Adv. Mater.*, **28**, 1839 (2016)
343. H.Zheng, Y.Zhang, L.Liu, W.Wan, P.Guo, A.M.Nystrom, X.Zou. *J. Am. Chem. Soc.*, **138**, 962 (2016)
344. M.Wen, G.Li, H.Liu, J.Chen, T.An, H.Yamashita. *Environ. Sci.: Nano*, **6**, 1006 (2019)
345. E.V.Perez, C.Karunaweera, I.H.Musselman, K.J.Balkus Jr., J.P.Ferraris. *Processes*, **4**, 32 (2016)
346. F.Maya, C.P.Cabello, A.Figuerola, G.T.Palomino, V.Cerdà. *Chromatographia*, **82**, 361 (2019)
347. X.Hu, X.Yan, M.Zhou, S.Komarneni. *Microporous Mesoporous Mater.*, **219**, 311 (2016)
348. B.Gao, M.Huang, Z.Zhang, Q.Yang, B.Su, Y.Yang, Q.Ren, Z.Bao. *Chin. J. Chem. Eng.*, **27**, 818 (2019)
349. L.He, L.Li, L.Zhang, S.Xing, T.Wang, G.Li, X.Wu, Z.Su, C.Wang. *CrystEngComm*, **16**, 6534 (2014)
350. J.Ying, A.Herbst, Y.-X.Xiao, H.Wei, G.Tian, Z.Li, X.-Y.Yang, B.-L.Su, C.Janiak. *Inorg. Chem.*, **57**, 899 (2018)
351. M.-M.Ma, M.Li, F.-S.Ke. *Chin. J. Inorg. Chem.*, **34**, 1663 (2018)
352. I.Luz, M.Soukri, M.Lail. *Chem. Mater.*, **29**, 9628 (2017)
353. M.M.Abolghasemi, V.Yousefi, M.Piryaei. *J. Sep. Sci.*, **38**, 1187 (2015)
354. W.Zhang, Y.Hu, J.Ge, H.L.Jiang, S.H.Yu. *J. Am. Chem. Soc.*, **136**, 16978 (2014)
355. J.Kou, L.-B.Sun. *ACS Appl. Mater. Interfaces*, **10**, 12051 (2018)
356. Q.Qu, H.Xuan, K.Zhang, X.Chen, Y.Ding, S.Feng, Q.Xu. *J. Chromatogr. A*, **1505**, 63 (2017)
357. W.A.El-Mehalmey, A.H.Ibrahim, A.A.Abugable, M.H.Hassan, R.R.Haikal, S.G.Karakalos, O.Zaki, M.H.Alkordi. *J. Mater. Chem. A*, **6**, 2742 (2018)
358. X.Yan, X.Hu, S.Komarneni. *RSC Adv.*, **4**, 57501 (2014)
359. N.E.Tari, A.Tadjarodi, J.Tamnanloo, S.Fatemi. *Microporous Mesoporous Mater.*, **231**, 154 (2016)
360. C.Chen, N.Feng, Q.Guo, Z.Li, X.Li, J.Ding, L.Wang, H.Wan, G.Guan. *J. Colloid Interface Sci.*, **513**, 891 (2018)
361. Z.Ulker, I.Erucar, S.Keskin, C.Erkey. *Microporous Mesoporous Mater.*, **170**, 352 (2013)
362. K.Uma, G.-T.Pan, T.C.K.Yang. *Materials*, **10**, 610 (2017)
363. R.Saeedirad, S.T.Ganjali, M.Bazmi, A.Rashidi. *J. Taiwan Inst. Chem. Eng.*, **82**, 10 (2018)
364. G.-Q.Song, Y.-X.Lu, Q.Zhang, F.Wang, X.-K.Ma, X.-F.Huang, Z.-H.Zhang. *RSC Adv.*, **4**, 30221 (2014)
365. Z.Li, H.C.Zeng. *J. Am. Chem. Soc.*, **136**, 5631 (2014)
366. V.Pascanu, A.B.Gomez, C.Ayats, A.E.Platero-Prats, F.Carson, J.Su, Q.Yao, M.A.Pericas, X.Zou, B.Martin-Matute. *ACS Catal.*, **5**, 472 (2015)
367. O.Shekhah, L.Fu, R.Sougrat, Y.Belmabkhout, A.J.Cairns, E.P.Giannelis, M.Eddaoudi. *Chem. Commun.*, **48**, 11434 (2012)
368. X.Lian, B.Yan. *Dalton Trans.*, **45**, 2666 (2016)
369. T.Han, C.Li, X.Guo, H.Huang, D.Liu, C.Zhong. *Appl. Surf. Sci.*, **390**, 506 (2016)
370. A.S.Shalygin, A.L.Nuzhdin, G.A.Bukhtiyarova, O.N.Martyanov. *J. Sol-Gel Sci. Technol.*, **84**, 446 (2017)
371. J.Cui, Y.Feng, S.Jia. *Chem. Eng. J.*, **351**, 506 (2018)
372. A.Sachse, R.Ameloot, B.Coq, F.Fajula, B.Coasne, D.De Vos, A.Galarneau. *Chem. Commun.*, **48**, 4749 (2012)
373. F.G.Cirujano, I.Luz, M.Soukri, C.Van Goethem, I.F.J.Vankelecom, M.Lail, D.E.De Vos. *Angew. Chem., Int. Ed.*, **56**, 13302 (2017)
374. J.Zhang, Z.Li, X.L.Qi, D.-Y.Wang. *Nano-Micro Lett.*, **12**, 173 (2020)
375. Y.Li, J.Liu, K.Zhang, L.Lei, Z.Lei. *Ind. Eng. Chem. Res.*, **57**, 559 (2018)
376. X.Zheng, L.Wang, Q.Pei, S.He, S.Liu, Z.Xie. *Chem. Mater.*, **29**, 2374 (2017)
377. C.Guo, F.Duan, S.Zhang, L.He, M.Wang, J.Chen, J.Zhang, Q.Jia, Z.Zhang, M.Du. *J. Mater. Chem. A*, **10**, 475 (2022)
378. L.Feng, K.-Y.Wang, J.Willman, H.-C.Zhou. *ACS Cent. Sci.*, **6**, 359 (2020)
379. J.Yang, F.Zhang, H.Lu, X.Hong, H.Jiang, Y.Wu, Y.Li. *Angew. Chem., Int. Ed.*, **54**, 10889 (2015)
380. M.Lu, Y.Deng, Y.Li, T.Li, J.Xu, S.-W.Chen, J.Wang. *Anal. Chim. Acta*, **1110**, 35 (2020)
381. J.Liu, H.Zhang, J.Meng, C.Han, F.Liu, X.Liu, P.Wu, Z.Liu, X.Wang, L.Mai. *ACS Appl. Mater. Interfaces*, **12**, 54545 (2020)
382. S.-Y.Moon, E.Proussaloglou, G.W.Peterson, J.B.DeCoste, M.G.Hall, A.J.Howarth, J.T.Hupp, O.K.Farha. *Chem. – Eur. J.*, **22**, 14864 (2016)

383. R.Jin, Z.Bian, J.Li, M.Ding, L.Gao. *Dalton Trans*., **42**, 3936 (2013)
384. X.Wu, C.Yang, J.Ge, Z.Liu. *Nanoscale*, **7**, 18883 (2015)
385. M.S.Denny, M.Kalaj, K.C.Bentz, S.M.Cohen. *Chem. Sci*., **9**, 8842 (2018)
386. J.-L.Ling, K.Chen, C.-D.Wu. *Research*, 9835935 (2021)
387. Z.Wang, Q.Chen. *Green Chem*., **18**, 5884 (2016)
388. J.Chen, S.Wang, J.Huang, L.Chen, L.Ma, X.Huang. *ChemSusChem*, **6**, 1545 (2013)
389. G.Li, K.Zhang, C.Li, R.Gao, Y.Cheng, L.Hou, Y.Wang. *Appl. Catal. B*, **245**, 753 (2019)
390. M.P.Silva, A.M.Ribeiro, C.G.Silva, K.H.Cho, U-H.Lee, J.L.Faria, J.M.Loureiro, J.S.Chang, A.E.Rodrigues, A.Ferreira. *Separ. Purif. Technol*., **290**, 120803 (2022)
391. J.A.Greathouse, M.D.Allendorf. *J. Am. Chem. Soc*., **128**, 10678 (2006)
392. A.S.Jayasinghe, D.K.Unruh, A.Kral, A.Libo, T.Z.Forbes. *Cryst. Growth Des*., **15**, 4062 (2015)
393. M.Ding, H.-L.Jiang. *CCS Chem*., **2**, 2740 (2020)
394. X.Xia, W.Li, S.Li. *J. Nanopart. Res*., **21**, 39 (2019)
395. Y.Zhao, H.Ding, Q.Zhong. *Appl. Surf. Sci*., **284**, 138 (2013)
396. C.Petit, B.Levasseur, B.Mendoza, T.J.Bandosz. *Microporous Mesoporous Mater*., **154**, 107 (2012)
397. D.D.Zu, L.Lu, X.Q.Liu, D.Y.Zhang, L.B. Sun. *J. Phys. Chem. C*, **118**, 19910 (2014)
398. W.Chaikittisilp, K.Ariga, Y.Yamauchi. *J. Mater. Chem. A*, **1**, 14 (2013).
399. J.Tang, R.R.Salunkhe, J.Liu, N.L.Torad, M.Imura, S.Furukawa, Y.Yamauchi. *J. Am. Chem. Soc*., **137**, 1572 (2015)
400. S.J.Yang, C.R.Park. *Adv. Mater*., **24**, 4010 (2012)
401. L.E.Lange, S.K.Obendorf. *ACS Appl. Mater. Interfaces*, **7**, 3974 (2015)
402. Y.Shen, Z.Li, L.Wang, Y.Ye, Q.Liu, X.Ma, Q.Chen, Z.Zhang, S.Xiang. *J. Mater. Chem. A*, **3**, 593 (2015)
403. S.R.Shin, H.S.Cho, Y.Lee, S.Gim, Y.M.Jung, H.Kim, O.Terasaki, J.K.Kang. *J. Am. Chem. Soc*., **143**, 20747 (2021)
404. C.Xin, Y.Ren, Z.Zhang, L.Liu, X.Wang, J.Yang. *ACS Omega*, **6**, 7739 (2021)
405. S.J.Yang, J.H.Cho, K.S.Nahm, C.R.Park. *Int. J. Hydrogen Energy*, **35**, 13062 (2010)
406. A.A.Talin, A.Centrone, A.C.Ford, M.E.Foster, V.Stavila, P.Haney, R.A.Kinney, V.Szalai, F.El Gabaly, H.P.Yoon, F.Léonard, M.D.Allendorf. *Science*, **343**, 66 (2014)
407. Y.Zhang, X.Bo, A.Nsabimana, C.Han, M.Li, L.Guo. *J. Mater. Chem. A*, **3**, 732 (2015)
408. N.A.Travlou, K.Singh, E.Rodriguez-Castellon, T.J.Bandosz. *J. Mater. Chem. A*, **3**, 11417 (2015)
409. A.Saad, S.Biswas, E.Gkaniatsou, C.Sicard, E.Dumas, N.Menguy, N.Steunou. *Chem. Mater*., **33**, 5825 (2021)
410. S.Q.Xie, J.Y.Hwang, X.Sun, S.Z.Shi, Z.Zhang, Z.W.Peng, Y.C.Zhai. *J. Power Sources*, **253**, 132 (2014)
411. M.Alfè, V.Gargiulo, L.Lisi, R.Di Capua. *Mater. Chem. Phys*., **147**, 744 (2014)
412. P.C.Banerjee, D.E.Lobo, R.Middag, W.K.Ng, M.E.Shaibani, M.Majumder. *ACS Appl. Mater. Interfaces*, **7**, 3655 (2015)
413. Z.Zhang, H.Wang, X.Chen, C.Zhu, W.Wei, Y.Sun. *Adsorption*, **21**, 77 (2015)
414. H.Furukawa, K.E.Cordova, M.O'Keeffe, O.M.Yaghi. *Science*, **341**, 1230444 (2013)
415. Z.Wang, L.Liu, Z.Li, N.Goyal,T.Du, J.He, G.K.Li. *Energy Fuels*, **36**, 2927 (2022)
416. C.Petit, T.J.Bandosz. *J. Colloid Interface Sci*., **447**, 139 (2015)
417. A.H.Ismail, M.H.Yaacob, M.A.Mahdi, Y.Sulaiman. *Sens. Actuators A: Phys*., **335**, 113395 (2022)
418. A.Rosado, A.Borrás, J.Fraile, J.A.R.Navarro, F.Suárez-García, K.C.Stylianou, A.M.López-Periago, J.Giner Planas, C.Domingo, A.Yazdi. *ACS Appl. Nano Mater*., **4**, 12712 (2021)
419. X.Zhou, W.Huang, J.Miao, Q.Xia, Z.Zhang, H.Wang, Z.Li. *Chem. Eng. J*., **266**, 339 (2015)
420. Y.Huang, W.Lin, T.Huang, Z.Li, Z.Zhang, R.Xiao, X.Yang, S.Lian, J.Pan, J.Ma, W.Wang, L.-P.Sun, J.Li, B.-O.Guan. *Adv. Opt. Mater*., **10**, 2101561 (2021)
421. C.Ma, Y.Guo, H.Liu, X.Zhang. *Microporous Mesoporous Mater*., **322**, 111153 (2021)
422. X.Qiu, X.Wang, Y.Li. *Chem. Commun*., **51**, 3874 (2015)
423. M.Heydari, M.Gharagozlou, M.Ghahari, S.Sadjadi. *Inorg. Chem. Commun*., **130**, 108693 (2021)
424. J.-H.Cha, K.Noh, W.Yin, Y.Lee, Y.Park, T.K.Ahn, A.Mayoral, J.Kim, D.-Y.Jung, O.Terasaki. *J. Phys. Chem. Lett*., **10**, 2270 (2019)
425. Y.Qi, M.Wan, A.M.Abd El-Aty, H.Li, L.Cao, Y.She, Y.Shao, F.Jin, S.Wang, J.Wang. *Microchim. Acta*, **187**, 279 (2020)
426. J.Huo, G.Yu, J.Wang. *J. Hazard. Mater*., **412**, 125298 (2021)
427. K.P.Prasanth, P.Rallapalli, M.C.Raj, H.C.Bajaj, R.V.Jasra. *Int. J. Hydrogen Energy*, **36**, 7594 (2011)
428. Z.H.Huang, G.Liu, F.Kang. *ACS Appl. Mater. Interfaces*, **4**, 4942 (2012)
429. X.Sun, Q.Xia, Z.Zhao, Y.Li, Z.Li. *Chem. Eng. J*., **239**, 226 (2014)
430. K.Kamal, D.I.Grekov, A.M.Shariff, M.A.Bustam, P.Pré. *Microporous Mesoporous Mater*., **323**, 111246 (2021)
431. B.P.Biswal, D.B.Shinde, V.K.Pillai, R.Banerjee. *Nanoscale*, **5**, 10556 (2013)
432. C.A.F.de Oliveira, F.F.da Silva, G.C.Jimenez, J.F.D.Neto, D.M.B.de Souza, I.A.de Souza, S.Alves. *Chem. Commun*., **49**, 6486 (2013)
433. *Metal-Organic Frameworks for Chemical Reactions: from Organic Transformations to Energy Applications*. (Eds A.Khan, A.M.Asiri, A.L.Bilgrami, K.C.B.Naidu). (Amsterdam: Elsevier, 2021)
434. A.Singh, A.K.Singh, J.Liu, A.Kumar. *Catal. Sci. Technol*., **11**, 3946 (2021)
435. P.Coliaie, R.R.Bhawnani, A.Prajapati, R.Ali, P.Verma, G.Giri, M.S.Kelkar, A.Korde, M.Langston, C.Liu, N.Nazemifard, D.Patience, T.Rosenbaum, D.Skliar, N.K.Nere, M.R.Singh. *Lab Chip*, **22**, 211 (2022)
436. V.Stavila, J.Volponi, A.M.Katzenmeyer, M.C.Dixon, M.D.Allendorf. *Chem. Sci*., **3**, 1531 (2012)
437. M.T.Conato, A.J.Jacobson. *Microporous Mesoporous Mater*., **175**, 107 (2013)
438. I.Ahmed, N.A.Khan, S.H.Jhung. *Inorg. Chem*., **52**, 14155 (2013)
439. R.Hardian, S.Dissegna, A.Ullrich, P.L.Llewellyn, M.-V.Coulet, R.A.Fischer. *Chem. – Eur. J*., **27**, 6804 (2021)
440. H.Liu, L.-G.Gong, C.-X.Wang, C.-M.Wang, K.Yu, B.-B.Zhou. *J. Mater. Chem. A*, **9**, 13161 (2021)
441. A.Lerf, H.He, M.Forster, J.Klinowski. *J. Phys. Chem. B*, **102**, 4477 (1998).
442. S.Bashkova, T.J.Bandosz. *Microporous Mesoporous Mater*., **179**, 205 (2013)
443. J.H.Lee, S.Kang, J.Jaworski, K.Y.Kwon, M.L.Seo, J.Y.Lee, J.H.Jung. *Chem. – Eur. J*., **18**, 765 (2012)
444. Y.Wei, Z.Hao, F.Zhang, H.Li. *J. Mater. Chem. A*, **3**, 14779 (2015)
445. J.H.Lee, J.Jaworski, J.H.Jung. *Nanoscale*, **5**, 8533 (2013)
446. J.Duan, S.Goswami, S.Patwardhan, J.T.Hupp. *J. Phys. Chem. C*, **126**, 4601 (2022)
447. Y.Sun, J.Harloff, H.Kosslick, A.Schulz, C.Fischer, S.Bartling, M.Frank, A.Springer. *Mol. Catal*., **517**, 112005 (2022)
448. L.Jiao, J.Wang, H.-L.Jiang. *Acc. Mater. Res*., **2**, 327 (2021)
449. P.B.S.Rallapalli, M.C.Raj, D.V.Patil, K.P.Prasanth, R.S.Somani, H.C.Bajaj. *J. Energy Res*., **37**, 746 (2013)
450. M.Anbia, S.Sheykhi. *J. Ind. Eng. Chem*., **19**, 1583 (2013)

451. L.Li, X.L.Liu, M.Gao, W.Hong, G.Z.Liu, L.Fan, B.Hu, Q.H.Xia, L.Liu, G.W.Song, Z.S.Xu. *J. Mater. Chem. A*, **2**, 1795 (2014)
452. Y.Bai, C.Liu, Y.Shan, T.Chen, Y.Zhao, C.Yu, H.Pang. *Adv. Energy Mater.*, **12**, 2100346 (2022)
453. E.Rojas-Garcia, A.A.Castañeda, D.Angeles-Beltrán, R.López-Medina, A.M.Maubert-Franco. *Catal. Today*, **394**–**396**, 357 (2022)
454. D.P.Broom, C.J.Webb, G.S.Fanourgakis, G.E.Froudakis, P.N.Trikalitis, M.Hirscher. *Int. J. Hydrogen Energy*, **44**, 7768 (2019)
455. R.Jin, F.Ji, H.Lin, C.Luo, Y.Hu, C.Deng, X.Cao, C.Tong, G.Song. *J. Chromatogr. A*, **1577**, 1 (2018)
456. A.F.Sapnik, D.N.Johnstone, S.M.Collins, G.Divitini, A.M.Bumstead, C.W.Ashling, P.A.Chater, D.S.Keeble, T.Johnson, D.A.Keen, T.D.Bennett. *Dalton Trans.*, **50**, 5011 (2021)
457. R.A.Maia, B.Louis, W.Gao, Q.Wang. *React. Chem. Eng.*, **6**, 1118 (2021).
458. P.Karikkethu Prabhakaran, J.Deschamps. *J. Mater. Chem. A*, **3**, 7014 (2015)
459. S.Wang, C.Wang, Q.Zhou. *ACS Appl. Mater. Interfaces*, **13**, 29949 (2021)
460. R.R.Ozer, J.P.Hinestroza. *RSC Adv.*, **5**, 15198 (2015)
461. X.Li, R.Zhou, Z.Wang, M.Zhang, T.He. *J. Mater. Chem. A*, **10**, 1642 (2022)
462. I.E.Uflyand, V.N.Naumkina, V.A.Zhinzhilo. *J. Compos. Sci.*, **6**, 215 (2022)
463. O.V.Kharissova, V.A.Zhinzhilo, J.D.Bryantseva, I.E.Uflyand, B.I.Kharisov. *Mendeleev Commun.*, **32**, 661 (2022)
464. V.A.Zhinzhilo, A.Yu.Litvinova, V.M.Lyamina, G.I.Dzhardimalieva, I.E.Uflyand. *Bull. Univ. Karaganda — Chem. Ser.*, **107**, 239 (2022)
465. M.Bazargan, F.Ghaemi, A.Amiri, M.Mirzaei. *Coord. Chem. Rev.*, **445**, 214107 (2021)
466. T.K.Vo, T.P.Trinh, V.C.Nguyen, J.Kim. *J. Ind. Eng. Chem.*, **95**, 224 (2021)
467. N.Garg, A.Deep, A.L.Sharma. *Coord. Chem. Rev.*, **445**, 214073 (2021)
468. X.Wang, Y.Wang, Y.Ying. *TrAC — Trends Anal. Chem.*, **143**, 116395 (2021)
469. J.Xu, J.Ma, Y.Peng, S.Cao, S.Zhang, H.Pang. *Chin. Chem. Lett.*, (2022); https://doi.org/10.1016/j.cclet.2022.05.041
470. B.I.Kharisov, C.M.O.González, O.V.Kharissova, L.T.Gonzalez, Y.P.Méndez, I.E.Uflyand. In *Magnetic Nanocatalysis. Industrial Applications*. Vol. 2. (Eds R.S.Varma, B.Banerjee, De Gruyter). (Boston: Berlin, 2022). P. 37
471. G.I.Dzhardimalieva, A.K.Zharmagambetova, S.E.Kudaibergenov, I.E.Uflyand. *Kinet. Catal.*, **61**, 198 (2020)
472. Y.Peng, J.Xu, J.Xu, J.Ma, Y.Bai, S.Cao, S.Zhang, H.Pang. *Adv. Colloid Interface Sci.*, **307**, 102732 (2022)
473. Y.Dai, C.Liu, Y.Bai, Q.Kong, H.Pang. *Nanotechnol. Rev.*, **11**, 1005 (2022)
474. M.Zhang, Y.Shan, Q.Kong, H.Pang. *FlatChem*, **32**, 100332 (2022)
475. Y.Sun, L.Zheng, Y.Yang, X.Qian, T.Fu, X.Li, Z.Yang, H.Yan, C.Cui, W.Tan. *Nano-Micro Lett.*, **12**, 103 (2020)
476. X.Dao, M.Nie, H.Sun, W.Dong, Z.Xue, Q.Li, J.Liao, X.Wang, X.Zhao, D.Yang, L.Teng. *Int. J. Hydrogen Energy*, **47**, 16741 (2022)
477. Y.Xu, Q.Li, H.Pang. *Nano Futures*, **4**, 032007 (2020)
478. G.Chakraborty, I.-H.Park, R.Medishetty, J.J.Vittal. *Chem. Rev.*, **121**, 3751 (2021)
479. P.Rani, V.Kasneryk, M.Opanasenko. *Appl. Mater. Today*, **26**, 101283 (2022)
480. I.Kurzydym, I.Czekaj. *Techn. Transact.*, e2020012 (2020); https://doi.org/10.37705 / TechTrans/e2020012